Biostratigraphy and sequence stratigraphy of the Minjur and Marrat Formations (Upper Triassic to Middle Jurassic) in Kuwait

Sandra Crespo de Cabrera[1], Thomas De Keyser[3], Ghaida Al-Sahlan[2], Hajar A. Al-Wazzan[2] and Adi P. Kadar[4]

[1]*Building No. 4682, Road No. 2468, Block No. 324, Manama, Bahrain*
[2]*Kuwait Oil Company, Exploration Group, P. O. Box 9758, Ahmadi, Kuwait*
[3]*Technically Write Consulting, LLC, 21091 Powerline Road, Harrisburg, OR 97446*
[4]*Jl. Raya Gadobankong 178C, Ngamprah, Kabupaten Bangdung Barat, Indonesia*
email: tdkatvvf@gmail.com

ABSTRACT: This paper summarizes sedimentological and biostratigraphic data for the Minjur and Marrat Formations in Kuwait and places them within an expanded sequence stratigraphic framework based on the letter and number scheme initiated by Sharland and others (2001). Only two sequences (Tr80 and J10) were identified in this interval in the original scheme, whereas, between Tr80 and the top of the Upper Marrat, 18 sequences are now recognized and their sequence boundaries and maximum flooding surfaces identified and illustrated herein. One new sequence (Tr90) was proposed in the underlying Jilh A Member. Three new sequences (Tr100, Tr105 and Tr110) are recognized in the Minjur Formation (= Lower Minjur in Saudi Arabia). Four sequences (J02, J04, J06 and J08) and part of a fifth (J10) are recognized in the Lower Marrat. Seven sequences (part of J10 and J11-J16) are recognized in the Middle Marrat. Three sequences (J17, J18 and J19) are recognized in the Upper Marrat.

Biostratigraphic data are sparse for the Minjur and Marrat Formations. In the Marrat Formation, calcareous nannofossils are extremely rare, benthic foraminifers are relatively common but long-ranging and palynomorphs are sparse and most commonly non-age diagnostic. Published and unpublished proprietary data from 33 wells have been combined to determine the ages of the succession. Using palynology, the Minjur Lower Member was dated as Norian. An undifferentiated Norian-Rhaetian age range is assigned to the Middle and upper Members of the Minjur Formation. The Triassic/Jurassic boundary is placed just below the base of the Lower Member of the Marrat Formation, where cuttings samples from a thin interval of strata yielded long age-ranging palynomorphs. The Sinemurian/Pliensbachian boundary occurs in the Lower Marrat at the base of the S J06 transgressive systems tract. The Pliensbachian/Toarcian boundary, dated on the basis of *Nannoceratopsis triceras* and *Lotharingius crucicentralis*, is also in the Lower Marrat at the base of the S J10 transgressive systems tract. The contact of the Middle and Upper Marrat is unconformable and locally karsted but appears to correlate to the Toarcian/Aalenian boundary. The upper section of the Upper Marrat and the base of the overlying Dhruma Formation have not been cored but the Aalenian/Bajocian boundary is placed in the upper portion of Sequence J19. SB J20 is placed at the top of the Upper Marrat Member.

Change in the age of the Late Triassic Baluti Formation in Iraq has resulted in changes in correlations of the Minjur and Marrat Formations to each other and to other formations in the region. The Lower Marrat is shown to be the shallow marine equivalent of the Upper Minjur siliciclastics in the subsurface Rub al Khali Basin and in the shallow subsurface Arabian Basin near the outcrop belt in Saudi Arabia. The Lower Marrat correlates to the Adaiyah Formation and the Upper Sarki Formation in Iraq. The Middle Marrat correlates to the Mus and Alan Formations in Iraq and to all of the Marrat Formation as defined in outcrop in Saudi Arabia. The Upper Marrat is largely represented by an Aalenian-age hiatus in the Saudi Arabian outcrop belt but a thin, condensed Aalenian section is present in the subsurface, basinward of the outcrop belt, and correlated with the Lower Dhruma (D1-D2). The Upper Marrat is correlated to the lower Sargelu Formation in Iraq. These new and revised correlations clarify the timing of the Late Triassic (Norian) uplift of the Qatar Arch.

INTRODUCTION AND GEOLOGIC SETTING

The Arabian Plate contains several hydrocarbon-rich sedimentary basins, including the Arabian Basin, the Rub al Khali Basin and the Mesopotamian Basin (text-fig. 1). Together, these basins contain numerous giant and supergiant oil and gas fields of Permian to Miocene age, representing a significant portion of Earth's remaining hydrocarbon reserves. Deep exploration in Kuwait since 1975 has discovered significant reserves of condensate and gas in Marrat carbonate reservoirs in several fields (Alsharhan et al. 2014). Coring associated with development drilling since 2000 has provided much of the data for this and other Jurassic studies (Kadar et al. 2015; Crespo de Cabrera et al. 2019, 2020).

Plate reconstructions provide a key to understanding the Mesozoic stratigraphy of Kuwait. Triassic to Jurassic reconstructions show that the Arabian plate was at equatorial latitude, part of the northeastern margin of Gondwana, bordering the Neotethys ocean basin (text-fig. 2) (e.g., Sengor and Natal'in 1996; Stampfli and Borel 2002; Barrier et al. 2018). Kuwait was located on the subsiding, shallow-water passive platform margin of the Arabian Plate along the southwest margin of the Neo-Tethys Ocean (Sengor and Natal'in 1996; Sharland et al. 2001; Ziegler 2001; Barrier and Vrielynk 2008; Barrier et al. 2018) (text-fig. 2). The Lower Jurassic sediments in Kuwait are typically shallow water shales, carbonates, and evaporites of the uppermost beds of the Minjur Formation and the Lower and Middle members of the

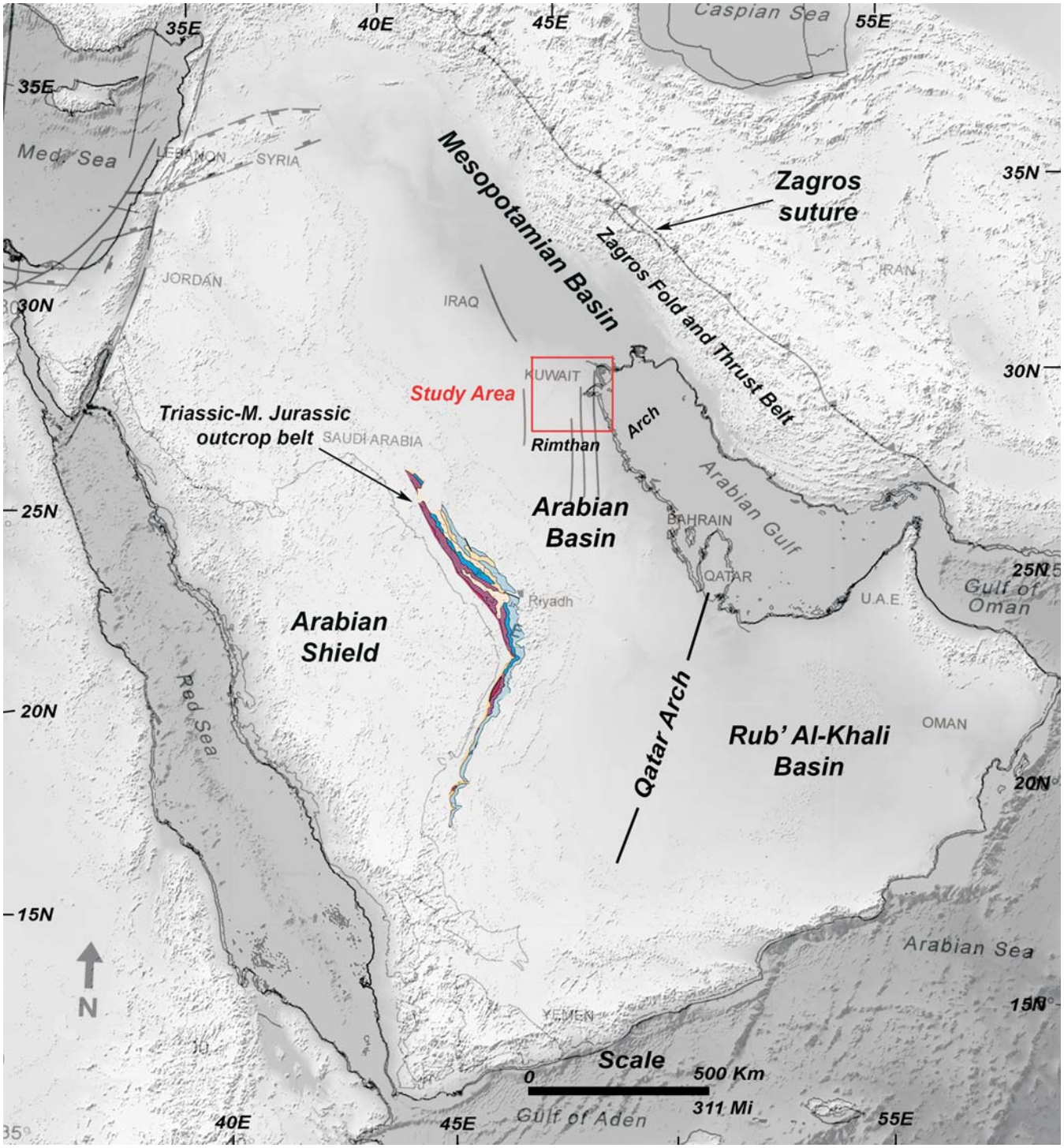

TEXT-FIGURE 1
Map of Arabian Plate, showing location of study area and principal features discussed in this paper.

Marrat Formation, a proven hydrocarbon reservoir (Al-Eiden et al. 2009). The Upper Marrat in Kuwait is Middle Jurassic in age. The Marrat platform was subdivided paleogeographically into two sedimentary environments; restricted carbonate platform in the west and open-marine carbonate platform in the east (Ziegler 2001; Barrier et al. 2018) (text-fig. 2). The Marrat Formation, divided into Upper, Middle, and Lower members (Kadar et al. 2015), conformably overlies the siliciclastics, carbonates, and evaporites of the Minjur Formation and is conformably overlain by the Middle Jurassic Dhruma Formation.

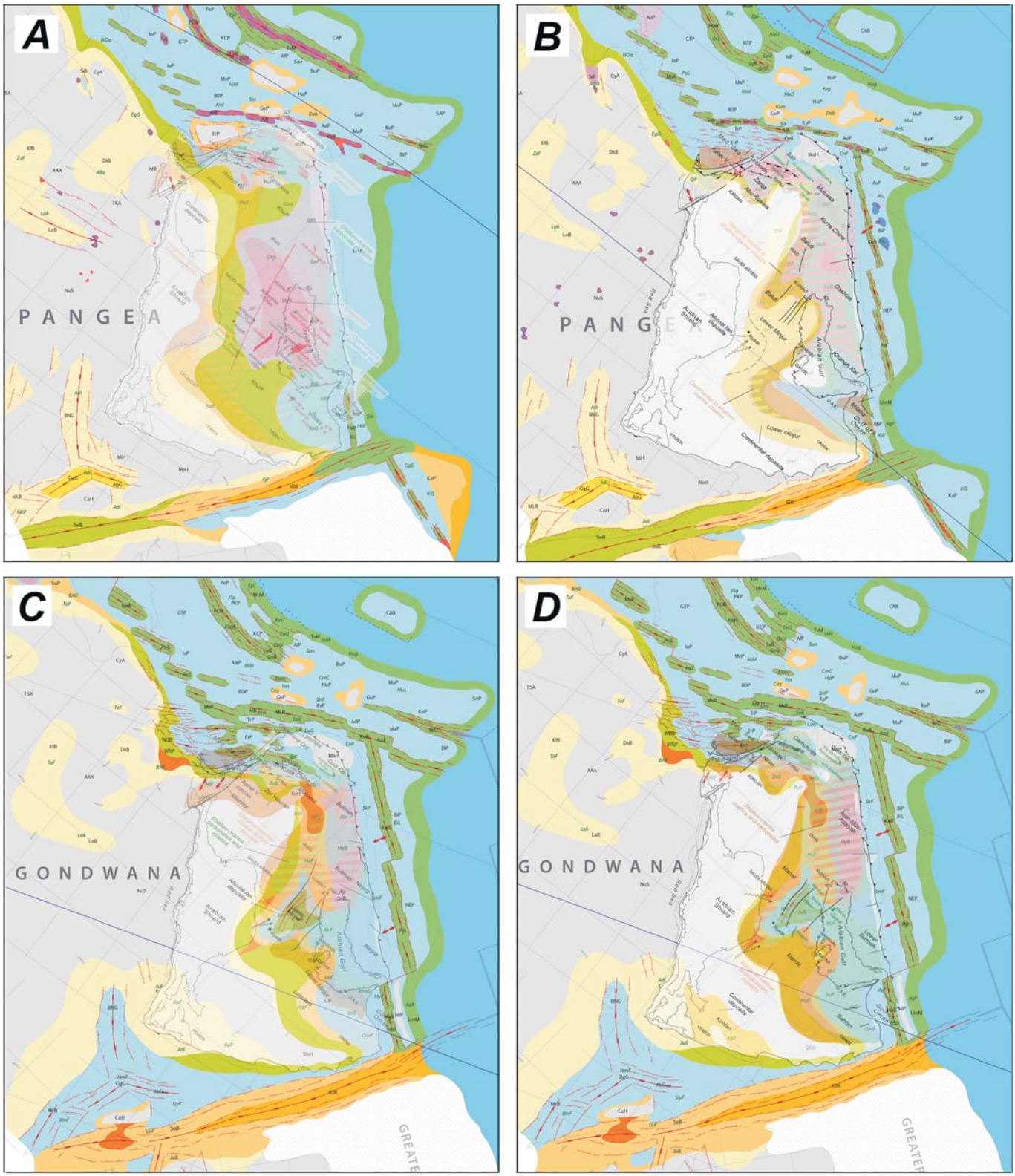

TEXT-FIGURE 2
Paleotectonic maps (Barrier et al. 2018) with paleofacies distribution superimposed (Ziegler 2001): (A) 247.2–242.0 Ma paleotectonics with paleofacies for Anisian; (B) 216.0–208.5 Ma paleotectonics with Carnian-Norian paleofacies; (C) 182.7–174.1 Ma paleotectonics with Toarcian paleofacies; (D) 182.7–174.1 Ma paleotectonics with Sinemurian-Aalenian paleofacies.

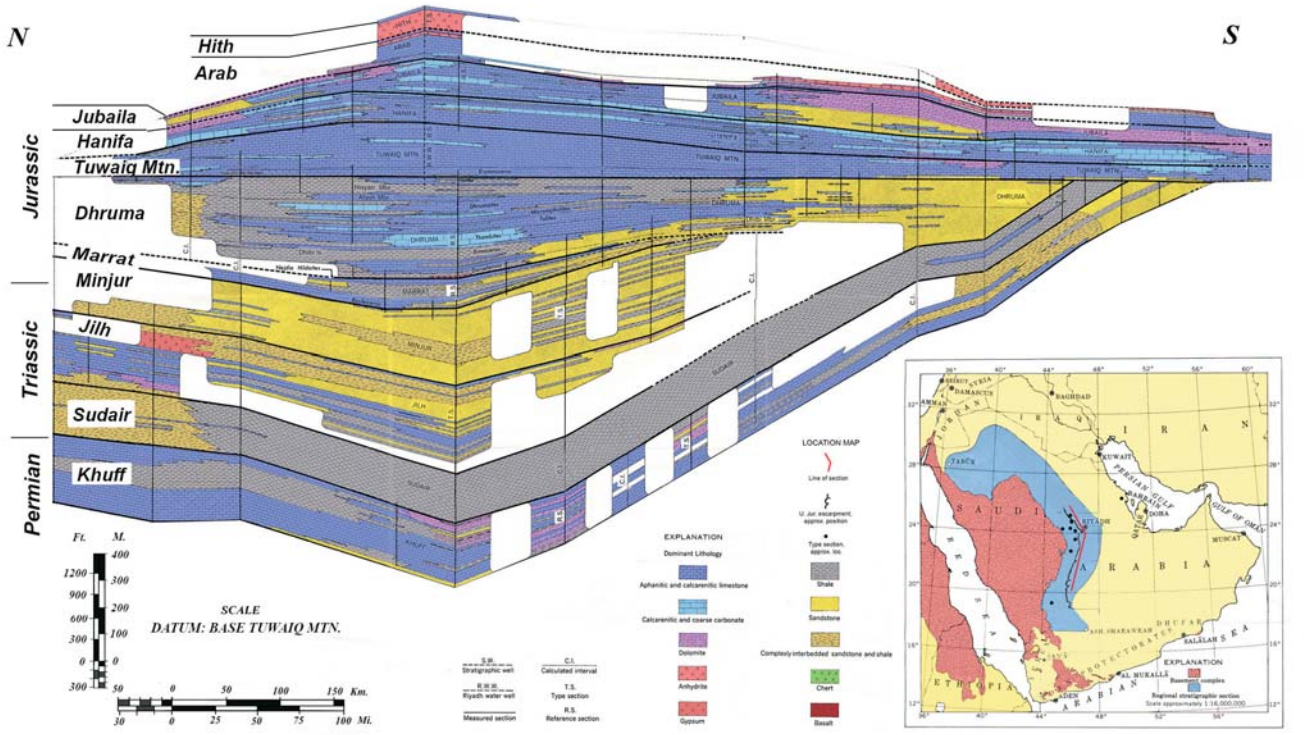

TEXT-FIGURE 3
Colorized excerpt of a cross-section of Upper Permian (Khuff) to Upper Jurassic (Hith) strata exposed in the Saudi Arabian outcrop belt as reconstructed by Powers et al. (1966). Note the changes in thickness distribution between pre-Minjur and Minjur strata and between Dhruma and younger Jurassic strata. Areas of non-exposure are shown as blank white spaces.

Despite being located in the interior of a passive plate margin, sedimentation was affected by intra-plate uplift, subsidence and faulting along reactivated structural boundaries. Uplift along the Qatar Arch during the Late Triassic influenced lithofacies distribution as a sediment source. Subsidence east and west of the uplift created depocenters in the Arabian and Rub al Khali basins, respectively. The large, rapid rise in sea level associated with MFS J11 caused a retreat of the Middle Marrat platform margin and formation of an intrashelf basin (ISB) within the Arabian Plate (De Keyser and Kendall 2014).

The Marrat ISB coincided with an oceanic anoxic event (T-OAE) and was a eustatic event without related uplift, erosion or changes in depositional thickness trends. Formation of the Rimthan Arch between Kuwait and Saudi Arabia and separation of the Arabian and Gotnia basins occurred during Middle and Late Jurassic time as described by Kadar et al. (2015) and Crespo de Cabrera et al. (2019, 2020). This paper describes the Upper Triassic and Lower and early Middle Jurassic sedimentological, biostratigraphic and sequence stratigraphic record in Kuwait. The brief structural episode that formed the Qatar Arch, separating the Arabian and Rub al Khali basins, and their subsequent infilling are further discussed in later sections of this paper.

LITHOSTRATIGRAPHY

Minjur Formation

The Minjur Sandstone was defined in outcrop exposures along the east-dipping margin of the Arabian Shield (Steineke and Bramkamp 1952, in: Arkell 1952; Powers et al. 1966; Powers 1968). It disconformably overlies the Jilh Formation and is conformably overlain by the Marrat Formation (text-fig. 3). The type section consists of 315 m (1,033 ft) of "sandstone, buff, commonly crossbedded, locally calcareous with several irregular zones of red, purple, and blue-gray shale, sandy shale, and shaly sand; black to brown ironstone at several levels form thin platy layers and concretionary masses which contain molds of fossil wood" (Powers 1968, p. 108) (text-fig. 3).

The regional cross-section published by Powers et al. (1966) shows the Jilh, Minjur and younger formations thinning and onlapping southward onto the tabular-shaped Sudair Formation (text-fig. 3). The Jilh and Minjur, where seen in outcrop, were interpreted to be relatively conformable with the subjacent and superjacent formations. The nature of the thinning and possible truncation was concealed beneath a large area of non-exposure (blank white areas in cross-section, text-fig. 3) and Powers et al. (1966, p. D36) concluded that the southward decrease in thickness of the Jilh could be due to erosion, thinning against the basin margin, or a combination of both.

The Minjur and the younger Jurassic formations appear to reach their maximum thickness in a depositional trough deepening northeastward at an acute angle to the outcrop section (see isopach map in Stewart et al. 2016, their Figure 8 and Issautier et al. 2019, their Figure 11) (also, see cross-sections by Stewart et al. 2016; Issautier et al. 2019; Lunn et al. 2019; Lunn 2020). Moreover, the Minjur represents a change from the carbonate-evaporite succession in the underlying formations to

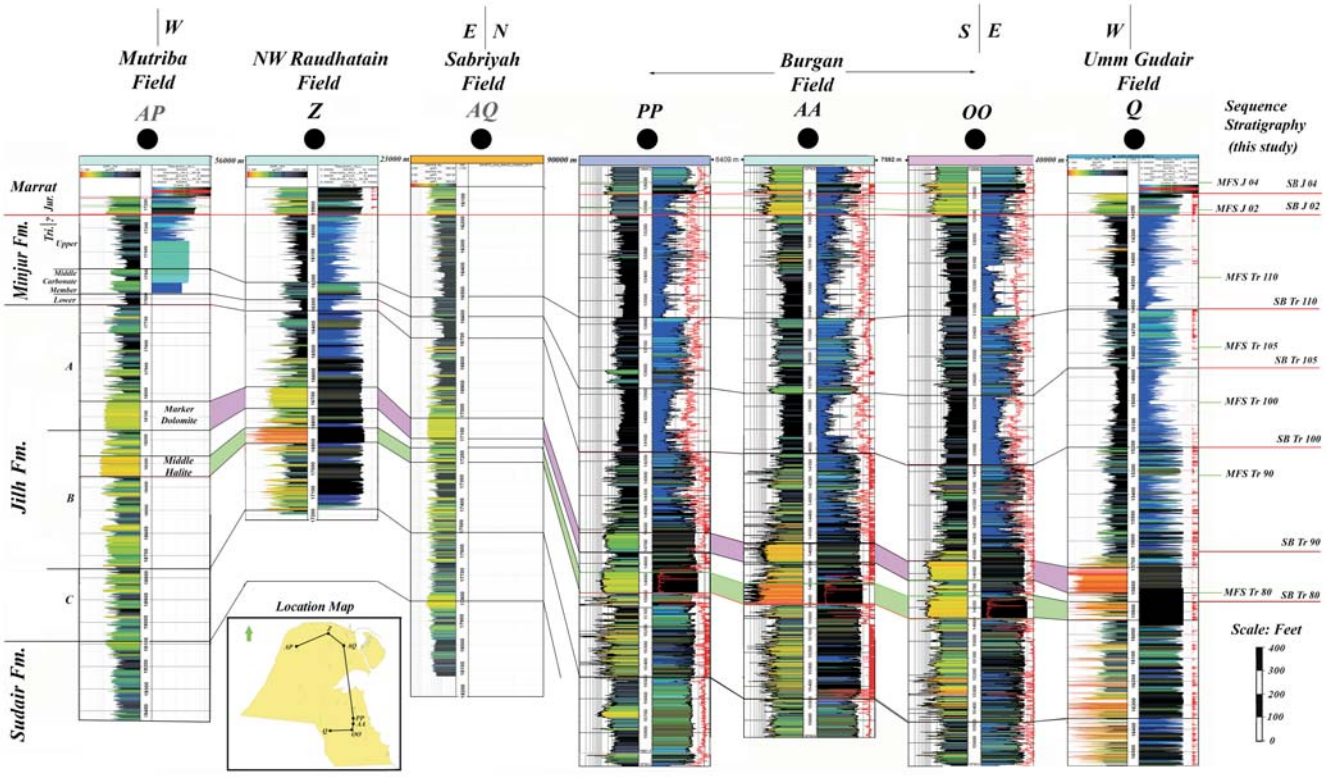

TEXT-FIGURE 4
A cross-section from Mutriba Field to Umm Gudair Field, showing the log character and thickness relationships of the Minjur Formation and the A and B members of the Jilh Formations. The sequence boundaries and MFSs shown on the right are based on Lunn et al (2019), Lunn (2020), Sharland et al. (2001) and this study. Biostratigraphic data suggest that the Triassic/Jurassic boundary is located in a thin indeterminate zone with mixed, long ranging flora just below the base of the Lower Marrat.

siliciclastics shed from uplifts to the south and west. The Minjur and the overlying formations up to the top of the Dhruma show thinning and onlap onto the Sudair. The formations above the Dhruma (Tuwaiq Mountain, Hanifa, Jubaila, Arab and Hith) extend southward beyond the pinchout of the Minjur Sandstone. Correlations of the Dhruma, Tuwaiq Mountain and Hanifa formations in Saudi Arabia to the Dhruma, Sargelu and Najmah formations in Kuwait are given in Kadar et al. (2015) and further documented in Crespo de Cabrera et al. (2019, 2020). Correlation of hiatuses in the Saudi Arabian outcrop belt to basinal strata in Kuwait are discussed in a later section of this paper.

The Minjur in Kuwait is comprised of a mixed assemblage of sandstone, shale, and limestone, divided into Lower (carbonate-siliciclastic), Middle (carbonate) and Upper (mixed carbonate-siliciclastic with minor dolomite and anhydrite) members based on dominant lithology. Alsharhan et al. (2014) further subdivided the lower and upper units and recognize five units, with their unit three equivalent to the Middle Carbonate shown in Figure 4. The Triassic/Jurassic boundary is placed near the top of the Upper member in Well AA (text-fig. 4), beneath a thin interval of mixed, long ranging Triassic–Jurassic flora obtained from cuttings samples just below the base of the Lower Marrat (Robertson Research 2000).

The Minjur Formation is a minimum of 390 ft (119 m) thick in northwest Kuwait (Mutriba Field) and thickens to 1,060 ft (323 m) in the Burgan Field, a 172% increase (text-fig. 4). Well penetrations are too few to allow even a generalized isochore map of the Minjur Formation. Of the more than 50 wells that penetrate the Minjur, only about a dozen penetrate to the underlying Jilh Formation and of those, six are in the Mutriba Field. A cross-section from the Mutriba Field through the NW Raudhatain Field, Sabriyah Field and Burgan Field, ending in the Umm Gudair Field shows the variations in thickness of the Minjur Formation and the A and B members of the underlying Jilh Formation (text-fig. 4).

The Minjur Formation thickens eastward in Kuwait from 390 ft in the northwest (Mutriba Field) to 520 ft in the northeast (Sabriyah Field), a distance of approximately 50 mi (80 km) (2.65 ft/mi or 0.5 m/km). The Minjur thickens southward from 520 ft (Sabriyah Field) to 1,060 ft (Burgan Field), a distance of approximately 42 mi (68 km) (13.1 ft/mi or 2.5 m/km). The formation thins westward to 983 ft (300 m) in Umm Gudair Field, a distance of approximately 25 mi (40 km) (3.1 ft/mi or 1.35 m/km). Thus, the Minjur thickens gently eastward but approximately five times more rapidly southward. Lunn et al. (2019, their Figure 9) showed the thickness increase from Mutriba to Burgan. Lunn (2020, their Figure 6) showed southward thinning of the Minjur Formation between the Burgan Field and the Ghawar Field, on

the northern flank of the Qatar Arch. The thinning there was attributed to the absence of the Upper Member of the Minjur Formation. Lunn et al. (2019) and Lunn (2020) consider the Lower and Middle members of the Minjur in Kuwait to be equivalent to the Lower Member of the Minjur as defined in Saudi Arabia.

Thickness relationships in the underlying A and B members of the Jilh Formation are different. The combined thickness of the Jilh A and B members decreases eastward from Mutriba Field where it is 1,117 ft (340.5 m) thick to Sabriyah Field (819 ft/249.7 m) over a distance of approximately 50 mi (80 km), a rate of 6.0 ft/mi (1.1 m/km). The Jilh A+B thickens southward from Sabriyah Field to a maximum of 1,188 ft (368 m) in the Burgan Field over a distance of approximately 42 mi (68 km), equivalent to 8.8 ft/mi or 1.7 m/km. The Jilh A+B thins westward from 1,188 ft (368 m) in the Burgan Field to 1,150 ft (351 m) in the Umm Gudair Field, a distance of 25 mi (40 km) or 1.5 ft/mi (0.2 m/km). Thus, the Jilh thickens southward and westward, while the Minjur thickens southward and eastward, suggesting a discordance or unconformity surface between the Jilh and Minjur formations. The northward thinning of the Minjur shown in Figure 4 and by Lunn et al. (2019) appears to be at least partly by basal onlap. Erosion at the top of the Jilh was shown by Khan (1989, Figure 5) in the Sabriyah Field (north Kuwait) but truncation is not evident in Figure 4. However, there does appear to be about 90 ft of truncation at the top of the Jilh Formation, westward from Burgan Field to the Umm Gudair Field (text-fig. 4) and one 4th-order cycle appears to have been eroded from the top of the Jilh A in Well Z (NW Raudhatain Field).

Marrat Formation

In Kuwait, the Marrat Formation (Steineke 1937, unpub. Aramco report; Steineke et al. 1958; Yousif and Nouman 1997) overlies the Upper Triassic Minjur Formation (Steineke and Bramkamp 1952) and is overlain by the Middle Jurassic Dhruma Formation (Steineke 1937, unpub. Aramco report; Steineke et al. 1958; Yousif and Nouman 1997; Kadar et al. 2015). The Marrat Formation in Saudi Arabia (Powers et al. 1966; Powers 1968) was divided into three units based on topography and lithofacies. It is important to point out that these are not time-equivalents of the three formally recognized members of the Marrat in Kuwait, discussed herein. The results of this study demonstrate that the Middle Marrat Member of Kuwait is equivalent to all three members of the Marrat Formation as described in the outcrop belt. In addition, the Lower Marrat Member of Kuwait is the equivalent of the Upper Minjur in subsurface Saudi Arabia. The Upper Marrat Member of Kuwait is represented by a regional late Toarcian-Aalenian hiatus in the type section.

The transition between the Minjur and Marrat formations has not yet been seen in core, but it is inferred from electrical logs at the top of the Minjur Formation in Well Minagish-27 (MN-0027), designated as the type section by Yousif and Nouman (1997). They applied the name for the first time in Kuwait and subdivided it into (top to bottom) A, B, C, D and E units. These subdivisions, have subsequently been replaced by the Lower, Middle and Upper Marrat members, based on the increased proportion of argillaceous sediments in the Lower and Upper members (Al-Eidan et al. 2009; Neog et al. 2010; Kadar et al. 2015) (text-fig. 5).

The contacts between the three members have been seen in core in several wells. The contact between the Lower and Middle Marrat Members is marked by the abrupt upward change from calcareous shale and argillaceous mudstone to pure skeletal wackestone. A karsted unconformity is locally present between the Middle and Upper Marrat members in northern Kuwait (Crespo de Cabrera et al. 2019). The lower and upper contacts of the Marrat Formation with the Minjur and Dhruma formations, respectively, have not been seen and described in core. The thickness of the Marrat Formation in onshore Kuwait varies from just over 1,300 ft (396 m) in the northwest to nearly 2,400 ft (732 m) in the southeast in the Burgan Field (text-fig. 6). It consists of complexly layered and interbedded limestone, dolomite, anhydrite, and shale.

Lower Marrat Member

In Kuwait, the Lower Member of the Marrat Formation is a thick carbonate-evaporite succession deposited on a broad, shallow-water platform and represents deposition in coastal sabkha, tidal flat, lagoon, shoal, and open marine platform depositional settings (Neog et al. 2010). It thickens uniformly from northwest to southeast, from less than 600 ft (183 m) to more than 900 ft (274 m) in southeastern Kuwait, north of where the Rimthan Arch would later develop (Kadar et al. 2015; Crespo de Cabrera 2019, 2020) (text-fig. 7). It consists of many thin cycles of 4th-order and higher, organized into four 3rd-order sequences and a fifth that extends up into the Middle Marrat Member. The Rimthan Arch did not form until Middle Jurassic time (Kadar et al. 2015; Crespo de Cabrera 2019, 2020) and it is likely that this thickness pattern and sequence framework may be extended into northeastern Saudi Arabia.

The Lower Marrat Member overlies the Minjur Formation with apparent conformity. The deepest portion of the Lower Marrat has not been seen in core. The character of the gamma ray (GR) and neutron-density logs, however, closely resemble those of the stratigraphically higher, cored portions of the Lower Marrat and are assumed to represent similar lithofacies. Based on study of core and logs from the shallower portion of the member, four 3rd-order sequences are recognized, each with recognizable lowstand, transgressive, and highstand systems tracts. A fifth sequence begins in the Lower Marrat and extends into the Middle Marrat (text-fig. 5). The depositional settings and lithofacies of the systems tracts will be discussed in the sedimentology section of this paper.

The age of the Lower Marrat Member is interpreted as middle or late Sinemurian to earliest Toarcian. During core description, probable fragments of the aberrant pterioid bivalve *Lithiotis* sp. were found in two wells. *Lithiotis* has a known range of early Pliensbachian to middle Toarcian (Fraser et al. 2004) and is consistent with the age range for the Lower Marrat Member proposed herein.

Middle Marrat Member

The Middle Marrat Member varies in thickness from about 600 ft in northwest Kuwait (Mutriba Field) to about 850 ft in the southeast, adjacent to where the Rimthan Arch developed during the Middle and Upper Jurassic (Crespo de Cabrera et al. 2019, 2020). There is a notable thinning in the area of the Magwa Field, at the north end of the Burgan Arch, in an area where the Middle Marrat lacks evaporite facies, possibly due to exposure and removal by dissolution (text-fig. 8). In general, however, the parallel north-south orientation and uniform spac-

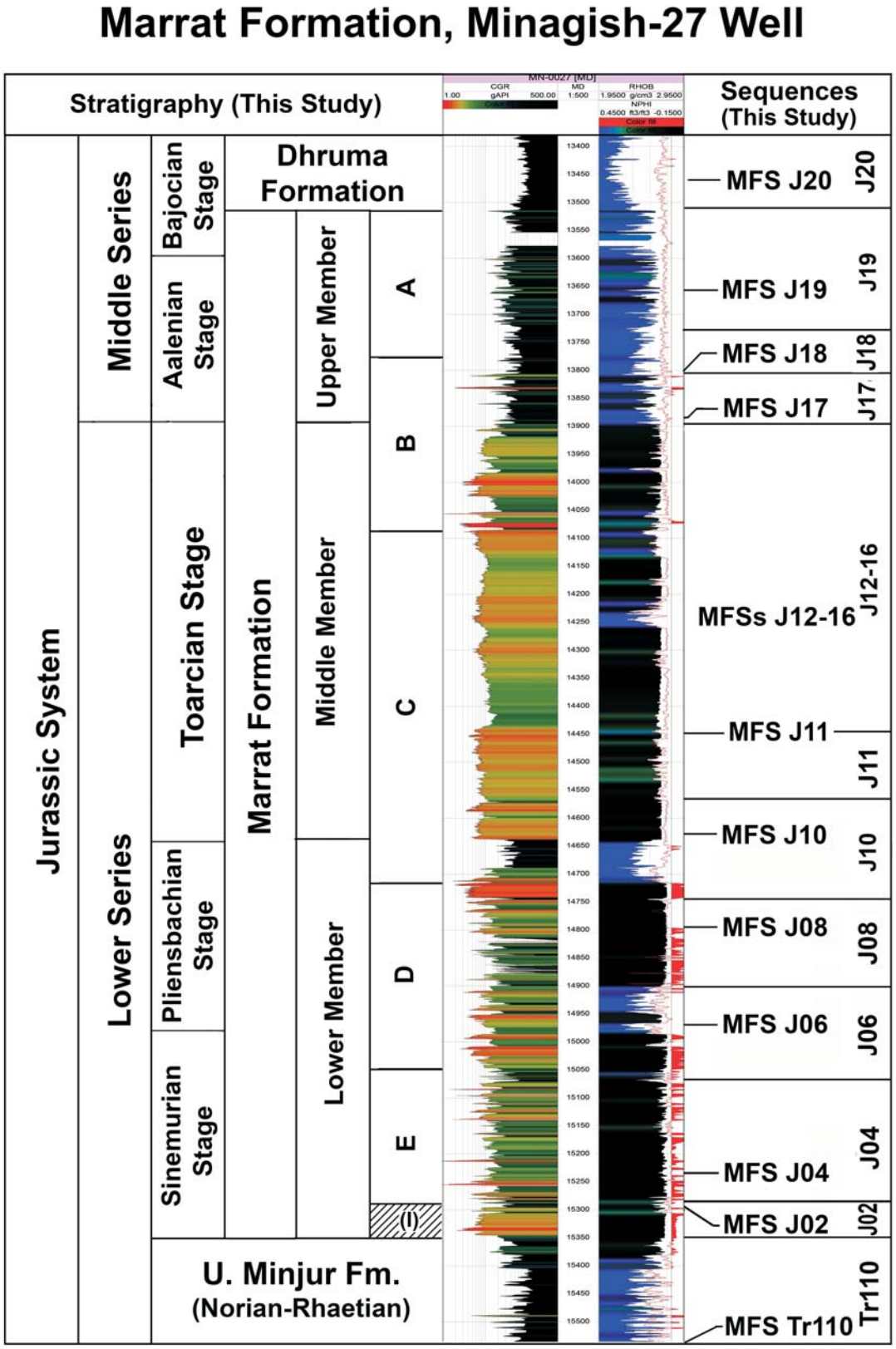

TEXT-FIGURE 5
Log display of the Marrat Formation in the Minagish-27 Well, comparing lithostratigraphic nomenclature of Yousif and Nouman (1977) and that used in this paper. On the right is shown the subdivision into 3rd-order sequences proposed in this paper. Sequences J12-J16 were deposited in the Toarcian intrashelf basin and correspond to sequences 2 to 6 of Neog et al. (2010) (modified after Kadar et al. (2015).

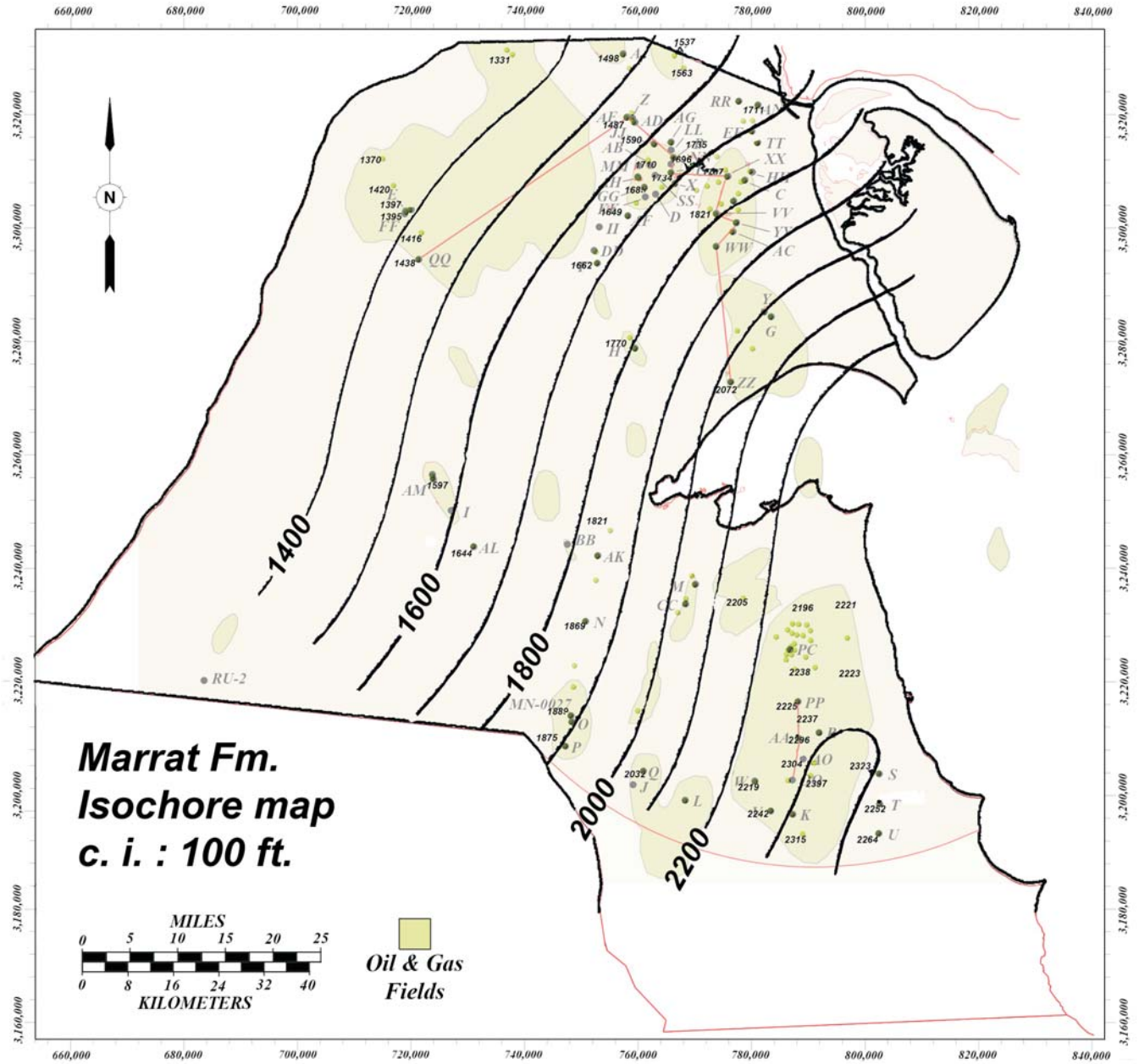

TEXT-FIGURE 6
Generalized isochore map of the Marrat Formation in onshore Kuwait. The map shows a gradual 50% increase in thickness eastward, with the maximum thickness occurring on the southern Burgan, just north of where the Rimthan Arch developed during the Middle Jurassic (Crespo de Cabrera et al. 2019, 2020).

ing of the contours suggests continuation into northeastern Saudi Arabia.

The Middle Member of the Marrat Formation is sedimentologically more diverse and complex than either the Lower or Upper Members. Although the Middle Marrat has not been further subdivided in Kuwait, four lithologically distinct stratal packages can be recognized. At the base of the member, a package of clean skeletal and peloidal lime mudstones, wackestones and mud-dominated packstones is present throughout Kuwait. This package is about 185 ft thick in the Mutriba Field and thins southeastward to about 140 ft Its upper surface is MFS J11. It is overlain by a depositional increment of strata which is approximately 240 ft thick in the northwest and thins abruptly to as little as 30 ft in the southeast. It consists of lime mudstones to grainstones, microbial boundstones, and anhydrite beds as well as reservoir-quality replacement dolostones. The superjacent sedimentary package averages about 80 ft thick in the northwest and thickens southeastward to 365-440 ft. It consists of thin cycles of lime mudstones to grainstones, cryptocrystalline dolostones and anhydrite in the northwest. In the southeast, it contains thick packages of argillaceous mudstones, wacke-

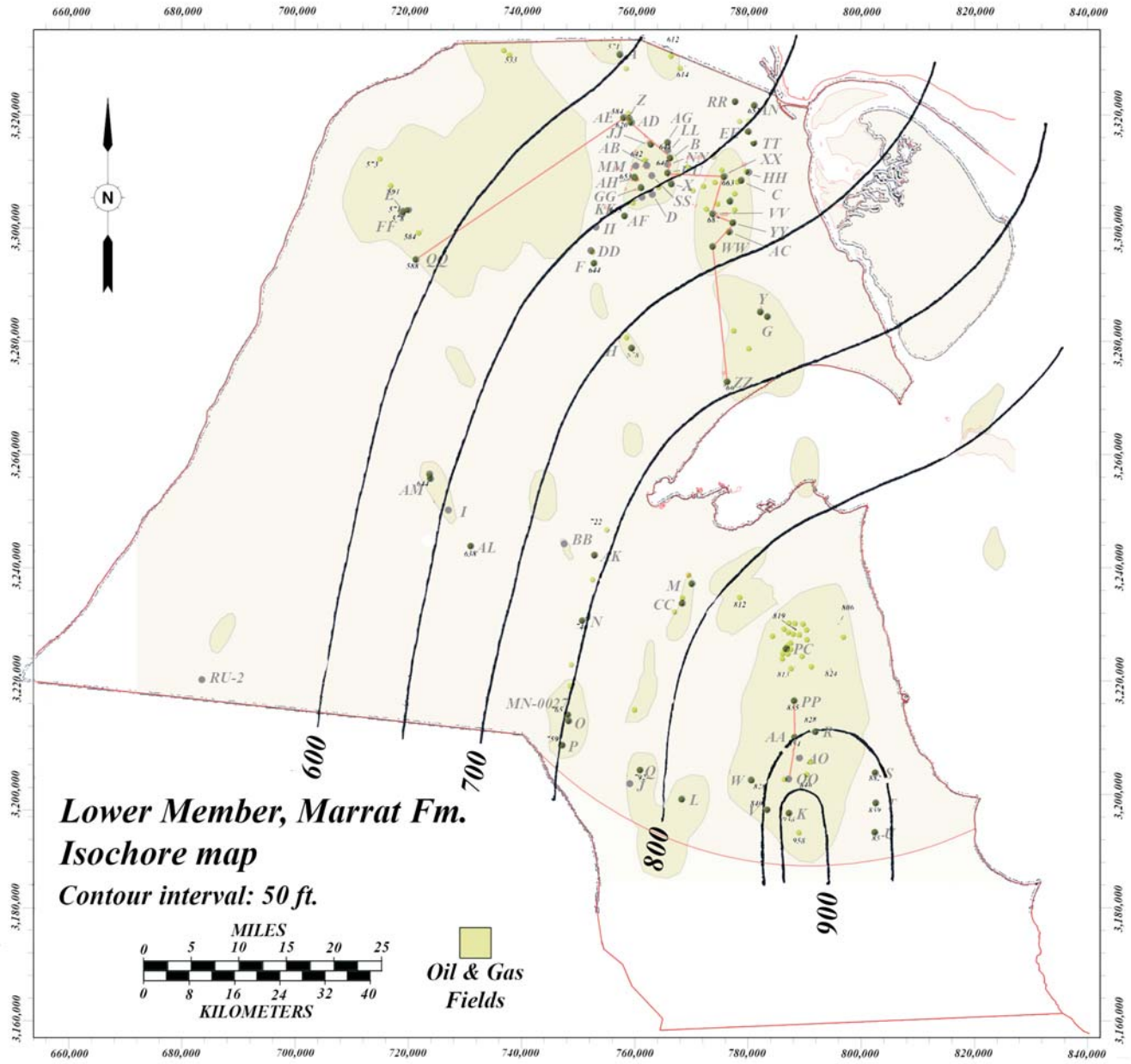

TEXT-FIGURE 7
Generalized isochore map of the Lower Member of the Marrat Formation. There is an approximately 50% increase in thickness toward the southeast, reaching a maximum on the southern Burgan Arch, just north of where the Rimthan Arch developed during the Middle Jurassic (Crespo de Cabrera et al. 2019, 2020).

stones and packstones but grainstones and anhydrite are occasionally observed. The uppermost package of strata in the Middle Marrat Member thickens gradually from about 130 ft in the northwest to 165 ft in the southeast and is comprised predominantly of mudstones and wackestones, occasional packstones and grainstones and only minor amounts of dolomite and anhydrite.

Much of the diversity of the Middle Marrat Member has been attributed to a large, rapid rise of sea level which resulted in drowning of the basal, open marine platform depositional settings, retreat of the platform margin, and formation of an intrashelf basin (Kendall and Schlager 1981; Al-Eidan et al. 2009; De Keyser and Kendall 2014) (text-fig. 5). As discussed by Kendall and Schlager (1981) drowning may occur if the rate of relative sea level rise exceeds the rate of carbonate production long enough for the depositional setting to be submerged below the euphotic zone. This may result from eustatic sea level rise, increased subsidence or some combination such that the relative rise exceeds the rate of sediment production and is greater than the depth of the euphotic zone. Published sedimentological and biostratigraphic data are too sparse outside of Kuwait to demonstrate the regional extent of the ISB at this time. During the remainder of Toarcian time, the platform margin redeveloped and

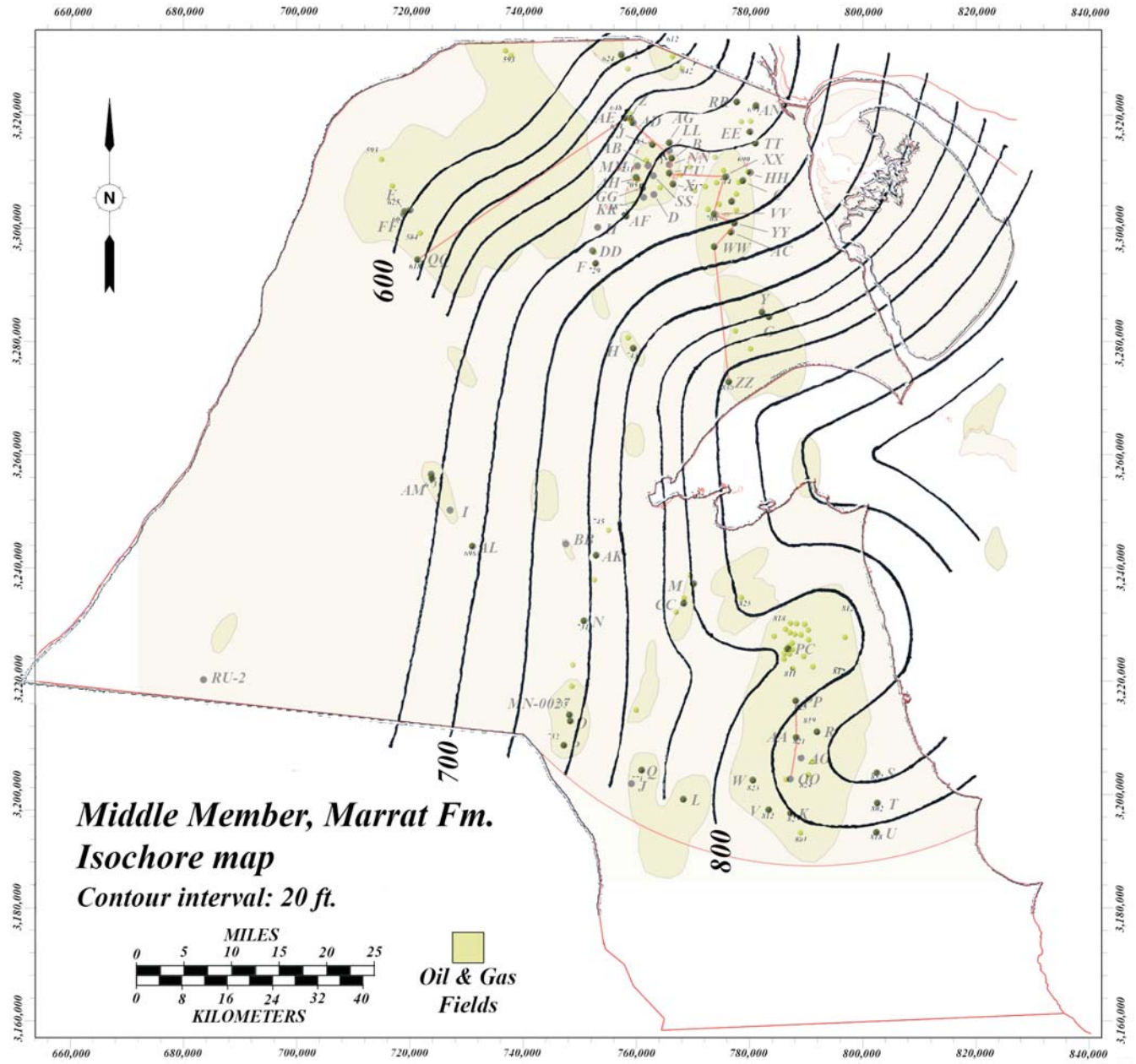

TEXT-FIGURE 8
Generalized isochore map of the Middle Member of the Marrat Formation. A general eastward thickening trend is visible but there is a prominent thinning in the area of Magwa Field, on the northern Burgan Arch, where evaporite deposits are missing from the Middle Marrat. The platform margin of the Middle Marrat ISB approximately falls between the 700 and 720 ft contours in north Kuwait.

prograded, infilling the intrashelf basin (De Keyser and Kendall 2014). Sedimentologic and biostratigraphic data presented in this paper support that interpretation and will be discussed further below.

In outcrop in Saudi Arabia, the Marrat Formation has been dated by ammonites as Toarcian (Arkell 1952; Enay et al. 1987). In Kuwait it has been extensively sampled for calcareous nannofossils but almost none have been recovered, probably due to non-preservation in these deeply buried, high temperature and pressure strata (Al-Moraikhi et al. 2014; Kadar 2015, pers. comm.). Palynomorphs and foraminifers provide most of the biostratigraphic data presented in this paper.

The depositional settings of the Middle Marrat have been described as a calciclastic shelf depositional model (Al-Eidan et al. 2009; Neog et al. 2010). Before extensive coring revealed the existence of a drowning unconformity (MFS J11) and deeper water lithofacies representative of an intrashelf basin (ISB) (De Keyser and Kendall 2014), the lithofacies of this

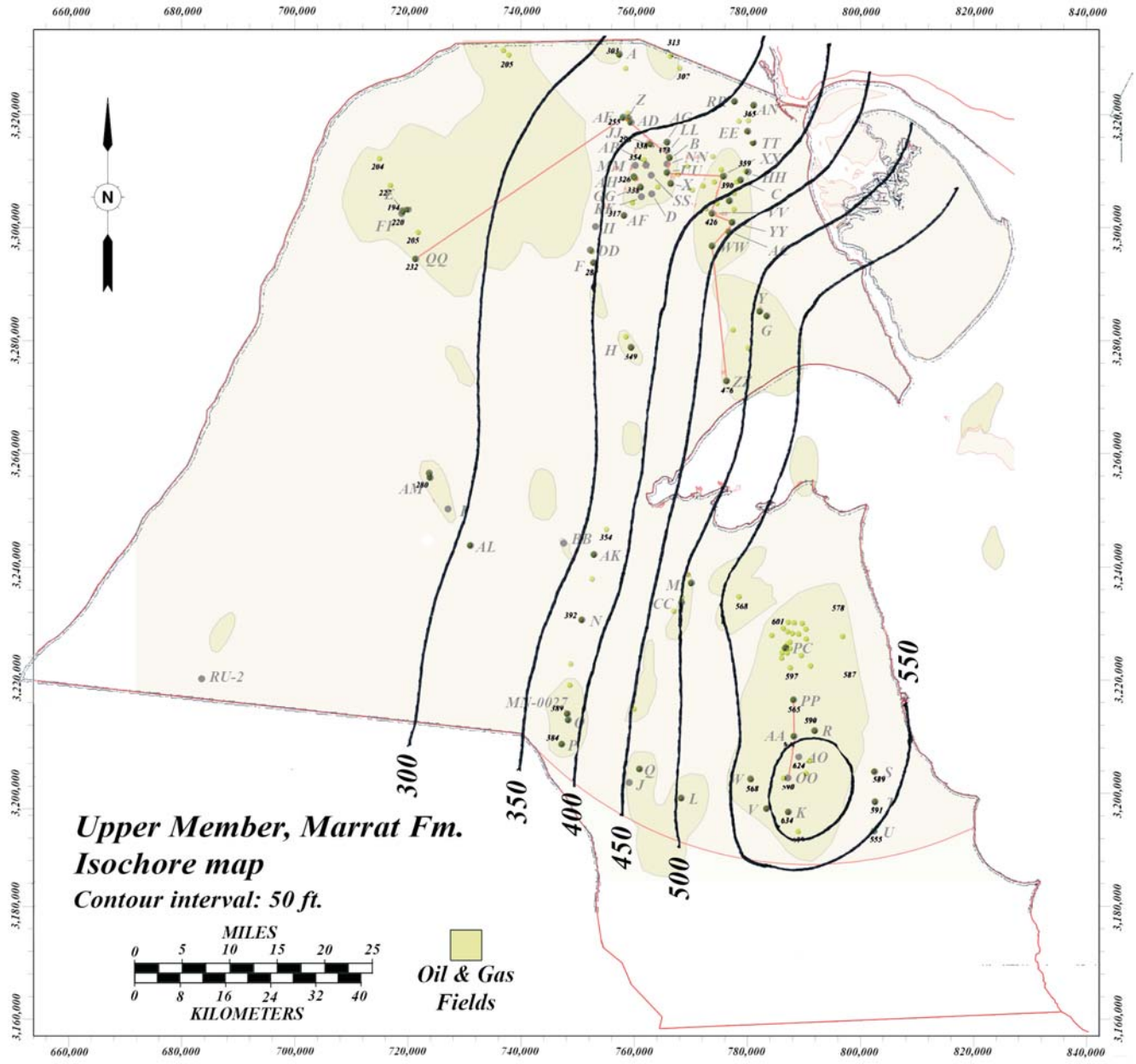

TEXT-FIGURE 9
Isochore map of the Upper Marrat Member of the Marrat Formation.

member were described within a ramp depositional model, divided into inner, middle, and outer ramp depositional settings. The lithofacies beneath the drowning unconformity consist of a succession of open marine platform lithofacies with echinoderms, gastropods, bivalves and foraminifers that suggests shallowing downward.

The large, rapid relative sea level rise (MFS J11) that marks the beginning of the Toarcian ISB caused the platform drowning and the regressive retreat of the platform margin. The platform margin at that time would initially have lacked a clearly defined barrier system separating platform from shelf and basin. Lowstands during subsequent high-frequency cycles shed packages of lime mudstone turbidites that downlapped onto the sediment-starved basin floor above the drowning unconformity. The platform margin quickly steepened and developed into the rimmed platform geometry described in the calciclastic shelf depositional model (Al-Eidan et al. 2009, Neog et al. 2010). Late highstands associated with the calciclastic shelf geometry were marked by an evaporitic lagoon which produced the dense, dolomitizing reflux brines which moved downward into the shelf mudstones and wackestones that became the prolific Middle Marrat dolomite reservoirs of north Kuwait (Neog et al. 2010).

Upper Marrat Member

The Upper Member of the Marrat Formation was informally recognized in Kuwait until formalized by Kadar et al. (2015). Yousif and Nouman (1997) divided the Marrat Formation into units A to

E, with the Upper Marrat being equivalent to unit A and the upper portion of Unit B. On electrical logs, the top of the Marrat Formation in Kuwait is placed where the interbedded calcareous shale, limestone, dolomite, and anhydrite beds of the Upper Marrat Member, are replaced by basinal shales with high API gamma-ray counts of the overlying Dhruma Formation. The contact appears to be conformable but has not been seen in core. In the outcrop belt along the eastern margin of the Arabian Shield, the Toarcian Marrat Formation (= Middle Marrat of Kuwait) is separated from the Bajocian Dhruma Formation by a Toarcian-Aalenian unconformity (Le Nindre et al. 1990; Sharland et al. 2001; Al-Mojel et al. 2018).

The Upper Marrat is less than 300 ft thick in northwest Kuwait but thickens eastward to more than 550 ft in southeastern Kuwait (text-fig. 9). As in the Lower and Middle Marrat members, there is a slight thickening southward and the overall pattern suggests continuation southward into northeastern Saudi Arabia. The formation is comprised of thin cycles of argillaceous mudstones, wackestones, dolostones, nodular anhydrite, and uncommon grain-supported beds that are interpreted to have been deposited in a ramp-like setting with very gentle eastward dips. The lithofacies are representative of sabkha, tidal flats, and lagoonal depositional settings. These probably represent a lowstand wedge deposited on the submerged and tilted platform of the Middle Marrat and appear to pre-date development of the Middle and Upper Jurassic Gotnia Basin.

MATERIAL AND METHODS

Detailed sedimentological core descriptions and biostratigraphic studies of the Late Triassic to Middle Jurassic wells have produced a large and valuable data set for stratigraphic analysis of this interval. Following earlier studies (Kadar et al. 2015; Crespo de Cabrera et al. 2019, 2020) that mainly focused on Middle to Late Jurassic nannofossils and planktonic foraminifera (Dhruma to Jubaila interval) and sequence stratigraphy of Kuwait and Saudi Arabia, this study compiles the benthonic foraminiferal, palynological associations and uncommon, low-resolution strontium isotopes data of the Upper Triassic to Middle Jurassic Minjur and Marrat formations. It also presents a revised and expanded Jurassic chrono- and sequence stratigraphy of Kuwait and adjacent areas and correlates it to the Jurassic Arabian Plate maximum flooding surfaces and sequence boundaries (Sharland et al. 2001, 2004; Davies and Simmons 2018; Horbury 2018; Lunn et al. 2019; Lunn 2020).

Biostratigraphy

Taxa range charts and biostratigraphic summaries from unpublished proprietary reports are the basis for the biostratigraphic framework here presented. Approximately 1375 samples from 33 wells (text-fig. 10) were biostratigraphically analyzed (Robertson Research 2000, 2004; Fugro-Robertson 2009; Packer et al. 2015, 2018, 2019), most of these, approximately 50 % were collected from the Middle Marrat Member, the most extensively cored interval. The micropaleontological study was carried out in petrographic thin sections, with approximately 580 samples studied to document benthonic foraminifera and other organisms such as bivalve fragments, echinoderm plates and spines, microgastropods, juvenile ammonites and sponge spicules.

For palynology, approximately 790 samples were processed to characterize the succession, recording scarce dinocysts and sporomorphs, as well as diverse palynodebris. Samples were macerated and treated with HCl, HF and HNO3 to disaggregate and extract the organic matter from the rock material. These were sieved and washed before preparing smear slides for each sample. Quantitative and semi-quantitative data are shown in summaries, as well as in taxa range charts used for palynostratigraphic and paleoenvironmental interpretations. Many smear slides for calcareous nannofossils were analyzed, both within Kuwait Oil Company and outsource, using a polarized light DM 4500P Digital Leica microscope at 1000x magnification. In the Triassic section the samples were barren of nannofossils, with generally poor results in the Marrat Formation.

Strontium Isotopes

The low-resolution of the resultant biostratigraphic framework was complemented with $^{87}Sr/^{86}Sr$ isotope ratios. Fugro-Robertson (2009), using standard processing techniques (sample grounding, washing, wet chemistry, ion exchange chromatography and thermal ionization mass spectrometry) analyzed 15 samples from four wells. NBS 987 and HMC standards were also measured with the samples to monitor mass spectrometer performance.

In assigning age dates the best-fit value of the sea water Sr calibration data was used. Most samples yielded mixed results regarding definitive chronostratigraphic dates, which is most probably due to diagenetic alterations. Nonetheless, data from two of these wells, (TT and X) compatible with biostratigraphic and/or stratigraphic position were integrated to increase the Lower Jurassic stratigraphic resolution. The timescale used in this study (Fugro-Robertson 2009) was Gradstein et al. (2004).

Sedimentology

Detailed description and sedimentological study of more than 16,000 feet of core from more than 100 wells has allowed identification of lithofacies, depositional environments and sequence stratigraphy of the Marrat Formation. Slabbed cores were etched in HCl acid to remove surface effects of slabbing before being described under a binocular microscope. Many dolomite and anhydrite core slabs were selectively polished and lightly acid etched. Selected core segments were digitally scanned at resolutions from 300 to 1200 dots/inch (dpi). Mosaics of scanned digital images of many core segments were assembled into mosaics to document important features and cycles. High-resolution photomicrographs of the core slabs were acquired while viewed under the binocular microscope. Approximately 6,500 scanned images, 500 photomosaics and 300 photomicrographs were included in the study.

Petrophysics

The Middle Member of the Marrat Formation is typically free of argillaceous material and the gamma ray (GR) curve has very low API values. Recognition of cyclicity and correlation between wells may be difficult or impossible. Many geologists have displayed Marrat GR logs on very short linear scales, e.g., 0–10 to 0–30 to overcome this problem. This helps distinguish bed and cycle sets in the clean carbonates but results in the stratigraphically significant thin argillaceous units being off-scale. Two techniques have helped to overcome this problem. First, we have displayed GR on a logarithmic rather than a linear scale, 1–120 for example. This has the advantage of expanding the display at very low values to emphasize cyclicity while still allowing display of argillaceous rock units (De Keyser et al. 2020). In the Upper Jurassic, where source rocks of

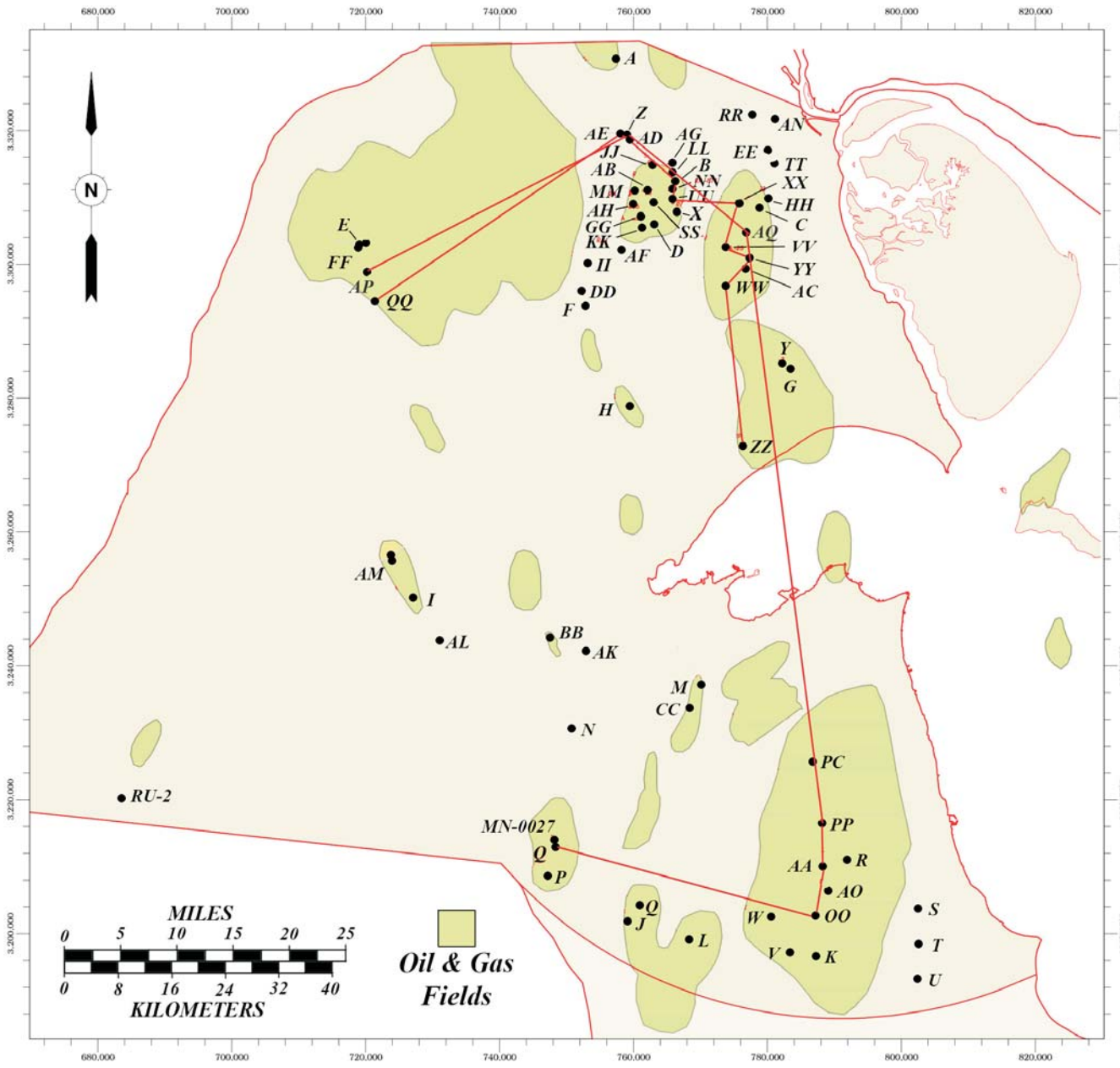

TEXT-FIGURE 10
Map of onshore Kuwait, showing oil and gas fields, wells and cross-sections discussed in this paper. Well abbreviations are the same as were used in Kadar et al. (2015) and Crespo de Cabrera et al. (2019, 2020).

the Najmah Formation have very large API values, clean carbonates can be shown with source rocks at scales up to 1-500 or more while still recognizing cyclicity.

Second, the GR curve is color-filled to distinguish between "clean," grain-supported and massive evaporitic lithofacies and increasingly argillaceous units such as mudstones and shales. A spectral color scheme is used, with "hot" colors (red, orange and yellow) for the clean, low-GR units (high-energy grainstones and pure anhydrites) and "cool" colors (green, blue and black) for progressively shalier lithofacies. To maximize the effect of the methodology, the curves are normalized so that all grainstones are a uniform red or yellow. In the Marrat, bulk shifts were found to be simple and effective. Where employed in siliciclastics, statistical methods were found to be more reliable. The displays are calibrated to core descriptions and the range of colors can be interactively adjusted or "tuned" to approximately match the percentages of grainstones and shales (De Keyser et al. 2020). Color fills are also utilized for the neutron and density logs. In particular, the density log curve is color-filled red above a density of 2.8 g/cm^3 to highlight anhydrite occurrences.

The data presented in this paper allow us to determine the age and depositional environments of the Upper Triassic to Middle Juras-

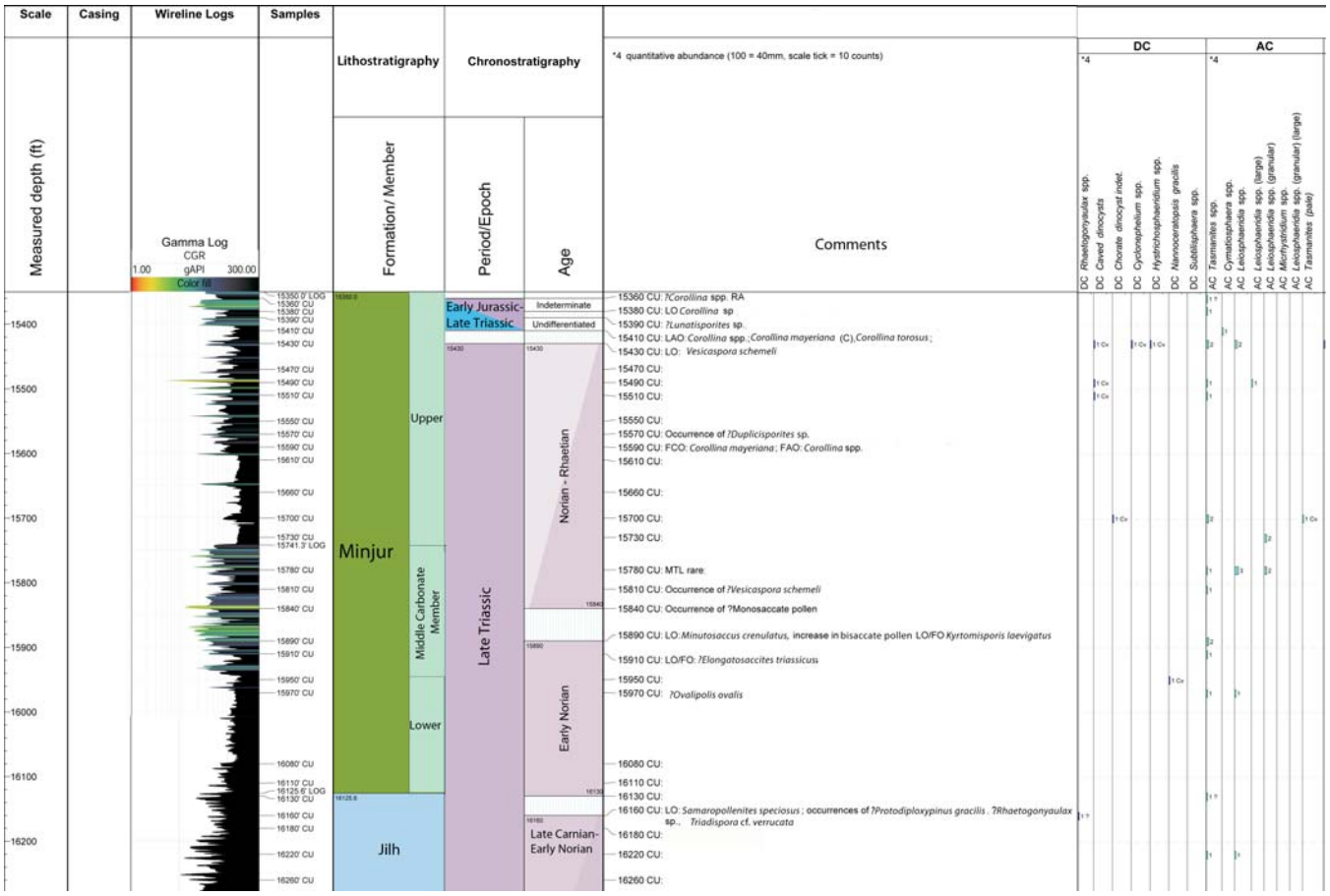

TEXT-FIGURE 11, Part 1
Biostratigraphy, lithostratigraphy and palynomorph distribution in the MN-0027 Well, Minagish Field, onshore Kuwait. Explanation: Cv = interpreted as caved; Rw = interpreted as reworked; Cu = cuttings sample; Co = core sample; DC: Dinoflagellate cysts; AC: Acritarchs; FT: Microforaminiferal test linings; SP: Spores and Pollen. Adapted from Packer et al. (2018).

sic stratigraphic units in onshore Kuwait, and to correlate them to other formations in the region. This new chronostratigraphic scheme differs from that published by Yousif and Nouman (1997) who designated a type section for Kuwait's Jurassic formations in the Minagish-27 Well. Improved bio- and sequence stratigraphy allow more detailed interpretation of the relationships between relative sea level, subsidence and sediment supply as well as their perturbation by tectonism. The paper concludes with a summary of the interpreted depotectonic history of the Kuwait region during the Late Triassic and Early Jurassic.

BIOSTRATIGRAPHY

Biostratigraphic data are sparse in the Triassic Minjur and Lower and Middle Jurassic Marrat formations. Proprietary unpublished data are the main source for age determinations which most frequently are based on microfossils, since the greatest sampling density and well coverage have been placed on this discipline. Palynofloral recovery is generally poor, though occasionally abundant in the Minjur and in the Upper Marrat unit. The scarcity of age-diagnostic palynomorphs and paucity of flora does not provide sufficient information for the establishment of a workable biozonation scheme in the Marrat Formation, though in the Minjur a low-resolution chronological framework is proposed. Nannofloral data are extremely sparse and mainly non-age diagnostic.

In the Minjur Formation of Kuwait only a few biostratigraphic studies are available (Robertson Research 2000) generally using a low-density sampling scheme. Recently however, microfossil and palynological studies have been completed in cores and cutting samples. The most conclusive results were obtained through palynology since shallow water depositional environments and/or diagenetic processes prevented benthic assemblages from proliferating or from being identified (Packer et al. 2018, 2019). In the Marrat Formation however, microfossils and in particular foraminifera, have played a significant role for the determination of a biostratigraphic framework (Fugro-Robertson 2009; Robertson Research 2004; Packer et al. 2015).

MINJUR FORMATION

The age of the Minjur Formation has been debated since Robertson Research (2000) biostratigraphically characterized the Precambrian to Triassic interval in onshore Kuwait. It was a ground-breaking regional study which included twenty wells and 496 palynology samples. Only a small percentage of sam-

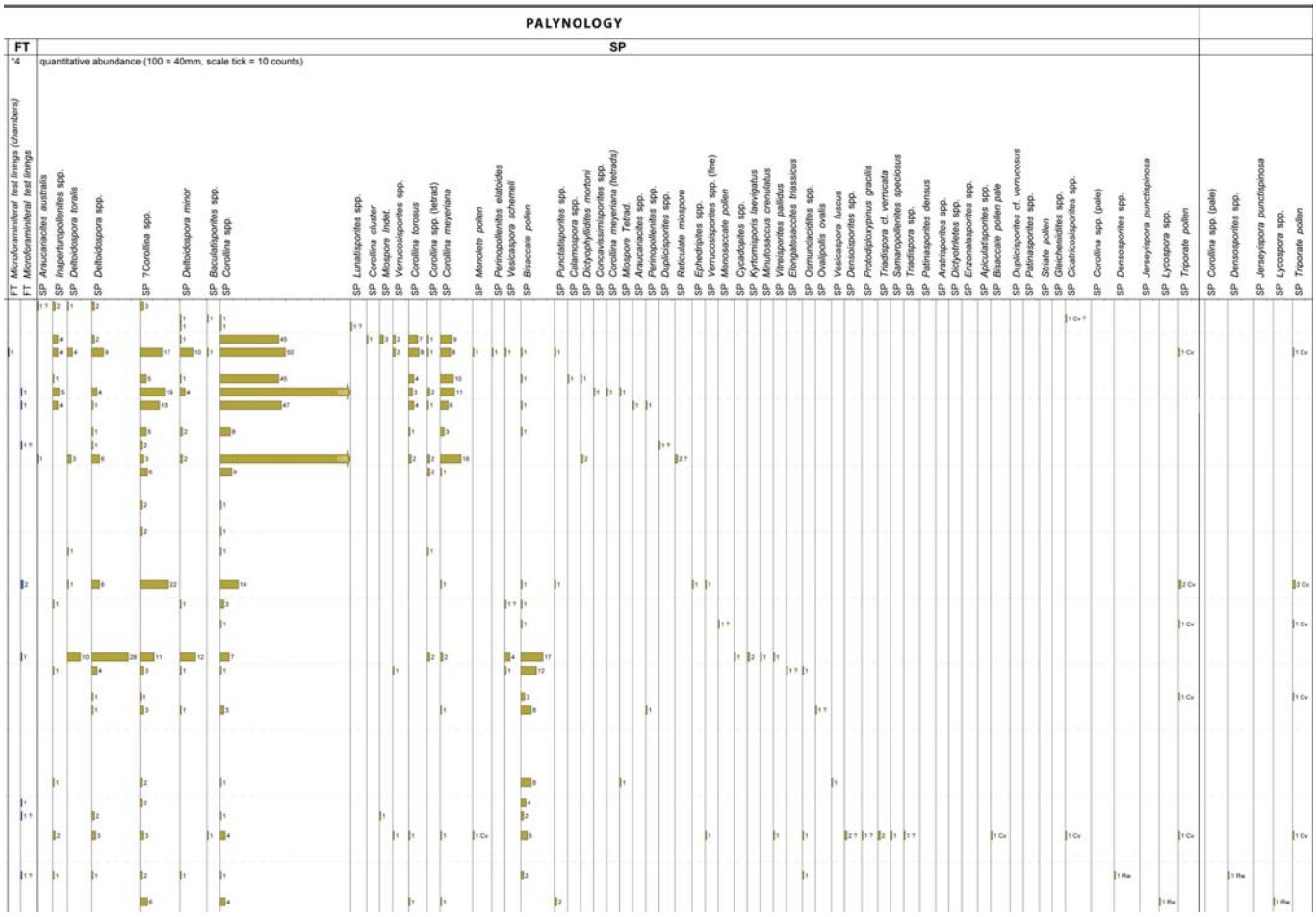

TEXT-FIGURE 11, Part 2
Continued.

ples (approximately 20 %) though, was collected from the Minjur Formation, especially from the Burgan Field, resulting in a low-density sampling interval of approximately 100 ft. That study placed the Triassic/Jurassic boundary within the Middle Minjur.

More recently Kuwait Oil Company (KOC) carried out a multidisciplinary regional study to assess leads and plays within the Triassic. A systematic, higher resolution biostratigraphic study of 497 palynology samples from ten wells was included (Packer et al. 2018, 2019), with 102 samples collected from the Minjur Formation. Sample spacing averaged approximately 22 ft, in some wells reaching as little as 2 ft, depending on the availability and type of samples. Palynomorph recovery in the Minjur Formation is moderate to good, with rare dinocysts, leiospheres, tasmanitids and localized influxes of microforaminiferal test linings. The resultant biostratigraphic framework, with some exceptions, generally confirms earlier Robertson Research's results (2000) for the Jilh and Sudair formations (out of the scope of the present work), but places the Triassic/Jurassic boundary near the top of the Upper Member of the Minjur Formation. The earlier age interpretation of Early Jurassic for the upper Middle and Upper Member of the Minjur was based on the assumption that the Triassic bioevents found within the Upper Minjur are reworked (Robertson Research 2000). The latest studies (Packer et al. 2018, 2019) document a similar assemblage to the one observed by Robertson Research (2000). It is characterized by long-ranging palynomorphs, none of which show a first stratigraphic occurrence (FO) constrained to the Jurassic, co-occurring with Triassic markers. In this regard an analysis of these bioevents is carried out specifying the lithostratigraphic level where these are observed.

Bioevents

Classopollis classoides Pflüg 1953

The generic name *Classopollis* has recently been used to replace *Corollina* and *Circulina* which are commonly used for the same fossil pollen forms (Traverse 2004, 2008). In the study area, the *Classopollis/Corollina* Zone (Robertson Research 2000), described the interval characterized by common to abundant *Classopollis classoides* and *Corollina meyeriana*. The assemblage constitutes long ranging species such as *Dictyophyllidites harrisii, Corrollina meyeriana, C. torosus* and *Kyrtomisporis laevigatus.*

C. classoides was originally described by Pflüg (1953) in the Liassic of Germany and has been recorded from the Norian to

Rhaetian and younger sediments of Europe, Australia, the Americas, Madagascar and India (Goubin 1965; Helby et al. 1987; Tripathi and Ram-Awatar 2006; Cirilli 2010). The increase in abundance of this taxon is the basis to suggest a Hettangian age for the *Classopollis/Corollina* Zone (Robertson Research 2000). However, it has been recorded in great abundance in Norian as well as in Rhaetian sediments (Yaroshenko and Imam 1995; Schneebeli-Hermann et al. 2017). In the Minjur Member of Kuwait (Robertson Research 2000) it occurs in wells OO (Upper Minjur: 13140 ft, 13270 ft); PP (Upper Minjur: 13240 ft, 13340 ft, 13390 ft); AA (Upper Minjur: 13340 ft); AD (Upper Minjur: 15950 ft, 16050 ft, 16200 ft); Q (Upper Minjur: 14310 ft, 14400 ft).

Packer et al. (2018, 2019) shows records of rare/common to abundant *Corollina,* (species such as *meyeriana, torosus*) in the Upper Minjur of Q, AQ, Z, AS, EF and MN-0027.

Elongatosaccites triassicus Cameron 1974

This taxon, together with *Kyrtomisporis corrugatus,* was first described by Cameron (1974) in the Upper Triassic of the Minjur Formation in Saudi Arabia and Iraq. It has also been observed in the Norian-Rhaetian of Syria (Yaroshenko and Imam 1995) where a great abundance of forms such as *Classopollis*/*Corollina* and *Vesicaspora schemeli* resemble the Norian-Rhaetian and Rhaetian deposits of England (Fisher 1972; Warrington 1978), Germany (Brenner 1986), and Austria (Morbey 1975); Norian-Rhaetian deposits of northeastern Spain (Baudelot and Taugourdeau-Lanti 1986). This association was dated as Late Norian (Yaroshenko and Imam 1995) on the grounds of the absence, among others, of *Rhaetipollis germanicus*. However, the occurrence of the dinoflagellate *Rhaetogonyaulax rhaetica* typical of the Syrian Assemblage VII, could suggest a Rhaetian age (Helby et al. 1987; Riding et al. 2010; Schneebeli-Hermann et al. 2017). This bioevent is observed in the following wells:

AO (Lower Minjur: 13634 ft, 13652 ft, 13690 ft, 13707 ft and 13709 ft); MN-0027 (Middle Minjur: 15919 ft); OO (Lower Minjur: 13670-13970 ft; Jilh: 14050 ft, 14120 ft, 14200 ft).

Kyrtomisporis corrugatus Cameron 1974

Described by Cameron (1974) in the Arabian Peninsula as a Late Triassic taxon, it occurs with forms such as *K. laevigatus*, *Elongatosaccites triassicus, Classopollis*/*Corollina* and *Vesicaspora schemeli.* It has been dated as Late Norian though its occurrence with *Rhaetogonyaulax rhaetica* in Syria (Yaroshenko and Imam 1995) would suggest it ranges up into the Rhaetian. It is also part of the Late Norian – Rhaetian assemblage of the Well 628-5 (Issautier et al. 2019) in Saudi Arabia, where it is also found with *R. rhaetica*. In Kuwait this bioevent has been observed in wells:

AA (Middle Minjur: 13628 ft, 13657.5 ft); AO (Upper Minjur: 13404 ft, 13409 ft; Lower Minjur: 13825 ft, 13850 ft); AS (Upper Minjur: 17070 ft); MN-0027 (Middle Minjur: 15750 ft); OO (Upper Minjur: 13420 ft; Lower Minjur: 14500 ft); Z (Middle Minjur:16245 ft)

***Lunatisporites* spp.** Leschik 1955 emend. Scheuring 1970

This genus is considered Triassic or older in age (Helby et al. 1987; Cirilli 2010; Sha et al. 2011, 2015; Kustatscher et al. 2018); In the Minjur Formation several species of this genus (*L. acutus, L. noviaulensis*) are observed. In the Minjur Upper Member however, it is recorded only to a generic level (Packer et al. 2018, 2019). This bioevent occurs in wells:

AA (Middle Minjur: 13678 ft); AO (Upper Minjur: 13286 ft); AQ (Upper Minjur: 16420 ft; Lower Minjur: 16660 ft); AS (Upper Minjur: 16980 ft; Jilh: 18753 ft, 18763 ft, 18935 ft, 18955.7 ft, 18982 ft); MN-0027 (Upper Minjur: 15390 ft); OO (Jilh:14000 ft).

Minutosaccus crenulatus Dolby 1976

This species was originally described by Dolby and Balme (1976) and was assigned a Carnian-?Norian age. Brenner (1992) showed an age range for this bioevent from Carnian to Rhaetian based on previous work by Dolby and Balme (1976) and Helby et al. (1987). He nonetheless assigned a Carnian and Norian age to samples from different sites of South Western Australia where *M. crenulatus* co-occurred with the dinoflagellates *Heibergella balmei* and *Shublikodinium wigginsii*. *M. crenulatus* has previously been recorded from the mid Carnian - Early Norian of the Alpine realm (Brugman 1983) and from Carnian-Norian carbonates and evaporitic deposits of Syria (Yaroshenko and Imam 1995).

In the study area (Packer et. al 2018, 2019) this bioevent occurs in wells:

AA (Middle Minjur: 13628 ft, 13652 ft); AO (Middle Minjur: 13487 ft; Lower Minjur: 13614 ft, 13622 ft); MN-0027 (Middle Minjur: 15890 ft; Jilh 16350 ft); Q (Middle Minjur: 14840 ft; Lower Minjur: 14930 ft; Jilh: 15440 ft).

Rhaetogonyaulax Sarjeant 1966

Helby et al. (1987) described the *Shublikodinium* Superzone in the Bonaparte Basin and assigned it a Middle Triassic to Pliensbachian age. It was later named *Rhaetogonyaulax* Superzone, since Stover and Evitt (1978) and Lentin and Williams (1989) considered *Shublikodinium* a junior synonym of *Rhaetogonyaulax*. In the Middle Triassic to Early Jurassic the marked provincialism of dinoflagellates cysts and microflora in general resulted in the absence from Europe of five out of the twelve dinoflagellates cysts illustrated by Helby et al. (1987) in the *Rhaetogonyaulax* Superzone. The six taxa known from Europe are: *Beaumontella langii*, *Dapcodinium priscus*, *Heibergella*? *kendelbachia*, *Rhaetogonyaulax rhaetica*, *Suessia swabiana* and *Sverdrupiella* spp. Australasian–European provincialism is accentuated by the presence of low diversity assemblages of undescribed dinoflagellate cysts in the latest Carnian-Sinemurian interval (Helby et al. 1987a; Riding et al. 2010). The Triassic dinoflagellate cyst record in Europe is confined to the Rhaetian, where the flora is dominated by the cosmopolitan species *Rhaetogonyaulax rhaetica* (Orbell 1973; Riding et al. 2010; Cirilli 2010). Despite the marked provincialism the FO of this bioevent in both areas, Australia and Europe, seems to be synchronous.

In the study area *Rhaetogonyaulax* spp. is observed (Packer et al. 2018, 2019) in wells:

AO (Upper Minjur: 13409 ft; Middle Minjur: 13420 ft, 13482 ft, 13489 ft; Lower Minjur: 13614 ft); MN-0027 (Upper Minjur: 15390 ft; Jilh: 16160 ft).

Samaropollenites speciosus Goubin 1965

This bioevent was described by Goubin (1965) in Madagascar as a Middle to Late Triassic taxon. It has been used as a

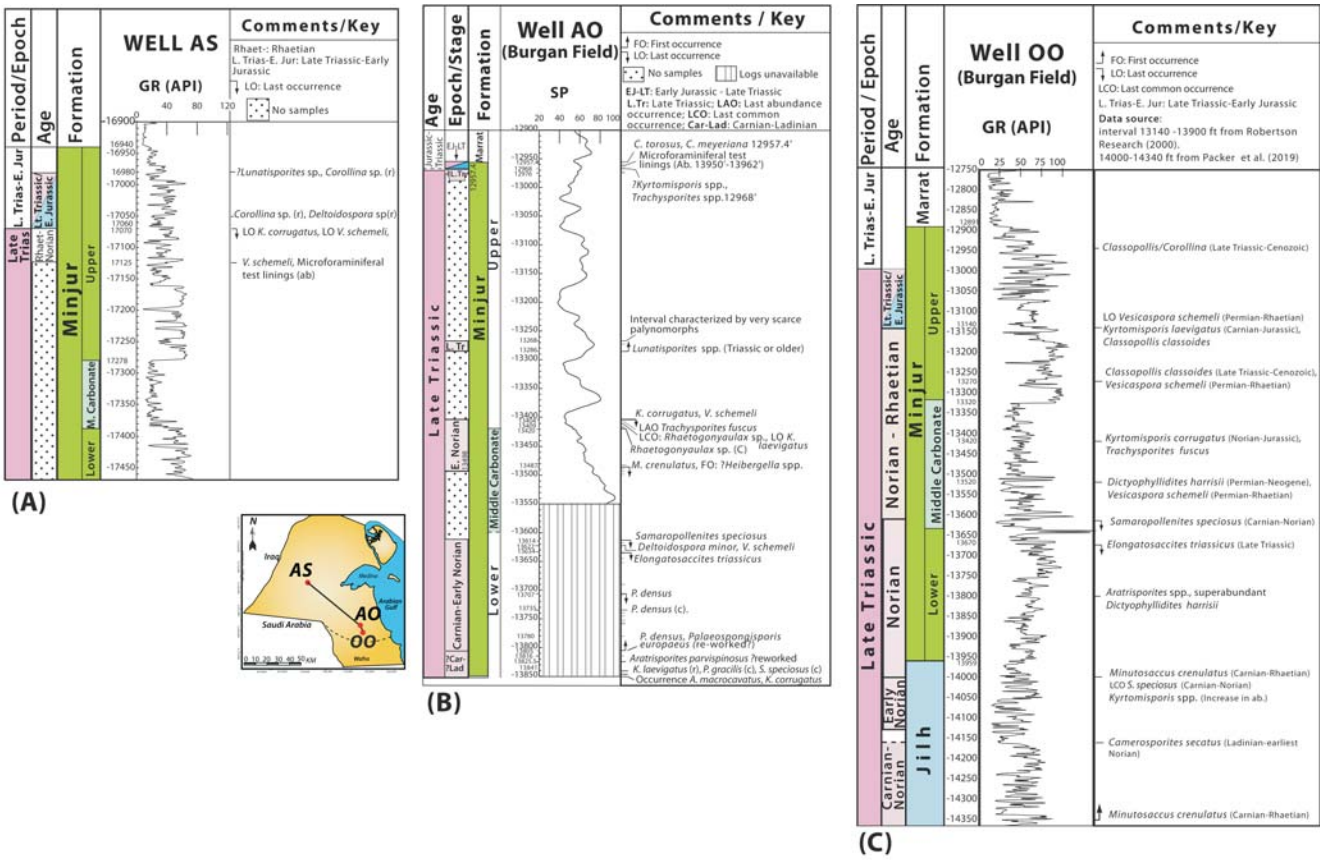

TEXT-FIGURE 12
Biostratigraphic summaries of the Minjur Formation in wells AO and OO in the Burgan Field and Well AS, located to the north in the Kra Al Maru Field. Biostratigraphic data for wells AS and AO from Packer et al. 2018, 2019 and for Well OO from Robertson Research (2000).

Carnian-Norian marker (Cirilli 2010) although Brugman (1983) assigned a Late Ladinian-Norian age. Yaroshenko and Iman (1995) observed this taxon in the Carnian-Norian of Syria, whereas in Western Australia Helby et al. (1987) used it to designate the Carnian. In the study area this bioevent is observed in wells:

AA (Middle Minjur: 13642 ft, 13672 ft, 13683 ft); AS (Jilh: 18753 ft, 18757 ft); AO (Lower Minjur: 13614 ft, 13841 ft); EF (Jilh: 18832 ft, 18914 ft, 18943 ft); OO (Middle Minjur: 13657.5 ft, 14540 ft'); MN-0027 (Jilh: 16160 ft); Z (16200 ft, 16325 ft, 16445 ft, 17310 ft); Q (Lower Minjur: 14760 ft; Jilh: 16020 ft, 16040 ft).

Vesicaspora schemeli Klaus 1963

This bioevent was originally described from the Permian of the Southern Alps (Klaus 1963). In Saudi Arabia, Hemer (1965) recognized similar monosaccate pollen grains to *V. schemeli.* Subsequently, Cameron (1974) extended its stratigraphic range up into the Late Triassic of the Arabian Peninsula, though he did not provide distribution range charts, nor specify the range within the Late Triassic. Robertson Research (2000) described a *Vesicaspora schemeli* Zone and assigned a Norian to Early Rhaetian age, whereas Loutfi and Sattar (1987) in the United Arab Emirates constrained this zone to the Rhaetian. This bioevent has been observed in wells:

AA (Middle Minjur: 13628 ft, 13638 ft, 13683 ft, 13687 ft); AO (Upper Minjur: 13404 ft, Lower Minjur: 13622 ft, 13759 ft); AS (Upper Minjur: 17070 ft); MN-0027 (Upper Minjur: 15430 ft; Middle Minjur: 15810 ft); OO (Upper Minjur: 13140 ft, 13270 ft; Lower Minjur: 13520 ft, 13759 ft; Jilh: 14000 ft, 14690 ft): Q (Middle Minjur: 14750 ft, 14760 ft); Z (Middle Minjur: 16245 ft; Jilh: 16590 ft).

DISCUSSION

Age determination of the Minjur Formation has been a difficult endeavor due to the paucity of biostratigraphic publications in the region. The unpublished palynological data from Robertson Research (2000) show a series of Triassic or older bioevents in the Upper Minjur Member, which these authors interpreted as a reworked assemblage. Consequently, after Robertson Research interpreted an Early Jurassic age for the Upper Minjur, several regional studies (Kadar et al. 2015; Davies and Simmons 2018; Issautier et al. 2019; Lunn et al. 2019) continued to assign an Early Jurassic age to the Upper Minjur of Kuwait. Al-Moraikhi et al. (2014) however, reported a Triassic age for the Minjur Formation based on palynological analysis, though no biostratigraphic data were presented. Establishing the precise stratigraphic range is difficult as most of the well-defined markers from the recognised palyno-zonation schemes are only occasionally recorded (Douban et al. 2001; Packer et al. 2019). A display of the predominant assemblage from the higher resolution latest work (Packer et al. 2018, 2019) however, shows that the absence of bioevents

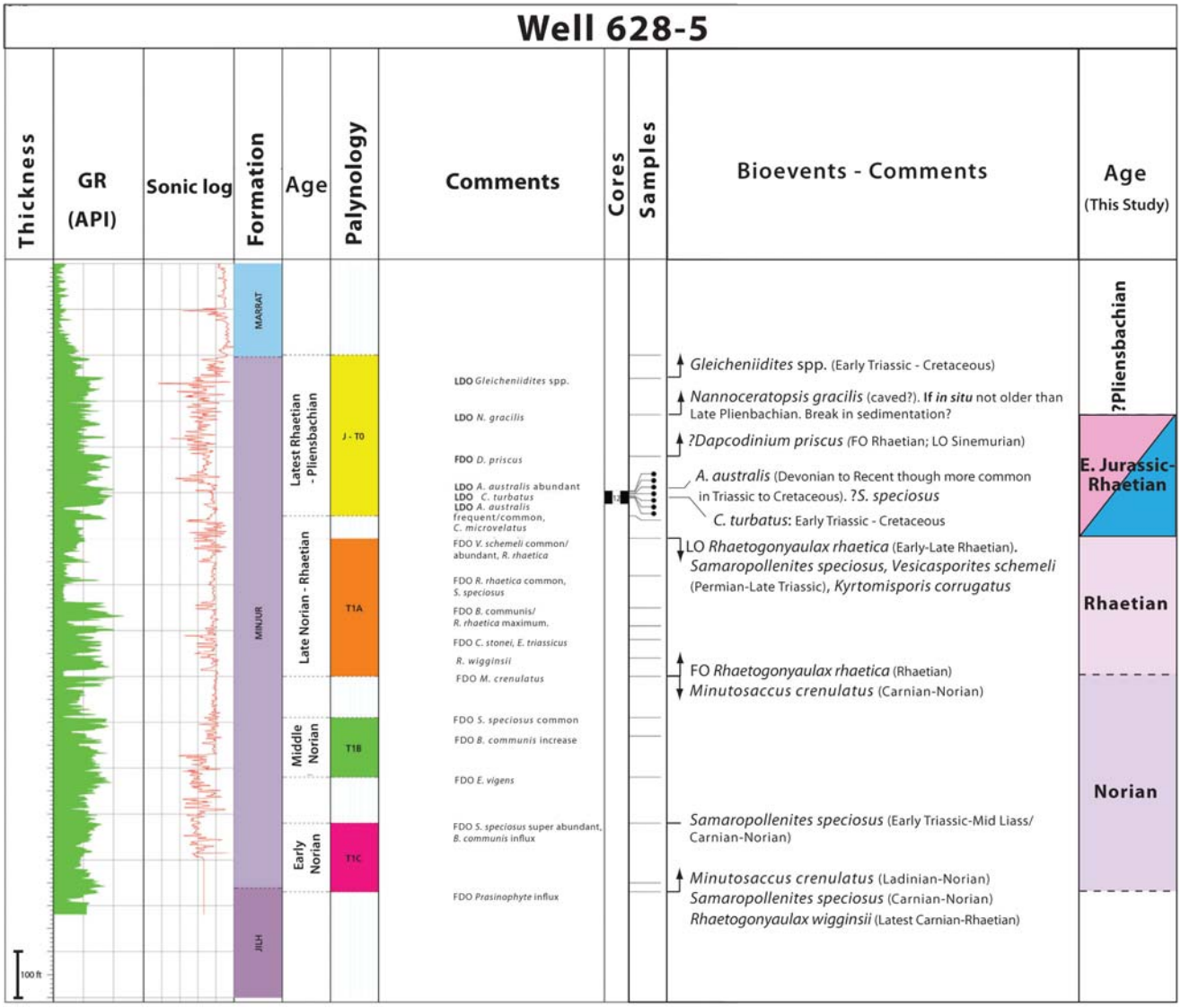

TEXT-FIGURE 13
Biostratigraphic summary and age reinterpretation for Well 628-5. Modified after Issautier et al. (2019).

constrained to the Early Jurassic could be the basis for a different age determination (text-figs 11, 12).

The Minjur Formation is 775 ft thick in Well MN-0027 (15350–16125 ft, MD). With the top of the Middle Carbonate Member picked at 15,741 ft Robertson Research (2000) studied the interval 15750–16810 ft, completely missing the Minjur Upper Member. Only five samples were analyzed in the Middle and Lower members, from 15750–16100 ft. The authors mentioned: "the impoverished flora does not allow age determination…. Wireline log correlation, however, suggests that the Jurassic-Triassic contact is likely to occur at 15860 ft (log)". This depth however, falls in the Minjur Middle Carbonate Member, dated Rhaetian to Norian (text-fig. 11) in the latest study (Packer et al. 2018), where 24 palynology samples were analyzed, 15 from the Minjur Upper Member. Packer et al. (2018) assigned an undifferentiated Early Jurassic-Late Triassic age for the interval from 15390–15410 ft since the assemblage basically consisted of *Corollina* spp. with questionable *Lunatisporites* spp. The underlying interval 15430–15840 ft is assigned an age range of Rhaetian to Norian based on the LO of *Vesicaspora schemeli* at 15430 ft (text-fig. 11). This interpretation is supported by the underlying LO of *Minutosaccus crenulatus* (Carnian–Early Norian) (Brugman 1983; Yaroshenko and Imam 1995) observed at 15890 ft, considered the top of the Early Norian (Packer et al. 2018).

Palynological analyses in Well AO interval 12957 – 12968 ft (text-fig. 12, B) is assigned an undifferentiated Late Triassic to Early Jurassic age (Packer et al. 2018, 2019) since the interval is characterized by long ranging palynomorphs such as *C. torosus* and *C. meyeriana*. In the core sample 12968 ft *Trachysporites* spp. co-occurs with ?*Kyrtomisporis* spp. The former has an age range of Late Norian to Hettangian whereas the latter is a miospore that tentatively suggests a Late Triassic age (Early Triassic–Late Jurassic according to Kustatscher et al. 2018;

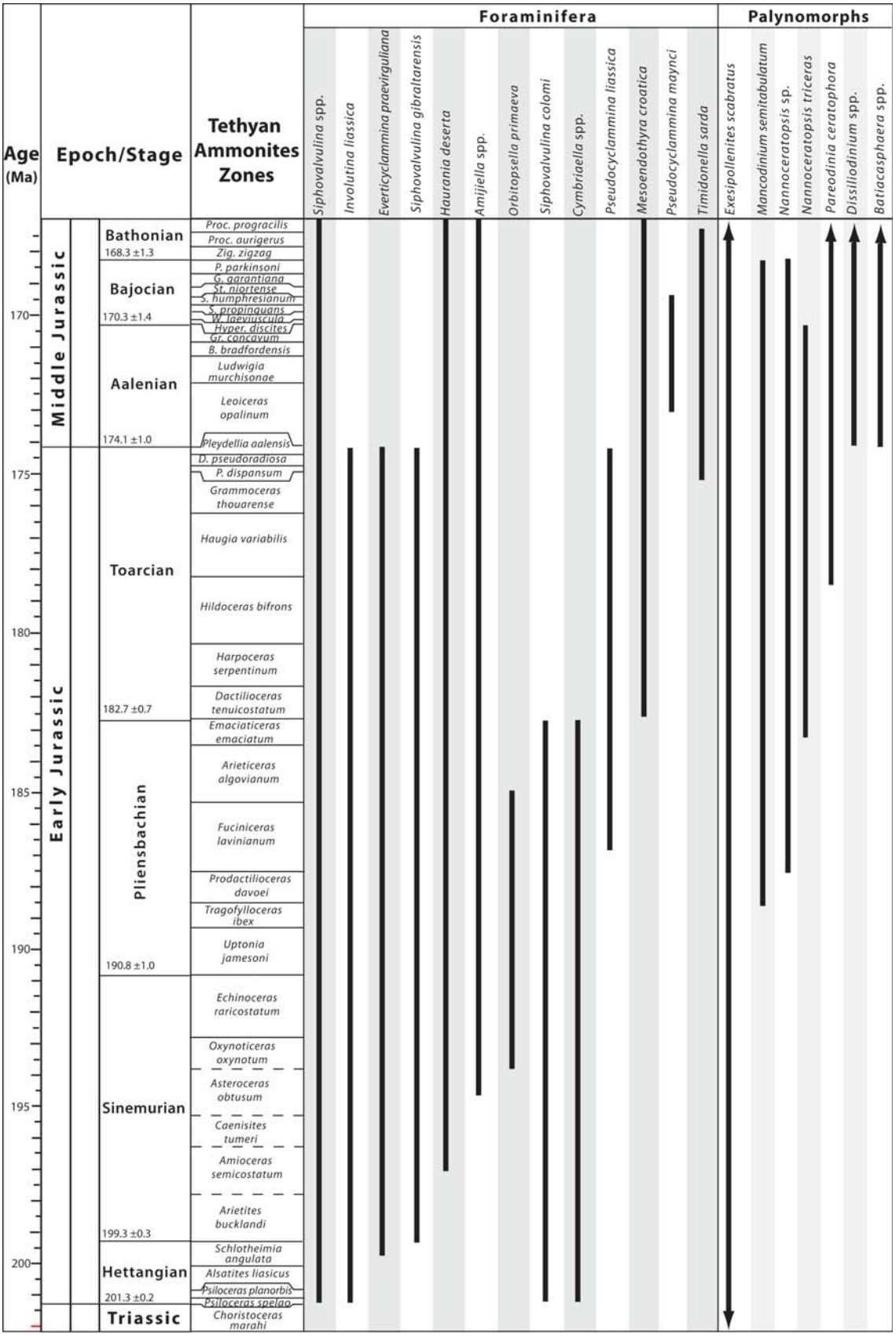

TEXT-FIGURE 14

Age-diagnostic foraminifers and palynomorphs observed in the Marrat Formation. Age range after Velić (2007), Boudagher-Fadel (2008), Ibrahim et al. (2002, 2003) and Williams and Bujak (1989). Timescale after Gradstein et al. (2012).

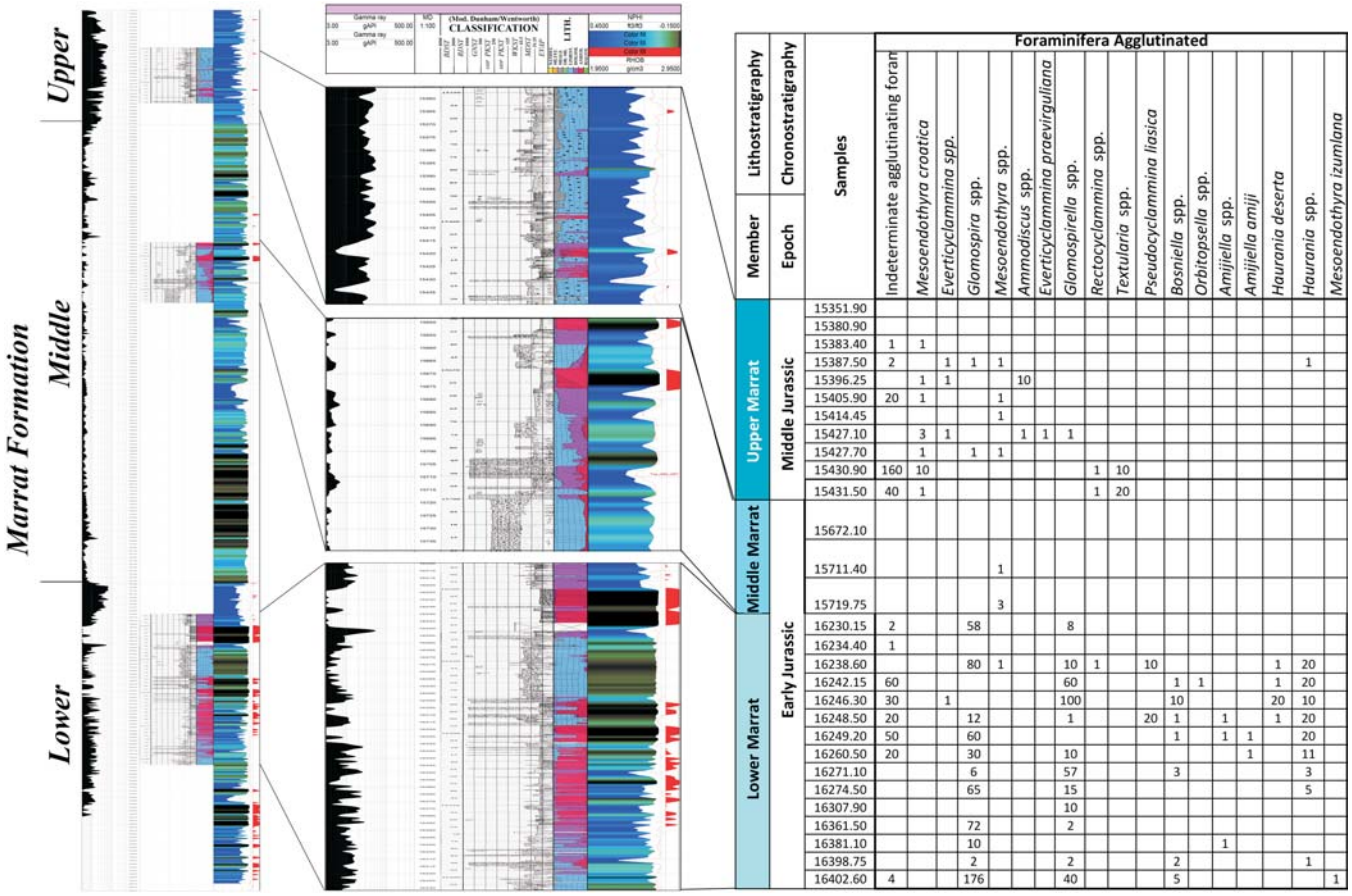

Samples	Indeterminate agglutinating foram	Mesoendothyra croatica	Everticyclammina spp.	Glomospira spp.	Mesoendothyra spp.	Ammodiscus spp.	Everticyclammina praevirguliana	Glomospirella spp.	Rectocyclammina spp.	Textularia spp.	Pseudocyclammina liasica	Bosniella spp.	Orbitopsella spp.	Amijiella spp.	Amijiella amiji	Hauranina deserta	Hauranina spp.	Mesoendothyra izumiana
15351.90																		
15380.90																		
15383.40	1	1																
15387.50	2		1	1	1												1	
15396.25		1	1			10												
15405.90	20	1			1													
15414.45					1													
15427.10		3	1			1	1	1										
15427.70		1		1	1													
15430.90	160	10							1	10								
15431.50	40	1							1	20								
15672.10																		
15711.40					1													
15719.75					3													
16230.15	2			58				8										
16234.40	1																	
16238.60				80	1			10	1		10					1	20	
16242.15	60							60				1	1			1	20	
16246.30	30		1					100				10				20	10	
16248.50	20			12				1			20	1		1		1	20	
16249.20	50			60								1		1	1		20	
16260.50	20			30				10							1		11	
16271.10				6				57				3					3	
16274.50				65				15									5	
16307.90								10										
16361.50				72				2										
16381.10				10										1				
16398.75				2				2				2					1	
16402.60	4			176				40				5						1

TEXT-FIGURE 15, Part 1
Ages, lithostratigraphy and microfossils distribution in the Marrat Formation, Well II, onshore Kuwait. Modified after Packer et al. (2015)

Mangerud et al. 2020), which is consistent, though not restricted, to the assigned age. From this interval down to 13286 ft, a general Late Triassic age is suggested (not older than ?Late Norian), based on the presence of *Lunatisporites* sp. at 13286 ft. *Lunatisporites* is frequently observed in the Permian-Norian interval though often it has been mentioned in younger sections. In eastern Asia basins the Triassic/Jurassic boundary is placed at the LO of the pollen taxon *Lunatisporites rhaeticus* (Helby et al. 1987; Cirilli 2010; Sha et al. 2011, 2015; Kustatscher et al. 2018). In the Sverdrup Basin, Suneby and Hills (1988) reported this taxon as extending to the top of the Triassic. Warrington (1997) also recorded *L. rhaeticus* in the Rhaetian of Dorset and Paterson and Mangerud (2015) recorded this genus in the Norian–Rhaetian Svenskøya Formation on Hopen Island, in the south-east of the Svalbard Archipelago. Additionally, Cirilli (2010) assigned a latest Norian to Rhaetian age to this species. Therefore *Lunatisporites* sp. constitutes the basis to assign this interval a Late Triassic age, within the Upper Minjur Member, with no evidence of this bioevent being reworked.

The proposed Norian age (Packer et al. *op. cit*.) for the interval 13404 – 13498 ft (text-fig. 12B) is based on the association of:

1) Last common occurrence of *Kyrtomisporis* spp., a palynoevent previously recorded from the central and northern North Sea (Goldsmith et al. 2003) in the Early Norian

2) *Rhaetogonyaulax* spp., considered a Norian - Rhaetian dinoflagellate cyst (Warrington 1984; Riding 2010)

3) The LO at 13415 ft of the dinoflagellate cyst recorded as questionable *Heibergella* sp. is similar to a form of *Heibergella* recorded from the Norian of Northeast Iran (Ghasemi-Nejad et al. 2008)

4) The LO of *Minutosaccus crenulatus* at the core sample 13487 ft. The reported age for this taxon is mid Carnian - Early Norian in the Alpine realm (Brugman 1983).

Accordingly, the association of palynomorphs from this interval is considered to suggest an Early Norian age (Packer et al. 2018, 2019, *op. cit*.).

In the AO well, the interval from 13614–13805 ft has been assigned an undifferentiated Carnian to Early Norian age. This part of the section is characterized by *Minutosaccus crenulatus* and undifferentiated bisaccate pollen such as *Deltoidospora minor* and *Vesicaspora schemeli*. As noted above, these associations of palynomorphs suggest a Carnian - Early Norian age. Another bioevent, with an age range of Ladinian to Early Norian (Brugman 1983; Cirilli 2010), the LO of *Samaropollenites speciosus* at 13614 ft (text-fig. 12B), is compatible with this proposed age. Cirilli (2010) however, constrains its FO

Foraminifera Calcareous																		Ostracods		ALAD			Miscellaneous Microfossils																			
Frondicularia spp.	Indeterminate calcareous benthics	*Lenticulina* spp.	Miliolidae (undifferentiated)	*Aeolisaccus* spp.	*Nodosariid* spp.	Ophthalmidium spp.	*Siphovalvulina* spp.	*Siphovalvulina colomi*	*Lingulina spp.*	*Quinqueloculina* spp.	*Siphovalvulina gibraltarensis*	*Cymbriaella lorigae*	*Cymbriaella* spp.	*Involutina liassica*	*Involutina* spp.	*Aeolisaccus dunningtoni*	*Nodosaria* spp.	Ostracods (articulated)	Ostracods (disarticulated)	*Clypeina* spp.	Algal fragments	*Thumatoporella parvovesculifera*	Bivalve fragments	Bivalve fragments (small)	*Bositra buchi*	*Bositra* spp.	Echinoid fragments	Microgastropods (undifferentiated)	Bivalve spat	Echinoid spines	Inoceramus fragments	Rovearinids (undifferentiated)	Brachiopod spines	Fish debris	Microgastropods (high spired)	Sponge spicules	Sponge spicules (axial)	Sponge spicules (Monoaxon)	Sponge spicules (Triaxon)	Bioclastic debris (fine)	Microgastropods (large)	Core Shift (ft)
1	1																	10	400	20			60	130	1	20	10	1														
	2																		2				96			6	46		2	6	4											
	1	1	1															1	70				30	840			1500			1	1											17.1
	10	10																	60				6	840				1			1											
	10	5		1	3	1													40					2550		90	10	30		10	20											
							4																10	130			1220	20		10	10											
	20	1					11	1															70	2990			70	10		20	10	1										
		1					2	1	1									3						690			700	10		10			10									21.2
						10	8												1				180	1620		7	80	10		10	1											
	2	1				10	1			1									50					370			30	20														
	70					1	2												10					550		20	160	20		40	1			10	10							
	1			2			5	1																			3															
							24				2																															23.1
							24																				1															
																			2				18						4	2						1						
																								2110	1	10	2				3											
			10				10																260				40			1					1		210	30				
	4		20	10			40	40				2	1	1	1			10	20		20		70				30	1		1												
	20			1			180	10			10	1		1		2						20	40				1										1		10			
	20				2							1					1		1			1	130				220			1	1						7					
						1	50	1				1							50				130				80	1		10					2							
			1	10			11	1					1			3			120			1	30							20										150		23.3
			9	12			27	6					1			3			3			3	18	3			30															
		5							5					5					15		3			105		15			5		5				1		2			485	7	
			1																				720			50	2				30											
				6															4							2	6	4												15		
					1	1						1											210						1		1				1						8	
				12	1											6						2		14				14			12				1							
			16		4		4			4	1		1						4				12	76																		

TEXT-FIGURE 15, Part 2
Continued.

to the Early Carnian, which would further support the age range. Additionally, an increase in abundance of *Patinasporites densus* at 13735 ft with a reported age of Carnian to Rhaetian (Brugman 1983; Cirilli 2010; Kürschner and Herngreen 2010) would be consistent with this age range. The first downhole occurrence (FDO) at 13805 ft of a definite specimen of *Palaeospongisporis europaeus,* generally considered a Ladinian marker but has been recorded within the Early Carnian (Warrington 1984; Brugman 1983) at 13805 ft, does not appear to be consistent with the age assignment for this section of the Minjur, which is no older than Norian (Packer et al. 2018, 2019). It is therefore considered reworked.

The interval from 13816–13850 ft (text-fig. 12B) is characterized by poorly preserved undifferentiated bisaccate pollen and palynomorphs (Packer et al. 2018, 2019), with an increase in *Aratrisporites* spp. at 13816 ft. A single *Aratrisporites parvispinosus* occurs at 13825.50 ft which if *in situ* is most characteristic of Middle Triassic, although it has also been reported from the Carnian of Siberia (Ilyina and Egorov 2008). At 13847 ft a few occurrences of questionable *Aratrisporites parvispinosus,* and *Samaropollenites speciosus* are present. *Duplicisporites* spp. is regarded as a Ladinian - Early Norian marker (Visscher and Brugman 1981) though it has been also observed in the Rhaetian (https://paleobotany.ru/palynodata/genus/4513; Tripathi and Ram-Awatar 2006) while *S. speciosus,* originally described from Early Triassic to Middle Liassic of Madagascar (Goubin 1965) is considered a Late Ladinian - Early Norian marker (Brugman 1983; Helby et al. 1987; Riding et al. 2010). Accordingly, the co-occurrence of these various taxa tentatively suggests a questionable Late Ladinian - Early Carnian age for this interval. The older age compared to equivalent intervals in wells of the study area, is based on species of *Aratrisporites,* which alternatively may be present due to reworking.

The age dating for the Minjur Formation in the Well OO (text-fig. 12C) stems from bioevents identified in ten samples from a 1065 ft thick Minjur Formation (Robertson Research 2000, *op. cit.*). In this well, Packer et al. (2019) concentrated on the Jilh Formation and older sediments, (out of the scope of the current work). Species such as *Classopollis classoides* and *Corollina meyeriana* constitute the dominant assemblage in the upper part of the Upper Minjur (Robertson Research 2000). Both taxa, however, are abundant in the Rhaetian of Europe (Morbey 1978; Schneebeli-Hermann et al. 2017).

The main criteria used by Robertson Research (2000) for assigning a Hettangian age to the Upper Minjur Member is based on the occurrence of the taxa *Trachysporites fuscus* and

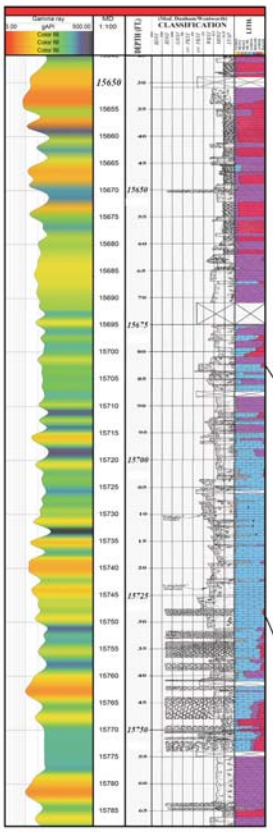

Lithostratigraphy		Chronostratigraphy	Core Samples	Foraminifera Agglutinated																
Formation	Member	Epoch		*Everticyclammina* spp.	*Glomospira* spp.	*Indeterminate agglutinating foram.*	*Pseudocyclammina liasica*	*Reophax* spp.	*Ammodiscus* spp.	*Glomospirella* spp.	*Mesoendothyra croatica*	*Mesoendothyra* spp.	*Amijiella amiji*	*Bosniella* spp.	*Textularia* spp.	*Amijiella* spp.	*Everticyclammina praevirguliana*	*Rectocyclammina spp.*	*Haurania deserta*	*Haurania* spp.
Marrat	Lower Marrat	Early Jurassic	15682.35	7	14	26	1	2												1
			15685.45	1																1
			15686.25		4	14		1	2	28	1	4								
			15693.20																	
			15694.65		200	1				40		1	1	4	20					3
			15695.45		110	50							1	1	90	2	1			1
			15696.40			40				20					1	2	4			1
			15713.65		10	35	1			25								5		1
			15720.30		95	50				25					15			5		
			15724.75		10					25				6	2					
			15728.75		150					180		1		1	1	1				
			15728.95		60					10									1	1

TEXT-FIGURE 16, Part 1
Ages, lithostratigraphy and Microfossil distribution in the Marrat Formation, Well KK, onshore Kuwait. Modified after Packer et al. (2015).

the abundance of *Classopollis classoides* and *Corollina meyeriana*, naming this interval the *Classopollis-Corollina* Zone. This is equivalent to the *Classopollis* Dominance Zone of Loutfi and Sattar (1987) and the *Corollina meyeriana* Abundance Zone of Bujak and Williams (1976); the latter ranges down to the Rhaetian, though. Nonetheless, the age range of *C. classoides* and *C. meyeriana*, is not constrained to the Early Jurassic. The former has been reported from the Carnian to the Cenozoic in Australia, Canada, Europe and North America (Barss et al. 1979; Liqin Li et al. 2018; Schneebeli-Hermann et al. 2017; Kustatscher et al. 2017). The other marker *Corollina meyeriana,* shows a range of Carnian to Cenozoic (Pacyna 2014; Kustatscher et al. 2017). In this regard the occurrence of *Vesicaspora schemeli* ranging from Permian to Rhaetian (Hemer 1965; Cameron 1974) at 13140 ft in conjunction with *Classopollis* and *Corollina* (text-fig. 12C) could well be considered the LO of this taxon since no species with a FO in the Early Jurassic or younger are observed. *V. schemeli* is also present in the underlying sample at 13270 ft, which could be additional supporting evidence to suggest that this taxon is *in situ*. In sections generally characterized by intervals with sparse palynomorphs such as in this formation, abundance is not reliable as an age defining criterion, though many taxa exhibit acme and abundance commonly associated to specific age intervals.

In the Upper Minjur of the AS Well (text-fig. 12, A) these Triassic markers show the same distribution. A sparse assemblage occurs between 16980-17050 ft with *Corollina* spp., *Deltoidospora* sp. and a questionable occurrence of *Lunatisporites* sp. suggesting an undifferentiated Early Jurassic–Late Triassic age (Packer et al. 2018). In the underlying sample at 17060 ft the LO of *Kyrtomisporis corrugatus* and *Vesicaspora schemeli* indicates a Late Triassic, probably Rhaetian-Norian age (Packer et al. 2018), showing a consistent, similar distribution as observed in the Well OO discussed above (text-fig. 12C).

In Saudi Arabia, a Pliensbachian to Rhaetian age has been assigned to the upper part of the Minjur Formation (the J-T0 Palynozone of Issautier et al. 2019). This ample range allows for a "flexible" age interpretation which could either be Early Jurassic or Late Triassic for the interval (text-fig. 13). The criteria for this assignment (Issautier et al. 2019) are based on:

1. The first stratigraphic occurrence (FO) of *Nannoceratopsis gracilis* (Pliensbachian or younger). If *in situ, N. gracilis* constitutes the main basis to assign an Early Jurassic age.

2. *Dapcodinium priscus* which has an age range of Rhaetian to Sinemurian/Pliensbachian (Williams and Bujak 1985; Helby et al. 1987; Warrington 1997; Larson 2009; Riding et al. 2010; Williams et al. 2017; Schneebeli-Hermann et al. 2017) in Alaska, Europe and Australia.

3. *Gleicheniidites* spp. described from the Lower Lias (Rhaetian-Toarcian) of Boulonais (Danze-Corsin et al. 1963)

Foraminifera Calcareous												Ostracods		ALAD		ALCO	Miscellaneous Microfossils												Core shft
Nodosaria spp.	Miliolidae (undifferentiated)	*Ophthalmidium* spp.	*Spiroloculina* spp.	*Aeolisaccus* spp.	*Cymbriaella* spp.	*Nodosariid* spp.	*Quinqueloculina* spp.	*Siphovalvulina gibraltarensis*	*Siphovalvulina* spp.	*Involutina* spp.	*Siphovalvulina colomi*	Ostracods (articulated)	Ostracods (disarticulated)	Algal fragments	*Thumatoporella parvovesculifera*	*Bacinella* spp.	Bivalve fragments	Bivalve fragments (small)	Bivalve spat	Brachiopod spines	Echinoid fragments	Echinoid spines	*Inoceramus fragments*	Microgastropods (high spired)	Microgastropods (large)	Microgastropods (undifferentiated)	Rovearinids (undifferentiated)	Sponge spicules	Sponge spicules (axial)	Sponge spicules (Triaxon)	
2																		66					1							
												5					1	325			10	10				5				
	8	1											1										14			2				
												21	6					75							1	2				
					2	1	1					1	40	270			560		30		1		1	2						
		3	20	1	1		1	20	20				1		7		40					2								20 ft.
													10					310								1				
3													10					325			5		1	1			1		5	
			80	1				5	80				1		120	60						1								
			25	5		1			25	1							160			1	1	1	5	1						
			4	100	1				4		1	10	20			12		30								1				
						2							30					280					1			20		20	90	10	

TEXT-FIGURE 16, Part 2
continued.

but also known from the Rhaetian (Solomon et al.1976; Herngreen and Boer 1974).

As observed, apart from *N. gracilis* which occurs in the upper part of the zone (text-fig. 13), no species with a FO in the Jurassic are mentioned. It is not clear the reason for determining a Pliensbachian – Rhaetian age range for the J-T0 Zone since a single occurrence of *Nannoceratopsis gracilis* at 145 ft from the top of Minjur could be the result of cavings within the Upper Minjur beds. In that case, there is a possibility that the interval could be older than Early Jurassic, probably Late Rhaetian. Should *N. gracilis* be considered *in situ* and not caved from the Marrat Formation, it could be the basis for proposing a sedimentary break and establishing Pliensbachian or younger age at this level. *Dapcodinium priscus* is observed as a questionable occurrence in the Well 628-5 (Issautier et al. 2019) within the J-T0 Zone, approximately 90 ft below the FDO of *N. gracilis* (text-fig. 13). In Well 355-3 *D. priscus* occurs approximately at 120 feet below the FDO of *N. gracilis* (Issautier et al. 2019, enclosure 2). This taxon is not observed in the Kuwait samples where species such as *Lunastiporites* sp., *Vesicaspora schemeli, K. corrugatus*, *Rhaetogonyaulax* sp. occur in the Minjur Upper Member (70–300 ft from the top of Minjur, Packer et al., *opt. cit.*) and would suggest a Rhaetian-Norian age range. The top of the T1A Zone is marked by *Vesicaspora schemeli* (Permian–Late Triassic) which occurs at 400 ft below the top of Minjur, with *Samaropollenites speciosus* observed 80 ft lower, at 480 ft from the Minjur upper boundary.

There is also a possibility of determining a more precise age for the underlying T1A Zone in Well 628-5 where Issautier et al. (2019) interpreted a range of Late Norian to Rhaetian. The distribution (FO and LO) of *Rhaetogonyaulax rhaetica,* is quite significant, considering the mentioned age ranges for this taxon (early-latest Rhaetian: Riding 2010; Early-Mid Rhaetian: Helby et al. 1987). Its FO and LO at 460 ft and 760 ft, respectively, above the base of the Minjur Formation (text-fig. 13) would support a Rhaetian age interpretation for this interval, instead of a Late Norian - Rhaetian range. The co-occurrence of the LO of *R. rhaetica* with the LO of *S. speciosus* at ~500 ft from the top of Minjur could be explained by considering the original age determination for the latter taxon, ranging from Early Triassic to Early Jurassic (Goubin 1965).

MARRAT FORMATION

Biostratigraphic studies recently carried out in the Middle and Late Jurassic (Kadar et al. 2015; Crespo de Cabrera et al. 2019, 2020) have constrained the age framework for the Marrat Formation, which can be no younger than Early Bajocian. The foraminiferal-based biozonation proposed for this formation (Fugro-Robertson 2009) is based on a series of long ranging taxa which in most instances are extremely scarce (e.g. *P. maynci* and

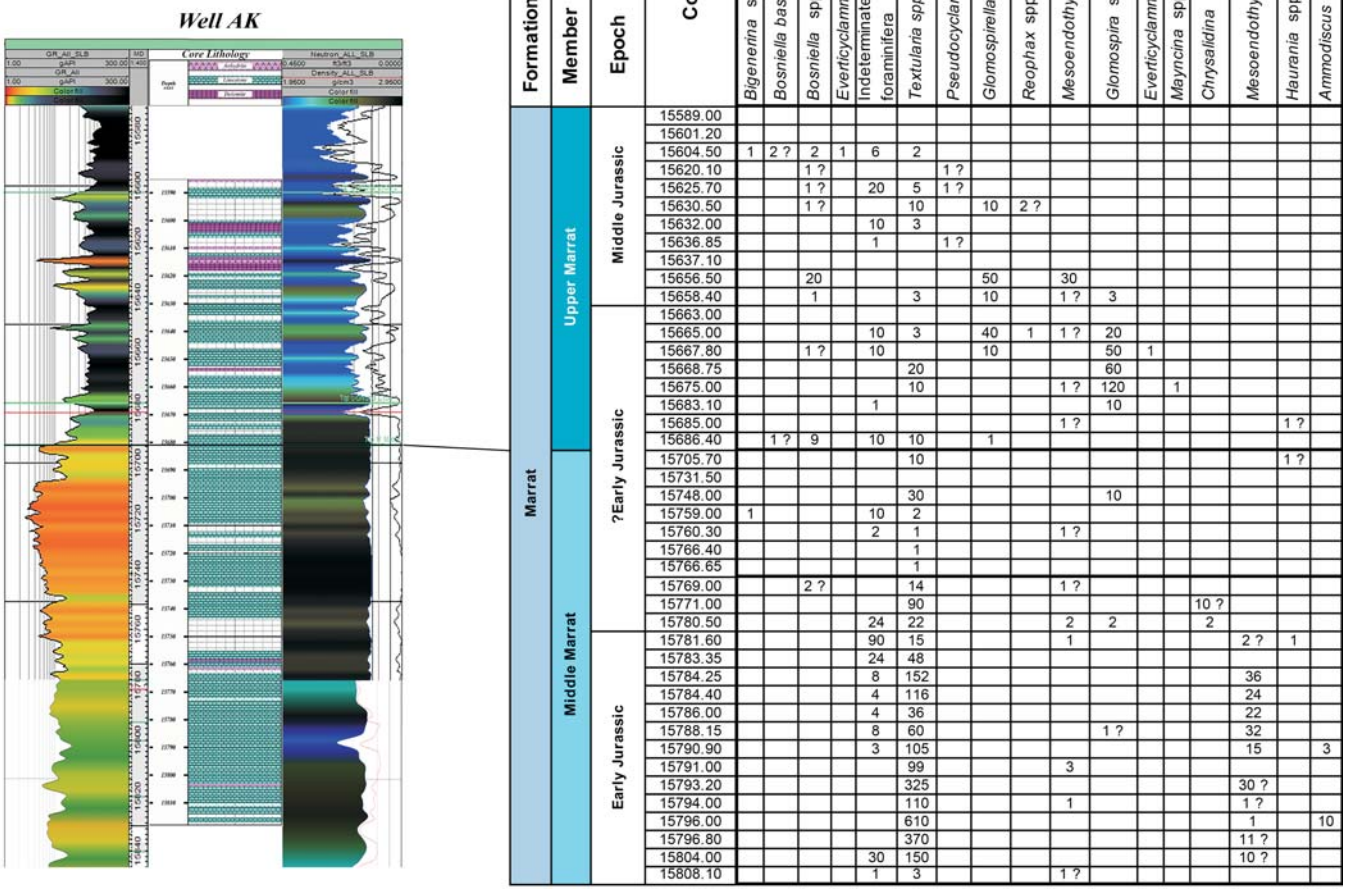

Core Samples	Bigenerina spp.	Bosniella bassoulleti	Bosniella spp.	Everticyclammina praevirguliana	Indeterminate agglutinating foraminifera	Textularia spp.	Pseudocyclammina spp.	Glomospirella spp.	Reophax spp.	Mesoendothyra croatica	Glomospira spp.	Everticyclammina spp.	Mayncina spp.	Chrysalidina spp.	Mesoendothyra spp.	Haurania spp.	Ammodiscus spp.
15589.00																	
15601.20																	
15604.50	1	2 ?	2	1	6	2											
15620.10			1 ?				1 ?										
15625.70			1 ?		20	5	1 ?										
15630.50			1 ?			10		10	2 ?								
15632.00					10	3											
15636.85					1		1 ?										
15637.10																	
15656.50			20					50		30							
15658.40			1			3		10		1 ?	3						
15663.00																	
15665.00					10	3		40	1	1 ?	20						
15667.80			1 ?		10			10			50	1					
15668.75						20					60						
15675.00						10				1 ?	120		1				
15683.10					1						10						
15685.00										1 ?						1 ?	
15686.40		1 ?	9		10	10		1									
15705.70						10										1 ?	
15731.50																	
15748.00						30					10						
15759.00	1				10	2											
15760.30					2	1				1 ?							
15766.40						1											
15766.65						1											
15769.00			2 ?			14				1 ?							
15771.00						90								10 ?			
15780.50					24	22				2	2			2			
15781.60					90	15				1					2 ?	1	
15783.35					24	48											
15784.25					8	152									36		
15784.40					4	116									24		
15786.00					4	36									22		
15788.15					8	60					1 ?				32		
15790.90					3	105									15		3
15791.00						99				3							
15793.20						325									30 ?		
15794.00						110				1					1 ?		
15796.00						610									1		10
15796.80						370									11 ?		
15804.00					30	150									10 ?		
15808.10					1	3				1 ?							

TEXT-FIGURE 17, Part 1
Ages, lithostratigraphy and microfossils distribution in the Well AK. Modified after Packer et al. (2015).

Amijiella amiji). No biozonation was presented by Packer et al. (2015) who generated a stratigraphic framework based on the integration of palynological and microfossil results of approximately 800 samples from fourteen wells regionally distributed in onshore Kuwait. In both reports, the co-occurrence of long-ranging taxa occasionally enabled age determination. Despite limitations intrinsic in the difficulties of achieving taxon identification to species level using thin sections, foraminifera proved to be the most viable way to establish a stratigraphic framework. Nonetheless, calibration of the foraminiferal markers with published literature is hampered by the lack of refined age ranges in terms of substages or ammonite zones (Fugro-Robertson 2009). This frequently results in loosely constrained Tethyan microfaunal stratigraphic frameworks for the Early Jurassic, characterized by low taxonomic diversity within the carbonate platforms deposited on the margins of the Tethys (Boudagher-Fadel and Bosence 2007; Velić 2007).

LOWER MARRAT

The foraminiferal faunas present are generally abundant and diverse. Typical taxa recorded include *Glomospira* sp., *Glomospirella* sp., *Involutina* sp., *Pseudocyclammina* sp., *Haurania* sp., *Amijiella* sp., *Cymbriaella* sp., *Involutina liassica*, *Siphovalvulina* sp., *Lenticulina* sp., *Aeoliasscus* sp., and nodosarids (Packer et al. 2015). Calcareous algae occur persistently through the interval, mostly *Thumatoporella* sp., *Lithocodium* sp. and *Bacinella* sp. The *incertae sedis* form *Cayeuxia* is also present. Ostracods are generally common or abundant. Associated macrofossil debris includes localized influxes of bivalves, echinoids, microgastropods and sponge spicules. Nannofossils are locally common or abundant, for example in well II.

Bioevents

Orbitopsella primaeva (Henson 1948)

In the study area it is very rare, observed only in Well AC at 15480 ft in the lower part of the Lower Marrat (Fugro-Robert-

Foraminifera Calcareous												FOP	Ostracods		ALAD				Miscellaneous Microfossils													ALIN	Allochems		
Dentalina spp.	*Lingulina* spp.	Miliolidae (undifferentiated)	Indeterminate calcareous benthics	*Spiroloculina* spp.	*Aeolisaccus* spp.	*Nodosaria* spp.	*Siphovalvulina* spp.	*Lenticulina* spp.	Nodosarid spp.	*Aeolisaccus dunningtoni*	*Globuligerina* spp.	Ostracods (articulated)	Ostracods (disarticulated)	Algal fragments	*Thumatoporella parvovesculifera*	*Lithocodium* spp.	*Bacinella* spp.	Bivalve fragments	Echinoid fragments	Echinoid spines	Fish debris	Inoceramus fragments	Microgastropods (high spired)	Roveacrinids (undifferentiated)	*Bositra* spp.	Microgastropods (undifferentiated)	Bioclastic debris (fine)	Sponge spicules (Monoaxon)	Microgastropods (fragmentary)	*Bositra buchi*	*Favreina* spp.	Sponge spicules	*Cayeuxia* spp.	Ooids (undifferentiated)	Peloids (undifferentiated)	Core Shift (ft)
												1	10					1800	60	20	10	40														
																		1540	70				10													
													230					780		10		80	40													
												2	160					220	60	10		20														
1	2	1											100						2370	9	1	20													
	1		1									1	20					740	20			80		20											
				1																					3590										
																		1470	90	1		1	1		40	6									
	1																	650	1230	1		1				1									
	1	50			1	10	1 ?											430	70			10	10												
1							1	6				2	30					290	100			10				20	1760								
																		420	10			10			1920	1									
					1		10						1					80	430	30		20				10	200									
							20 ?						30					70	300			10				20	30									
							10		10			2	70					220	230				1		20	120		10								
									2			10		3				130	110	20					10	60	80		10							
									1				10					220	10			10	30		20		250		50							
									2				10					120	50				10	10	1		180		10							
																		50	20	10			10		10	50	120								
									1									240	10			3	10			60	60			1	1 ?					
													10					110	40	1		3			10		390	30								
					2														100								270	1								20
																		130	20							20									
													10					290	30			10			2				10		4					
																		200																	
																			1								100									
			2								1 ?		16					38		1						4						2				
					10		4						90					200	10							6										
	1		1		6		11			1			2				12 ?	1																	
					80		10		1			1	30		1 ?			10					10									15				
							24									1			6							1								60		
							8																												
							12												8			4				1								60		
																			1	4			1			9						1	30		
																			4	4													30		
							10												2			1											30		
							9					1	3																					30		
					1		50						5						40	5													4		
					5		2						145					35	85															12	
					20		10			1			1					40	230	20															
					10		30						20					20	160															12	
					1		20						10					20	50												1 ?					
							1																									1	15		

TEXT-FIGURE 17, Part 2
Continued.

son 2009). According to Velić (2007), this taxon commonly occurs in the late Sinemurian to late Pliensbachian of the Adriatic carbonate platform of southeast Europe. It reaches its maximum abundance in the early Pliensbachian. In the study area it co-occurs with *Siphovalvulina gibraltarensis* which is assigned a Sinemurian-Toarcian age range (text-fig. 14).

Cymbriaella Fugagnoli 1999

This genus was described from the shallow water carbonates of the Calcari Grigi Formation (Hettangian-Pliensbachian) located in the Southern Alps, Italy. It characterizes the Rotzo Member of the formation, which is dated as late Pliensbachian. This genus is monospecific, represented by the species *Cymbriaella lorigae.* Fugagnoli assigned this taxon a late Pliensbachian age, though Boudagher-Fadel (2008) reported a Hettangian to Pliensbachian range. In the Lower Marrat it is rare in wells II (16242–16271 ft.; J06 HST) and KK (15695–15729 ft; J04 TST).

Amijiella Loeblich and Tappan 1985

This is a long-ranging genus described from Southwestern Asia and is commonly found in low numbers in the Lower Marrat or lower part of the Middle Marrat. It is usually associated with textulariids and *Siphonina* sp. In the study area, it has been observed in wells II, interval 16248.50–1638110 ft (J04 TST to J06 HST) (text-fig. 15), KK (15695–15728 ft; J04 TST) and AC (15240–15500 ft; J04 HST to J08 HST).

Haurania deserta Henson 1948

H. deserta is a larger agglutinated foraminifer with a reported age range of Sinemurian to Bajocian (Velić 2007) or Sinemurian to Bathonian (Boudagher-Fadel 2008). It has been observed in the Lower Marrat in wells AC (at 15380 ft (J08 LST) and 15460 ft (J06 TST)), II (co-occurring with *Pseudocyclammina liassica* at 16238.60 ft; J06 HST) and a questionable occurrence at 15728.95 ft (J04 TST) in well KK.

Pseudocyclammina liassica Hottinger 1967

Together with *Lituosepta recoarensis, Orbitopsella* and *Lituosepta compress,* this taxon is considered one of the most useful biostratigraphic markers in several carbonate successions of the southern Tethys. Fugagnoli (1999), observed this genus where *Cymbriaella* was described, in the Early Jurassic of the Venetian Prealps of northeastern Italy, where it was restricted to the late

Pliensbachian. Velić (2007) however, assigned a latest late Pliensbachian to early Toarcian age to this taxon. In the study area, it is observed in wells G in the uppermost Middle Marrat at 14818 ft (J15 HST) and II at 16248.5 ft (J06 HST) in the upper portion of the Lower Marrat. In well KK two samples, at 15695.45 ft and 15728.75 ft (J04 TST and HST) (text-fig. 16), contain single questionable occurrences of this taxon, both found within the Lower Marrat.

Additional taxa which are not restricted to any of the Marrat members are briefly mentioned here, such as *Involutina liassica, Siphovalvulina gibraltarensis* and *Everticyclammina praevirguliana.* These are long ranging species; the first two have a first stratigraphic appearance in the Hettangian, and the last species has a FO in the Sinemurian. In the absence of any younger taxa, they could be attributed an Early Jurassic age.

Involutina liassica (Jones 1853)

This taxon is observed in northeastern Italy in the Lower Jurassic deposits, but only in the rocks originating at the platform margins and slopes (Velić 2007). It was common in the early Sinemurian as well as in the Toarcian, where it seems to have been restricted to the NE marginal areas of the platform towards the Slovenian and Bosnian basin, in the Karlovac area, northern Herzegovina, Montenegro, and on the slopes towards the Budva–Cukali trough (Velić, 2007). This species is also an important component of the *Siphovalvulina colomi* biozone determined by BouDagher-Fadel and Bosence (2007), when studying the Early Jurassic foraminifera of the Western Mediterranean area. In the study area, it appears in the Lower Marrat of Well II, with its FO at 16274.5 ft (J04 TST).

Siphovalvulina gibraltarensis Boudagher-Fadel, Rose, Bosence and Lord 2001

This taxon is long ranging, from Sinemurian to Pliensbachian (Boudagher-Fadel 2008) and according to Velić (2007), extends into the Toarcian. This latter interpretation is used in this work since it is observed invariably within the Lower and Middle Marrat units. It commonly appears in the Middle Marrat in wells ZZ, F, II, AL, QQ, AE, AF, AK, AC, TT, and RR. In the Lower Marrat, it is scarce although occasionally common in wells KK, II, and AC. This taxon has also been observed in the SS Well in the Upper Marrat, which is supporting evidence for its long age range.

Everticyclammina praevirguliana Fugagnoli 2000

This taxon was described by Fugagnoli (2000) from the Early Jurassic of the Venetian Prealps (Calcari Grigi, Trento Platform), northern Italy. In a study of the Early Jurassic of the Western Mediterranean, Boudagher-Fadel and Bosence (2007) divided the Hettangian to Pliensbachian into four biozones, *Everticyclammnina praevirguliana* being the second one, determined on the basis of the FO of this taxon. It is found in micritic limestones with associated algae/cyanobacteria (*Cayeuxia*, *Thaumatoporella* and *Palaeodasycladus mediterraneus;* Boudagher-Fadel 2008). The assigned age for this species is latest Sinemurian to Pliensbachian (Boudagher-Fadel 2008), although Velić (2007) assigned a latest Hettangian to Toarcian age to this species in the Adriatic Carbonate Platform of southeast Europe. The latter age is more applicable to the studied area since it occurs invariably throughout the different units, though most abundantly and persistent in the Middle Marrat unit. The Aalenian age determined by Packer et al. (2015) is not sustainable since it occurs in intervals confidently assigned to Toarcian.

The occurrence of *E. praevirguliana* in the study area per well can be summarized as follows:

• Upper Marrat in wells II and G

• Middle Marrat in wells AK, AC, Y, ZZ, F, AL, TT, RR and N

• Lower Marrat in Well KK

MIDDLE MARRAT

Microfossils tend to be common to abundant with assemblages characterized by *Glomospira* sp., *Glomospirella* sp., *Involutina* sp., *Pseudocyclammina* sp., *Haurania* sp., *Amijiella* sp., *Cymbriaella* sp., *Siphovalvulina* sp., *Lenticulina* sp., *Aeoliasscus* sp., very rare *Mesoendothyra croatica* and nodosarids.

Bioevents

Sampling density is low in this interval which has a thickness ranging from 600 to 850 ft. Most of the available cores are taken from the mid and upper part of this unit, except for wells PC and AC. These cores are also the most extensive, spanning the former for 690 ft and the latter for 700 ft. The most densely sampled is Well PC, where 88 samples are studied; in well AC only 20 samples are analyzed throughout this unit. Well PC, however, documents the transition from the Lower Marrat to the Middle Marrat, which is very helpful when trying to understand the stratigraphic evolution within these units.

Mesoendothyra croatica Gušić 1969

This taxon has been assigned an Aalenian to Bathonian age (Sartorio and Venturini 1988). In this work, occurrence of this and other similar forms in older sections supports the use of the Toarcian to Bathonian age range proposed by Velić (2007). It occurs frequently within the study in very low numbers. In well PC, a single occurrence is observed at 12029.00 ft, 295 ft above the base of the Middle Marrat. It is scarce but consistently observed from 11677.20 ft, a depth which could well be considered its FO, approximately 219 ft below the top of the Middle Marrat. In Well II, its FO is observed at 15431.5 ft, in the lower 50 ft of the Upper Marrat. In Well AK, the abundance of this species increases considerably at some intervals within the Upper Marrat, compared to the previous wells. Its FO is observed at 15794 ft (text-fig. 17), about 102 ft below the top of the Middle Marrat. Well G is very densely sampled and this taxon is only identified in two samples (Fugro-Robertson 2009) at 14789.00 and 14751.00 ft, respectively.

Siphovalvulina colomi Boudagher-Fadel, Rose, Bosence and Lord 2001

In the Western Mediterranean, Boudagher-Fadel and Bosence (2007) divided the Hettangian to Pliensbachian into four biozones that correlate with strontium isotope dating. The *Siphovalvulina colomi* biozone was the oldest, of early Sinemurian age. In the Adriatic Carbonate Platform in southeast Europe, Velić (2007) extended this age range from the Hettangian to the Toarcian, which is the age applied in this study. It is frequently observed in the Lower Marrat in wells II and KK as well as in the Middle Marrat (AF, K, TT, Y, F, AL, QQ, AN, and N).

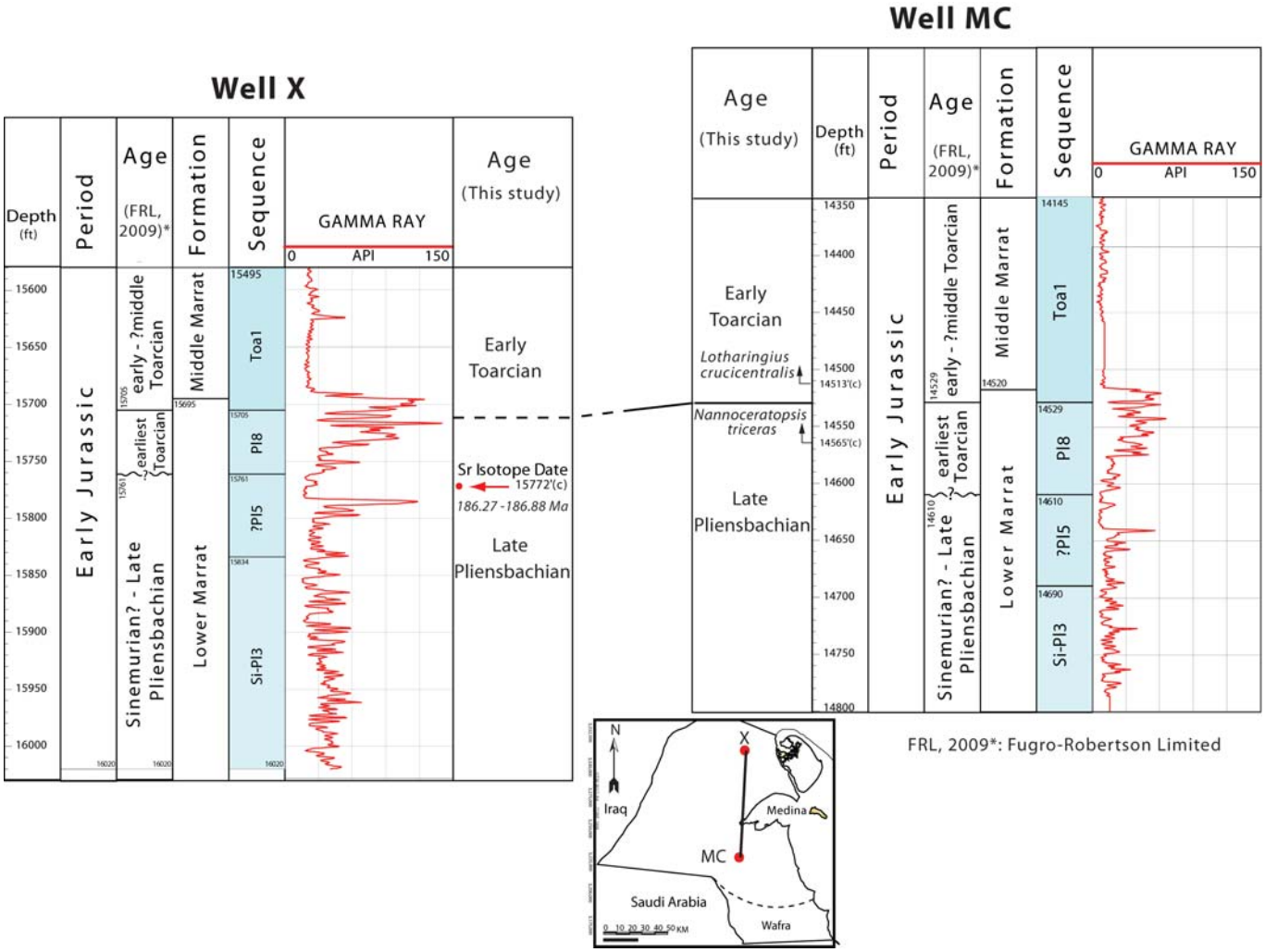

TEXT-FIGURE 18
Integrated biostratigraphy and Sr isotope stratigraphy in onshore Kuwait. Modified after Fugro-Robertson (2009).

UPPER MARRAT

Biostratigraphic data has been obtained from nine wells (AK, PC, II, SS, K, Y, G, AC and TT). The results are summarized in unpublished reports by Fugro-Robertson (2009) and Packer et al. (2015). In the former, two biozones *Bositra* sp. and *Pseudocyclammina maynci* are described, whereas in the latter no biozones were described. In this unit, recovery is generally relatively good and comprises locally common numbers of smaller benthic foraminifera with localized influxes of calcareous and agglutinating forms. Typical forms include *Lenticulina* sp., *Siphovalvulina* sp., *Textularia* sp., *Glomospira* sp., *Dentalina* sp., *Lingulina* sp., *Mesoendothyra croatica,* and *Everticyclammina praevirguliana.*

Bioevents

Sampling of the studied wells varies from high density, as in Well G where sampling is carried out at approximately 2 ft intervals to a 30–40 ft interval in Well ZZ. The upper part of this unit shows a sparse assemblage where ostracods, echinoderms and bivalves are most common, with occasional *Ophthalmidium* and miliolids. At approximately 200 ft from the top of the member in the north and 350 ft in the south, *Glomospira* spp., *Mesoendothyra* spp., *Lenticulina* spp. and *Siphovalvulina* appear. This assemblage is also common in the underlying Middle Marrat.

Pseudocyclammina maynci Hottinger 1967

This taxon is very rare and has only been recorded in Well G. The proposed age ranges from latest early Aalenian to the early Bajocian (Velić 2007). A Bajocian-Kimmeridgian range is determined by Boudagher-Fadel (2008). The age proposed by Velić (2007) in the Adriatic carbonate platform, southeast Europe, is applied in this study (text-fig. 14). This taxon defines the Upper Marrat biozone in onshore Kuwait (Fugro-Robertson 2009; Al-Sahlan et al. 2010). The upper half of this unit is characterized by a paucity of age diagnostic markers and abundance of ostracods, echinoderms and bivalves. It is not quite clear why this species was selected as the bioevent for the Upper Marrat Member since it is very rare, observed only in Well G at 14780 ft, 264 ft below the top of this unit. A questionable *Timidonella sarda* overlies this marker at 14645 ft, and *Mesoendothyra croatica* and *Siphovalvulina* spp. commonly occur at and below 14751 ft.

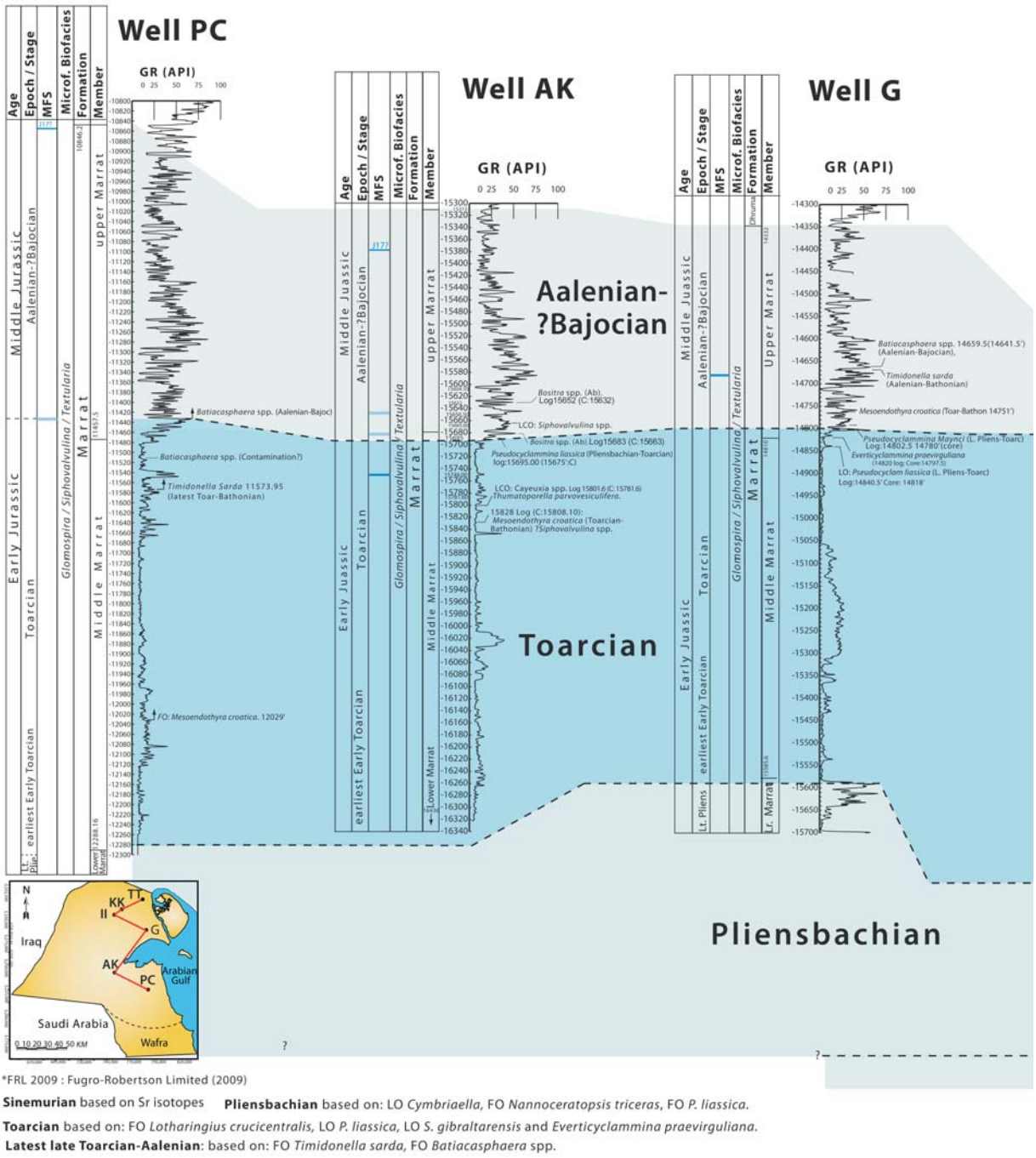

TEXT-FIGURE 19, Part 1
Biostratigraphic Regional Correlation of the Lower - Middle Jurassic Marrat Formation in onshore Kuwait.

Timidonella sarda Bassoullet, Chabrier and Fourcade 1974

This taxon has been assigned an Aalenian to Bajocian age (Velić 2007; Boudagher-Fadel 2008). Therefore, the observed forms within the Upper Marrat are Aalenian in age and considered to represent its FO. It is observed in Well G at 14645 ft, and a questionable occurrence is documented at 11573.95 ft (Middle Marrat) in Well PC.

AGE OF THE MARRAT FORMATION: A BIOSTRATIGRAPHIC AND ISOTOPE STRATIGRAPHY INTEGRATION

Scarcity of age-diagnostic bioevents and the generally poor recovery of microflora and microfauna have hindered the establishment of a practical biostratigraphic framework for the Marrat Formation. Additionally, it is known that Tethyan microfaunas of carbonate platform facies deposited on the mar-

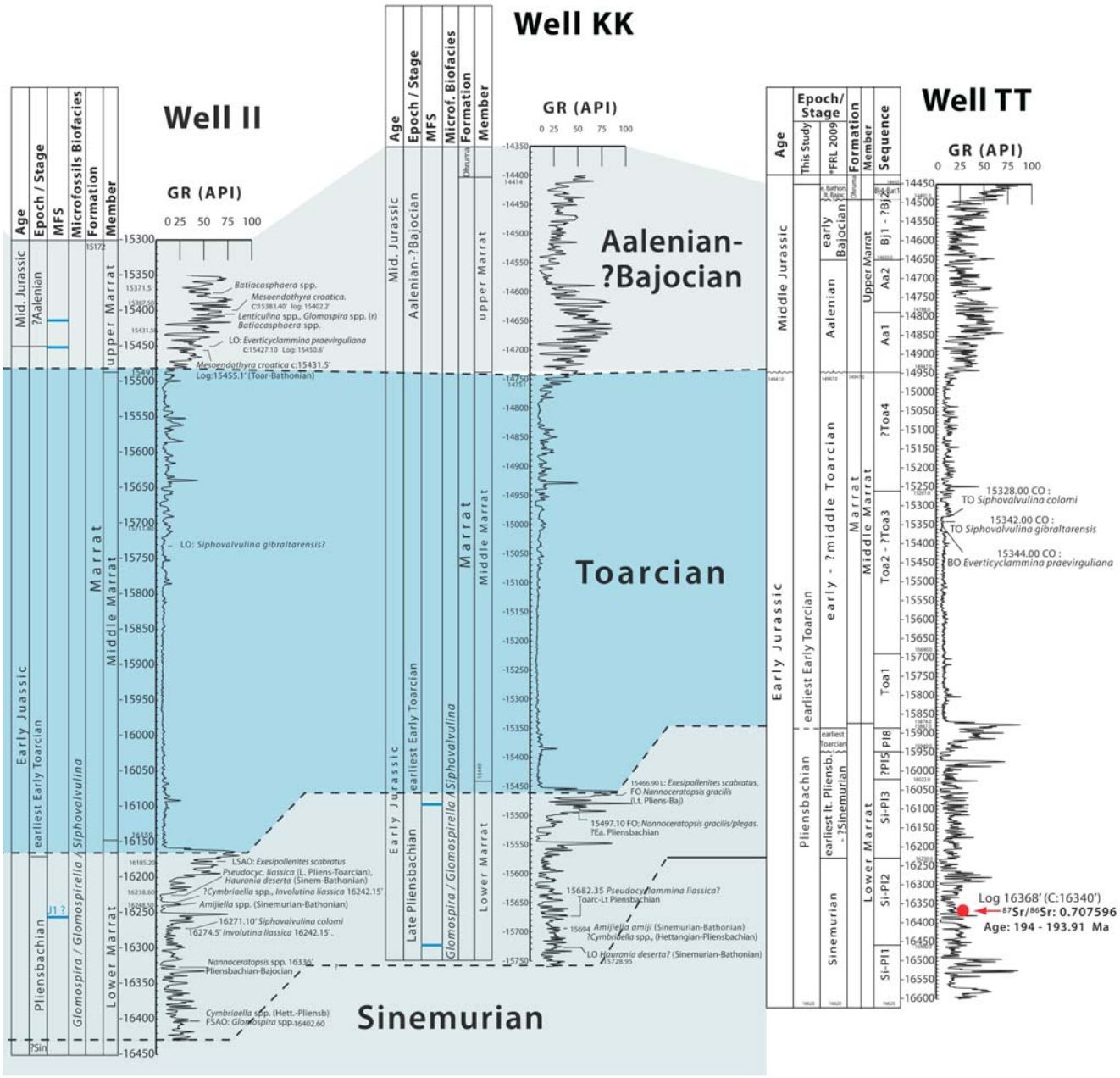

TEXT-FIGURE 19, Part 2
Continued.

gins of the Tethyan Ocean in the Early Jurassic as well as earliest Middle Jurassic show a low taxonomic diversity (Boudagher-Fadel and Bosence 2007; Velić 2007). To overcome these limitations, alternative tools such as Sr isotope stratigraphy has been incorporated, though with limited success. The base of the formation has proven challenging to determine since no bioevents are recovered from the top of the underlying Minjur Formation.

Samples studied from the uppermost Minjur and lowest 50 ft of the Lower Marrat in wells AO (12957 ft) and Q (14160–14210 ft) yielded long ranging palynomorphs such as *Corollina meyeriana* together with *E. scabratus* (text-fig. 14). In the absence of any Late Triassic age markers, an Early Jurassic - Late Triassic age is suggested for the lowermost Marrat Formation.

A low-confidence Sinemurian age based on Sr isotope analysis is proposed in a sequence stratigraphic framework presented by Fugro-Robertson (2009) where no age-diagnostic markers were observed (text-fig. 18). Only a few samples from four wells yielded coherent results within the Marrat Formation. In well TT at 16340 ft (Si-Pl2 Sequence; S J06 herein) a $^{87}Sr/^{86}Sr$ value of 0.707596 is converted to a Sinemurian age of 194.42 Ma–193.91 Ma in the Lower Marrat (Fugro-Robertson 2009). This agrees with age-diagnostic markers such as *Cymbriaella* sp., (Hettangian-Pliensbachian) and *Haurania deserta* (Sinemurian-

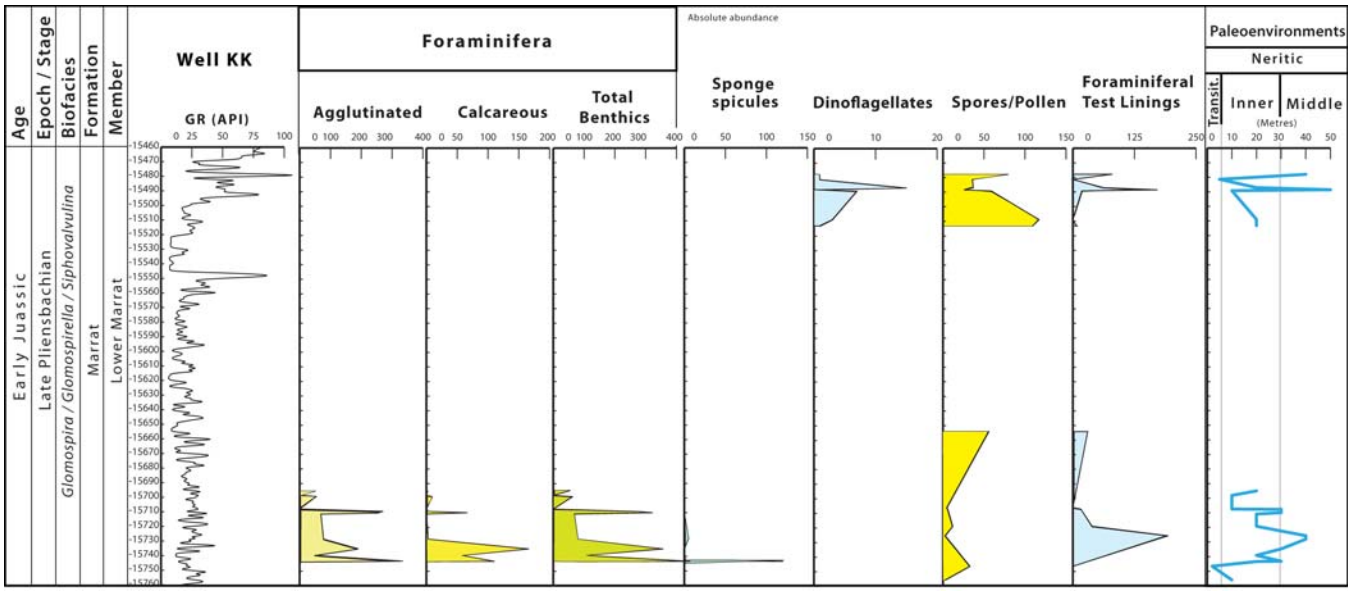

TEXT-FIGURE 20
Abundance of main microfossils groups, biofacies and paleoenvironmental interpretation in the Lower Marrat, Well KK, onshore Kuwait.

Bathonian) which co-occur in laterally equivalent intervals of wells KK and II (text-figs 15 and 16). Higher within the upper part of the Lower Marrat, a core sample from 15753–15772 ft (log) in well X, in the Sequence J10 lowstand systems tract (LST), considered to be the highstand systems tract (HST) of biosequence ?Pl5 by Fugro-Robertson (2009, *op. cit*.) yielded a Sr isotopic age of 186.27–186.88 Ma, equivalent to late Pliensbachian, early part of the ammonite zone *Fuciniceras lavinianum* (text-fig. 14). This isotopic age is in agreement with microfossil markers observed in wells KK and II where at laterally equivalent intervals, the LO of *Amijiella amiji* (Pliensbachian-Bathonian) *Pseudocyclammina liassica* (Late Pliensbachian-Toarcian) and *Cymbriaella* spp. (Hettangian-Pliensbachian) are observed (text-fig. 19).

Orbitopsella primaeva is a very rare taxon which ranges from late Sinemurian (*Oxynoticeras oxynotumis* Zone) to Pliensbachian (*Arieticeras algovianum* Zone) (text-fig. 14). In the study area, it is observed in the Lower Marrat in well AC at 15480 ft (J06 HST). This bioevent could well be considered the FO on the basis of the stratigraphic position, an interval correlated to the Well TT dated as Sinemurian using Sr isotope, 280 ft above the top of the Minjur Formation (text-fig. 19). Another long-ranging bioevent is *Cymbriaella* sp., with an assigned age of Hettangian to Pliensbachian. It has been observed higher up within the Lower Marrat and near the FO of *Haurania deserta* and *Amijiella* spp. These last two genera show a similar age range of late Sinemurian to Bathonian (text-fig. 14) and appeared in the upper half of this unit. As it is obvious, no bioevent so far mentioned enables any precise dating other than being not younger than Pliensbachian.

The appearance in the upper portion of the Lower Marrat of taxa such as *Pseudocyclammina liassica* with a shorter age range, (late Pliensbachian–Toarcian, *Fuciniceras lavinianum* to *Pleydellia aalensis* Zone), confirms a Pliensbachian age. Another bioevent considered to be no older than Pliensbachian, though it has predominantly been reported from the Toarcian, is the palynomorph *Nannoceratopsis* spp., with its FO in the Well II at 16336 ft (J06 HST), 177 ft below the top of the Lower Marrat (text-fig. 19). All the supporting biostratigraphic and isotopic evidence suggests that the Lower Marrat Unit can be assigned an age no older than Sinemurian in the lower part and Pliensbachian in the upper part (J10 TST). Likewise, a Pliensbachian or older age can be determined for most of the upper part of this unit. Within the upper part of the Lower Marrat (Sequence Toa1) in Well MC at 14565 ft, a Toarcian age was determined on the basis of palynology. Besides the occurrence of long ranging assemblages such as *Micrhystridium* sp., *Cymatiosphaera* sp., *Solisphaeridium* sp., *Deltoidospora* sp. and *?Corollina* sp., the dinoflagellate *Nannoceratopsis triceras* was observed. Williams and Bujak (1985) and several other authors agree on a FO for this taxon at the latest late Pliensbachian and not constrained to the earliest Toarcian, as was suggested by previous proprietary work (Fugro-Robertson, *op. cit.*). Williams and Bujak (1985) proposed a late Pliensbachian to Aalenian age, which is the basis to conclude a late Pliensbachian age for most of the upper part of the Lower Marrat (text-fig. 18). Additionally, the single occurrence at 14513 ft in Well MC of the calcareous nannofossil *Lotharingius crucicentralis* suggests an early Toarcian age (Mattioli and Erba 1999). The unconformity proposed by Fugro-Robertson (2009 *op. cit.*) at the base of their P18 Sequence cannot be corroborated since *N. triceras* ranges down into the latest Pliensbachian and *L. crucicentralis* has its FO during the earliest Toarcian. In this study, the base of Pl8 is correlated to the base of J10 TST and represents a lateral facies shift, i.e., a type 2 unconformity.

The latest Pliensbachian to earliest Toarcian age has been extrapolated throughout the study area, in the absence of additional age-diagnostic markers. The position of *Lotharingius crucicentralis* however, may fall within the topmost Lower Marrat (no core shift is available for Well MC) in which case the uppermost Lower Marrat could be earliest Toarcian. Higher within the Middle Marrat, there is a prevalence of *Sipho-*

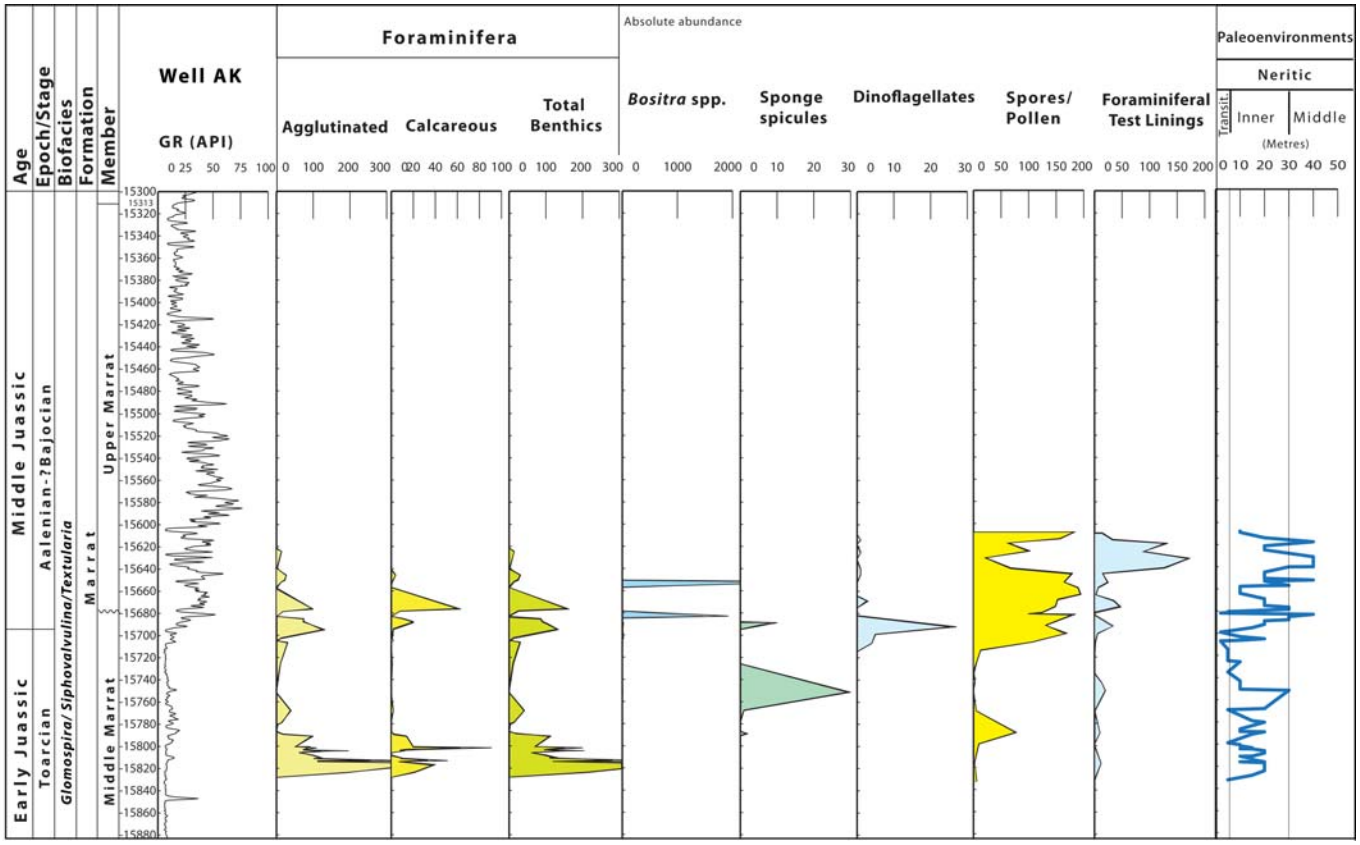

TEXT-FIGURE 21
Abundance of main microfossils groups, biofacies and paleoenvironmental interpretation in the Middle and Upper Marrat Units, Well AK, onshore Kuwait.

valvulina species together with *Pseudocyclammina liassica* and *Everticyclammina praevirguliana*. The last two species, though long-ranging, have their LO at the top of the Toarcian but cannot be used to delimit the top of the Pliensbachian-base of Toarcian. The FO of *Mesoendothyra croatica,* with an age range of Toarcian to Bathonian (Velić 2007), is the best candidate to suggest a Toarcian age. Its lowest appearance is observed in Well PC at 12029 ft, 259 ft above the base of the Middle Marrat. Therefore, on this basis and considering the previously described FO of *L. crucicentralis* in Well MC (text-fig. 18), a Toarcian age is assigned to the lower part of the Middle Marrat. This agrees with assemblages such as *E. praevirguliana, Siphovalvulina gibraltarensis,* and *Siphovalvulina* spp. (text-fig. 19). These taxa, though long-ranging, constitute reliable bioevents since their LOs are assigned at the top of the Toarcian (Velić 2007; Boudagher-Fadel 2008).

The upper part of the Middle Marrat Member (S J16 herein) has moderately common to abundant microfauna. They are composed primarily of indeterminate agglutinates, *Textularia* sp., *Siphovalvulina* sp., *Siphovalvulina gibraltarensis, Pseudocyclammina liassica* and abundant echinoderm and bivalve fragments. Ostracods are rare and *Bositra* sp. begins to appear. On the basis of the LOs of *S. gibraltarensis, P. liassica* and *Everticyclammina praevirguliana* a Toarcian age can be assigned to the upper part of the Middle Marrat. An unconformity is proposed based on sedimentological criteria at the base of the Upper Marrat in Well G (Fugro-Robertson 2009; Packer et al. 2015) and karst features indicative of an unconformity have been identified at this contact in core studies of other wells in Kuwait (Kadar et al. 2015) where the unit reaches a maximum thickness of 550 ft. Different lithofacies above and below the boundary further support emergence during that time. A hiatus from the late Toarcian to latest Aalenian is recognized in the Saudi Arabian outcrop belt (Powers 1966; Issautier et al. 2012a, 2012b), suggested by Le Nindre et al. (2003) as evidence of basin margin uplift. Paleogeographic reconstruction carried out on Middle-Upper Jurassic sediments in the study area reveals significant biostratigraphic and paleoenvironmental differences when compared to Saudi Arabia (Crespo de Cabrera et al. 2020). Depositional environments of the Marrat Formation in outcrop sections in Saudi Arabia vary from continental meandering fluvial deposits to tidal or wave-dominated mixed carbonate-siliciclastic inner-platform deposits (Al-Mojel et al. 2018). Progradation of the prevailing marine carbonate-neritic settings observed during this time in the study area could account for a shorter period of continental emergence and a briefer interruption in sedimentation. Most or all of the Aalenian absent in Saudi Arabia is present in Kuwait.

It is apparent that the use of benthic microfauna for biostratigraphy is limited by lack of calibration with ammonite zones. Nonetheless, in more recent research within the Tethyan realm, benthic microfossils occasionally have been calibrated by other

means, i.e. isotopic studies (Boudagher-Fadel and Bosence 2007). Dinoflagellates have also been useful to calibrate these benthic bioevents. *S. gibraltarensis* and *E. praevirguliana* have been widely studied (Boudagher-Fadel 2008; Velić 2007) and the age ranges applied in the current study is the one that better adapts to the observed distribution and co-occurrence with other bioevents. In both taxa, Velić's (2007) interpretation is the better option, considering their distribution within the formation. Both bioevents have their LO during the Toarcian.

Timidonella sarda, though scarce, is another piece of evidence to suggest more continuous sedimentation than has been proposed. The age of this taxon is latest Toarcian to Bathonian, with a FO starting at the *Grammoceras thouarense* ammonite zone and not in the Aalenian, as was used in previous studies (Fugro-Robertson 2009; Packer et al. 2015). A questionable FO of *Timidonella sarda* is observed in well PC at 11593.75 ft, in the upper part of the Middle Marrat. In well G, *T. sarda* occurs at 14645.0 ft within the Upper Marrat. In both cases, it appears within the assigned age range (Toarcian-Bathonian), although the FO in the Middle Marrat would be evidence of sedimentation during the Late Toarcian.

The dinoflagellate *Batiacasphaera* sp. is characteristic of ammonite-dated Aalenian assemblages documented from southern Germany (Burkhalter et al. 1997). It has been dated as 174.2 Ma (text-fig. 14) or base of the Aalenian, using the GTS 2012 timescale (Gradstein et al. 2012). This taxon is observed in wells EE, G, II, PC, KK, K, SS and VV. It is scarce to common throughout the Upper Marrat with its FO in the lowermost portion of this unit, except for an anomalous FO in Well PC within the upper Middle Marrat (Packer et al. 2015, *op. cit.*). This anomaly will need a careful review since it falls within sediments of Toarcian age, differing from the known range of this dinoflagellate.

With the observed bioevents, it is not possible to assess the exact time within the Aalenian or the corresponding ammonite zone in which this unit was deposited. It is nonetheless worth mentioning that *Batiacasphaera* occurs consistently from the lowermost Upper Marrat; in well VV its FO is at 14634.0 ft, ten feet above the base of the member. Its LO is observed in well G at 14636 ft, approximately 300 feet from the top of the Upper Marrat Member (text-fig. 19).

The overlying Dhruma Formation has been assigned an early Bajocian age (Crespo de Cabrera 2019, 2020) which suggests an Aalenian to earliest early Bajocian age for the Upper Marrat Member. Considering the time involved in the Aalenian, thickness of the unit and assuming sedimentation rates in the range of 150.0-66.0 ft/myr for the Upper Marrat (AL-Wazzan et al. 2021; Hawie et al. 2020) there was probably no major time break in sedimentation associated to the Toarcian-Aalenian unconformity. The upper range of 150 ft/myr would yield 600 ft thickness which is a value close to the maximum thickness observed towards the east in onshore Kuwait. This, however, does not exclude the possibility of a longer hiatus in different portions of the study area.

Another bioevent which would enable constraining an Aalenian age to the Upper Marrat consists of the presence of the dinoflagellate *Dissiliodinium,* considered to have a FO in the Upper Aalenian (*Ludwigia murchisonae* ammonite Zone). A questionable occurrence observed in well PC at 11630.0 ft is considered to be contamination. In well SS in the middle portion of the Upper Marrat a questionable specimen is recorded at 14982.0 ft as well as another questionable occurrence at 14630.0 ft in well VV. This taxon only confirms the Aalenian age assigned on the basis of *Batiacasphaera* spp. which occurs four feet below at 14634.0 feet.

Additional taxa used to define the Toarcian/Aalenian boundary (Fugro-Robertson 2009; Packer et al. 2015) such as *Everticyclammina praevirguliana* and *Mesoendothyra croatica* could provide some age constraint. The LO of the former is used to delineate the top of the late Toarcian, whereas the latter has a FO in the Toarcian and not in the Aalenian as previously assigned (Sartorio and Venturini 1988 and GTS 2012; Fugro-Robertson 2009; Packer et al. 2015). It has been documented throughout the Middle and Upper Marrat units (Truskowski et al. 2015).

PALEOECOLOGY

The paleoecological interpretation is fragmented due to the discontinuous availability of core sections, with most sampling concentrated in the Middle Marrat Member. Various microfossil biozones have been defined throughout the Tethyan realm for the Lower Jurassic but especially in carbonate platforms such as those found in Spain, Morocco, Italy and southeast Europe (Velić 2007; Boudagher-Fadel 2008; Sartorio and Venturini 1988; Fugagnoli 1999). In Saudi Arabia, the Marrat Formation was deposited on a continental to shallow-marine platform located in the tropics on a passive margin facing the Neo-Tethys Ocean (Murris 1980). No biozonation has been attempted for the Triassic section.

Marine shallow water conditions have been interpreted for the Minjur Formation with the most distal conditions proposed based on abundance of leiospheres, dinoflagellate cysts and microforaminiferal test linings (Stancliffe 1996; Digbehi et al. 2012; Packer et al. 2018, 2019). In the Middle Carbonate Member, paleobathymetry of inner-middle neritic are interpreted during early Norian time. Generally, a shallowing trend is observed in the upper half of the formation. In the uppermost Minjur Upper Member, non-marine conditions are interpreted in the north and northwest, though deeper neritic paleobathymetry is observed towards the south.

The Marrat Formation has been divided into microfossil units (Fugro-Robertson 2009) as follows: *Amijiella amiji* Zone (Pliensbachian-Toarcian), *Siphovalvulina* spp. Zone (Toarcian), *Pseudocyclamina maynci* Zone (Aalenian) and *Bositra* spp. Zone (Bajocian). In some instances, the index taxon is very scarce, or occurs throughout different units with little use for correlation. This stems from the fact that most microfossils are long ranging and observed throughout the different units. It is nonetheless possible to differentiate biofacies which could support paleoenvironmental interpretation. These have been determined based on the abundance of the prevailing taxa, regardless of their biostratigraphic significance. The microfossils observed in the Marrat Formation are mainly smaller and include scarce larger benthic foraminifera indicative of marine shallow water conditions, scattered miliolids and rare calcareous forms, composed mainly of nodosariids. Low faunal abundances and diversity suggest variable, adverse paleoenvironmental conditions; the frequency of anhydrite deposits (Fugro-Robertson 2009, *Op. Cit*.) indicate fluctuations in salinity.

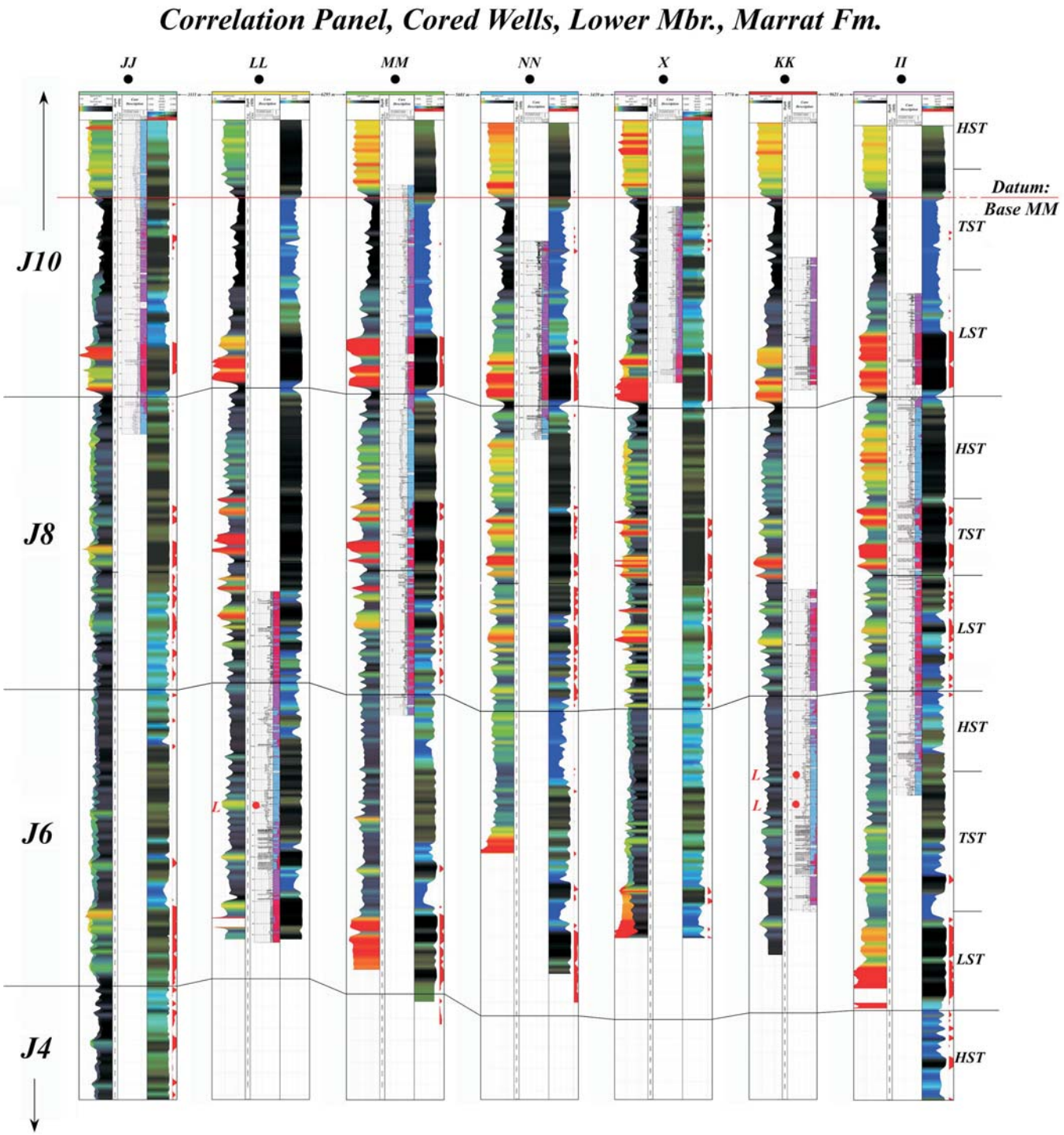

TEXT-FIGURE 22
Correlation panel through wells with cored sections of the Lower Marrat. The base of Sequence J4 is not shown. GR logs (left side of log track) have been normalized to show clean carbonates and anhydrite as red. Red shading of the density log values > 2.8 (right side, where available) indicates anhydrite. Cored sections are shown in center track. The neutron-density log was unavailable in Well KK. Abbreviations: LST, lowstand systems tract; TST, transgressive systems tract; HST, highstand systems tract; MM, Middle Marrat; L, *Lithiotis* occurrence.

Biofacies

Glomospira / Glomospirella / Siphovalvulina

This biofacies is identified in the Lower Marrat Unit where additional forms such as *Amijiella amiji, Haurania* sp. *Aeolisaccus* sp., and *Involutina liassica* are observed. Other common organisms include ostracods, bivalve fragments, sponge spicules and echinoderms. Small foraminifera such as those observed in this biozone were widespread on the platform and tolerant to a wide range of paleobathymetries, from inner platform to lagoonal and open marine settings (Septfontaine 1984; Fugagnoli 2004; Hughes 2004). Others such as *Involutina liassica* occurred throughout the Lower Jurassic deposits, but only in the rocks originating at the platform margins and slopes. Taxa such as *Haurania, Amijiella* on the other hand, indicate established shallow warm waters along Tethys in that period of the Early Jurassic (Boudagher-Fadel 2008). In this unit, paleobathymetry is determined based on the most common or abundant taxa, integrated with the occurrence of other forms such as dinoflagellates, spores and pollen, sponge spicules and foraminiferal test linings (text-figs 20 and 21, wells KK and AK). This approach should enable determining a more precise paleoenvironmental interpretation, considering the ample range of sedimentary environments tolerated by this assemblage. The common presence of anhydrites indicates a sabkha environment which would explain the occurrence of many barren samples. Shallow-water inner neritic paleobathymetry prevailed for most of the studied interval, but deeper middle neritic conditions at the lower and uppermost part of the biofacies coincided with peak abundances in microforaminiferal test linings and benthic foraminifera (text-fig. 20).

Glomospira / Siphovalvulina / Textularia

This biofacies is documented from the Middle Marrat and lowermost Upper Marrat. Besides the index taxa, this interval is characterized by abundant but less persistent *Mesoendothyra, Glomospirella, Aeolisaccus,* nodosarids and *Bosniella* sp. Other forms such as *Bositra* spp. start to appear, together with occasional *Lenticulina* spp. and more frequent *Nodosaria* spp. Miscellaneous microfossils such as ostracods, echinoderms and bivalves are generally abundant. Paleoenvironments are more distal when compared to the Lower Marrat. Paleobathymetry is generally deeper, ranging between inner to middle neritic, especially in the upper part of the biofacies corresponding to the lowermost Upper Marrat, where dinoflagellates and foraminiferal test linings tend to be more abundant. The appearance of the bivalve *Bositra* spp. indicates pelagic sedimentation with a paleobathymetry probably exceeding 50 m (Hart et al. 2012).

The upper half of the Upper Marrat unit lacks proper biostratigraphic study since six out of the eight studied wells were only cored in the lower half of the unit. Only two wells located in the northern area (Y and TT) contain a few samples from the whole unit. Thirteen samples along a 454 ft interval were studied in Y and twelve samples throughout a 456-foot interval in TT (Fugro-Robertson 2009, *op. cit*). No biofacies are described for the upper part of the Upper Marrat since most of the samples were barren of foraminifera, containing only occasionally common to abundant bivalves, echinoderms and ostracods. In both wells (Y and TT) this assemblage indicates a general shallowing trend from predominantly inner to middle neritic in the lower part of the Upper Marrat to mainly transitional, probably lagoonal conditions, towards the upper part of this unit. More detailed, higher density sampling of well AK (text-fig. 21) however, shows that biofacies *Glomospira / Siphovalvulina / Textularia* has a general deepening trend, from the upper part of Middle Marrat to the lower part of the Upper Marrat Member, indicating shorter term sea-level fluctuations within the Upper Marrat unit.

***Lithiotis* Bivalves**

Reef-building scleractinian corals were one of the casualties of the end-Triassic extinctions. Scleractinian reefs were consequently rare in the Early Jurassic. In their absence, microbes and other groups partially filled these vacant niches. One group which appeared during this time interval was the family of aberrant pterioid bivalves containing the genus *Lithiotis* and several other genera (Fraser et al. 2004).

Occurrences of "*Lithiotis*" facies bivalves are almost exclusively reported from the Tethyan realm, with the exception of some localities in Oregon, California and Nevada, USA (Dickinson and Vigrass 1965; Taylor 1982; Fraser et al. 2004; Posenato et al. 2018). In the Middle East, *Lithiotis* beds are reported by several authors (van Bellen et al. 1959 [2004]; James and Wynd 1965; Setudehnia 1972). The known range of "*Lithiotis"* facies bivalves is predominantly Pliensbachian to early Toarcian. Posenato et al. (2018) report that *Lithiotis* bivalves disappear abruptly in beds marking the onset of the Toarcian Oceanic Anoxic Event (T-OAE) in southern Italy.

In the Middle East, van Bellen et al. (1959) described an occurrence of "*Lithiotis* beds" in outcrops of the middle unit of the Sehkaniyan Formation, informally named the "*Lithiotis* limestone." In these beds, *Lithiotis* occurs with a *Spiriferina* fauna similar to one reported by Kent (1951) from southwestern Iran and thought to be Late Liassic in age (van Bellen et al. 1959, p. 190). The term Liassic dates from a time when the Lower, Middle and Upper Jurassic were named the Lias, Dogger and Malm, respectively, and will not be used in the remainder of this paper. The *"Lithiotis* limestone" of the Sehkaniyan was correlated to the Mus Formation in the subsurface of Iraq. A *Spiriferina* fauna also occurs in the Marratt Formation in the outcrop belt of Saudi Arabia and based on that occurrence van Bellen et al. (1959 [2004], p. 147) assigned a probable upper Liassic age to the Mus and tentatively correlated it to the Marrat of Saudi Arabia, dated by ammonites as Toarcian in age (Arkell 1952; Enay et al. 1987).

James and Wynd (1965) also reported the occurrence of *Lithiotis* from SW Iran, where it occurs with *Megalodon,* just above the base of the Surmeh Formation, unconformably overlying the Neyriz Formation. These occurrences were assigned a Late Liassic age. Occurrences of *Lithiotis* bivalves were recorded in the Lower Marrat (J 04 TST) in the subsurface of Kuwait and are dated herein as early or earliest Pliensbachian based on foraminifers. *Lithiotis* has not been identified from the Middle Member of the Marrat Formation in Kuwait or the Marrat outcrop belt of Saudi Arabia. Bendias and Aigner (2015) have recently reported multiple occurrences of *Lithiotis* in both the Upper and Lower Members of the Mafraq Formation in Oman. They note that the unpublished Jurassic biostratigraphic zonation used in Oman is based mostly on published literature and not on thin section study. If their identifications and ages can be confirmed, however, the range of the lithiotids could be extended to as old as Hettangian and as young as Bajocian.

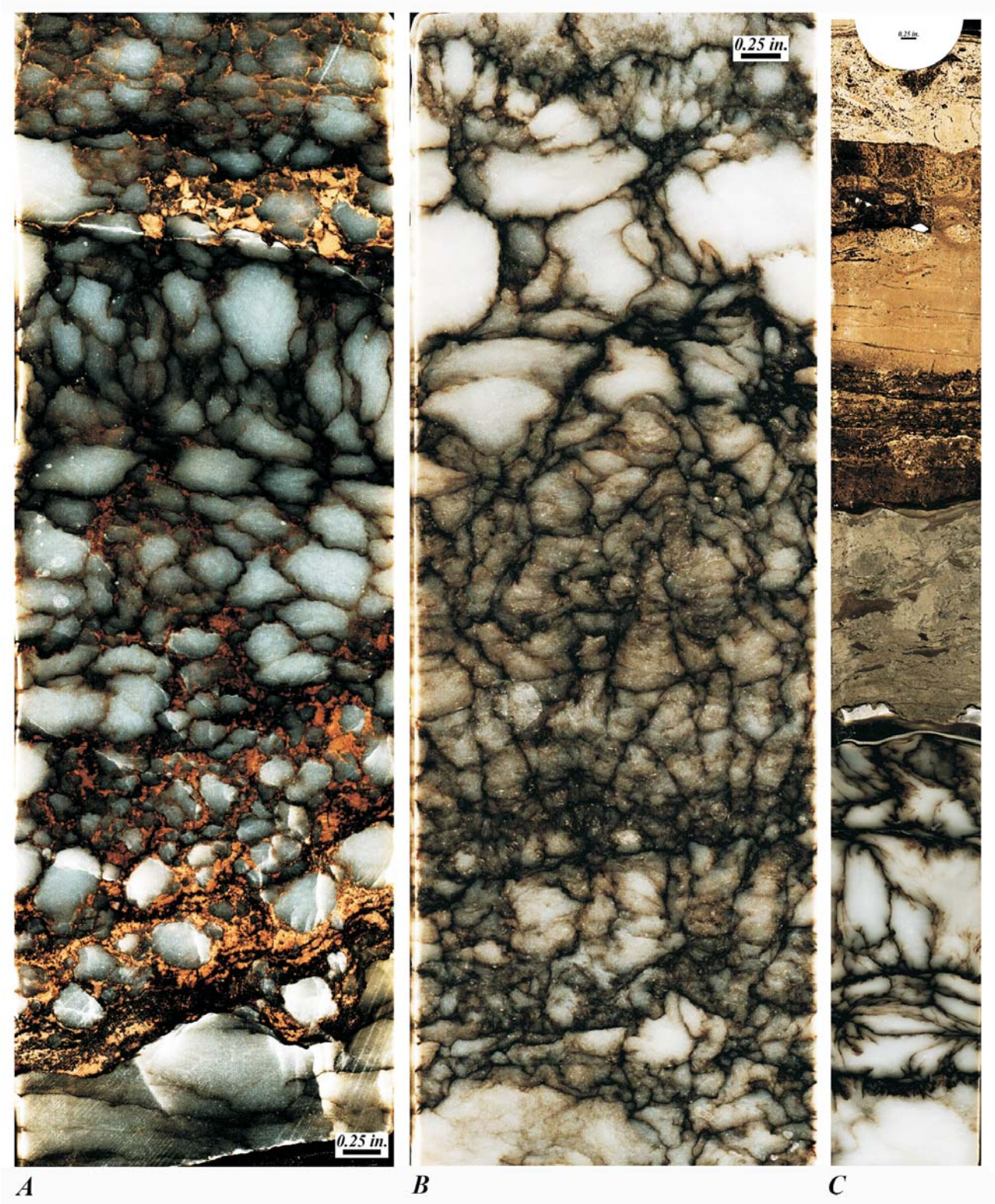

TEXT-FIGURE 23
Scanned images of core slabs from Well LL, showing lithofacies characteristic of the massive anhydrite unit of the LST of Sequence J06. (A) Nodular anhydrite typical of "chicken wire" fabric representative of sabkha depositional setting, becoming palmate upward, interrupted by thin microbial intervals (reddish in color) of probable intertidal setting (M.D., core, 15783.0–15783.7 ft). (B) Mixture of nodular and palmate anhydrite suggestive of ponded, intermittently flooded sabkha depositional setting, with upward growth of individual crystals through successive sedimentary surfaces (M. D., core, 15774.65 to 15775.35 ft). (C) Photomosaic showing abrupt contact of upright palmate anhydrite crystals (subaqueous) overlain by intertidal to subtidal, bioturbated mudstones and wackestones at contact with base of Sequence J06 TST (rounded hole at top is from removal of core plug) (M. D., core, 15768.9 to 15770.35 ft)

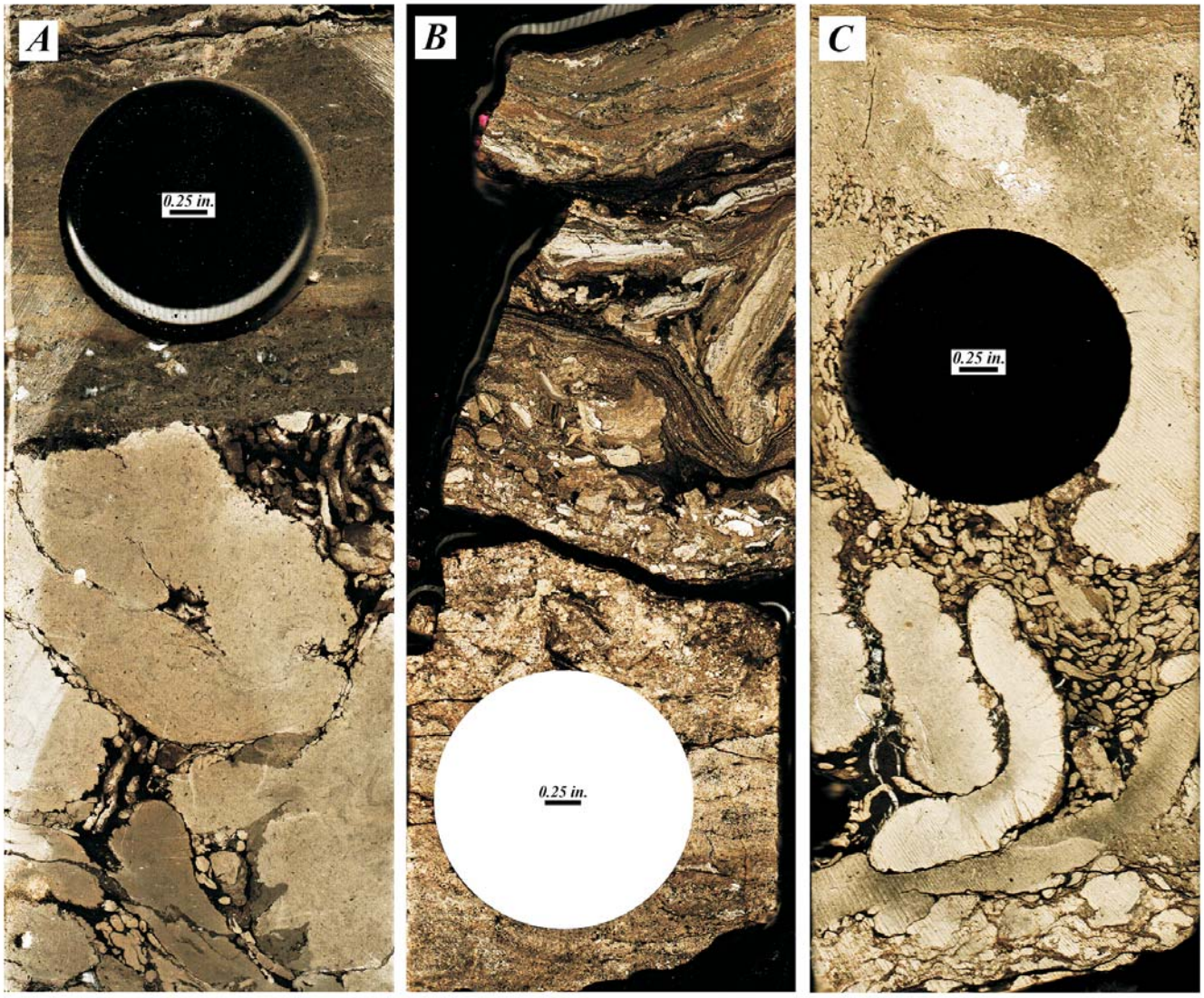

TEXT-FIGURE 24
Scanned images of core slabs, showing the breccia bed at the base of the J08 LST: (A) Well II, 16351.0 to 16351.6 S15351.0 to15351.6 ft; (B) Well KK, 15663.0 to 15663.65 ft; and (C) Well MM, 15924.85 to 15925.5 ft.

BIOSTRATIGRAPHIC SUMMARY

Age determination of the Minjur Formation has been debated due to the paucity of biostratigraphic publications in the region. Additionally, most of the well-defined markers from the recognised palynozonation schemes are only occasionally recorded (Douban et al. 2001; Packer et al. 2019). The unpublished palynological data from Robertson Research (2000, *op. cit.*) show a series of Triassic or older bioevents in the Upper Minjur Member, which these authors interpreted as a reworked assemblage, assigning an Early Jurassic age for the top of the Middle Carbonate and Upper Minjur Members. Recent work (Packer et al. 2018, 2019) proposed a different age interpretation, based on the recurrent appearance at the same stratigraphic level in several wells of species such as *Lunatisporites* spp., *Vesicaspora schemeli* and *Kyrtomisporis corrugatus.* The uppermost Upper Minjur Member is assigned an undifferentiated Early Jurassic-Late Triassic age since the assemblage basically consists of *Corollina* spp. (*C. torosus* and *C. meyeriana*) with questionable *Lunatisporites* spp. and *Kyrtomisporis* spp. The Late Triassic Rhaetian-Norian age assigned to the remaining of the Upper Minjur is based on *Lunatisporites* sp. and *Vesicaspora schemeli,* together with *Rhaetogonyaulax* sp. and *Kyrtomisporis corrugatus.* A Norian age is determined for the underlying Middle Carbonate Member on the basis of *Rhaetogonyaulax* spp. and *Minutosaccus crenulatus.* The Lower Minjur Member is assigned a Carnian-Norian age based on the LO of *Samaropollenites speciosus* co-occurring with *Patinasporites densus* (Carnian-Rhaetian) and *Elongatosaccites triassicus* (Norian-Rhaetian).

Age assignment for the Marrat Formation is complicated by the paucity of age-diagnostic markers, where long ranging benthic assemblages prevailed. The lower part of the Lower Marrat is devoid of biostratigraphic age-diagnostic markers. As an alter-

TEXT-FIGURE 25
Scanned images of core slabs from Well LL, showing subtidal microbial growth forms: (A) Stromatolitic microbial growth form with subaqueous anhydrite (Well LL, 15752.85–15753.25 ft); (B) Smaller, thinly laminated, stromatolitic growth framework (Well LL, 15737.0–15737.8 ft).

native, a date obtained from $^{87}Sr/^{86}Sr$ isotopes (194.42–193.91 Ma) has been used to assign a Sinemurian age to this unit. Pliensbachian is determined for the upper part of the Lower Marrat based on a few bioevents such as *Orbitopsella primaeva,* the LO of *Cymbriaella*, FO of *Nannoceratopsis triceras* and the FO of *P. liassica*. A Sr Isotope date of 186.27–186.88 Ma (Late Pliensbachian) agrees with the observed bioevents within this interval. In the uppermost Lower Marrat, the dinoflagellate *Nannoceratopsis triceras* underlies another age-diagnostic marker found at the base of the Middle Marrat, *Lotharingius crucicentralis,* which indicates an earliest Early Toarcian age.

Higher within the Middle Marrat, the FO of *Mesoendothyra croatica* is observed. Additional assemblages within the upper part of this unit include *E. praevirguliana, Siphovalvulina gibraltarensis,* and *P. liassica*, with their LO during the Late Toarcian. Within the lower part of the Upper Marrat, an Aalenian age is assigned based on the FO of *Batiacasphera* spp. which does not range below the Aalenian. Considering additional bioevents such as the FO of *Timidonella sarda,* which is considered as Late Toarcian within the top of the Middle Marrat, no significant time seems to be missing at the Middle-Upper Marrat Unconformity. This could well be supported by estimates of sedimentation rates carried out in recent stratigraphic modelling for this formation (Al-Wazzan et al. 2021; Hawie et al. 2020).

Using shallow water marine palynomorphs, transitional to inner neritic conditions have been determined for the Minjur Formation. The most distal, offshore environments are identified based on dinoflagellates and microforaminiferal test lining abundances; microfossils and calcareous nannofossils are very scarce or absent. The different units of the Marrat Formation are interpreted as fluctuating between shallow water conditions to sabkha-tidal flat for the Lower Marrat. The biofacies *Glomospira / Glomospirella / Siphovalvulina* is identified for this unit.

Benthic assemblages for most of the Middle Marrat suggest relatively shallow marine, transitional to inner neritic environments and the biofacies *Glomospira / Siphovalvulina / Textularia* is determined. The interpreted deeper conditions for the lower part of the Upper Marrat are based on the appearance of the pelagic bivalve *Bositra* spp. at the base of this unit. Lack of cores in the upper half of the Upper Marrat member prevents any paleoenvironmental interpretation, though the scarce data indicates probable lagoonal conditions and an overall shallowing trend for this interval.

SEDIMENTOLOGY AND SEQUENCE FRAMEWORK

Minjur Formation

Issautier and others (2012a, 2012b) have studied the Minjur Formation in detail, measured additional sections and mapped the depositional settings along the outcrop belt. They identified additional lithofacies and determined that the Minjur contains a succession of depositional settings: fluvial, coastal plain, tidal flat, and lagoon (Issautier et al. 2012a). They subdivided the Minjur into two 2nd-order sequences, referred to as the Lower and Upper Assemblages. They suggested that the lower portion (sequence 1) of the Lower Assemblage is equivalent to the upper Jilh Formation as previously mapped. The remaining three sequences of the Lower Assemblage were classified as 3rd-order sequences comprised mostly of coastal and marginal marine lithofacies, dated as Norian to Rhaetian in age. The Upper Assemblage, consisting of five 3rd-order sequences, is almost exclusively coarse siliciclastics (Issautier and others, 2012a). The Upper Minjur has not been biostratigraphically dated in outcrop and has been considered Triassic in age (Al-Mojel et al., 2018; Farouk et al. 2018). Paleontologic data, lithostratigraphy and sequence stratigraphy all support the existence of two 2nd-order sequences, one Upper Triassic and the other Early Jurassic, in the subsurface and argue for an early Jurassic age for the non-marine sandstone section at the top of the Minjur in outcrop exposures.

Reid et al. (2015) reported on a set of three shallow core holes, drilled on successive basinward escarpments southwest of Riyadh, Saudi Arabia. They were drilled in an area transitional between siliciclastics to the southeast and carbonates to the northwest and, with considerable overlap, provided a complete section from the top of the Minjur nearly to the top of the Dhruma Formation. The cores and the logged boreholes were comprehensively studied and carefully spliced together to form a single composite reference section. Microfossils recovered from fine-grained siliciclastics immediately below the Marrat carbonates in the new reference section were dated as late Pliensbachian to earliest Toarcian (Reid et al. 2015).

More recently, Stewart et al. (2016) extended the work of Issautier et al. (2012a) into the subsurface of Saudi Arabia and published a chronostratigraphic section accompanied by biostratigraphic data. They showed the Minjur Sandstone as consisting of two 2nd-order sequences, following Issautier and others (2012a, 2012b), with the Lower Minjur being latest Carnian to Rhaetian in age, equivalent to the upper portion of the Jilh Formation and the entire Minjur Formation as defined in Kuwait, i. e., Upper Triassic. The Upper Minjur was shown as Sinemurian to Pliensbachian in age, separated from the Lower Minjur by a hiatus encompassing the late Rhaetian, Hettangian and early Sinemurian, and conformably overlain by the Marrat Formation as defined in Saudi Arabia (Toarcian) (Stewart et al. 2016, their Fig. 4). They included a seismic section and a log cross-section showing onlap and thinning across the Qatar Arch and thickening into the Rub' Al-Khali basin to the south (Stewart et al. 2016, their Figs. 4, 5 and 6).

Issautier et al. (2019, Figure 3) reclassified the nine 3rd-order sequences described by Issautier et al (2012a, 2012b) as 4th-order, grouping them into three 3rd-order and two 2nd-order sequences. Like Issautier et al. (2012a, 2012b) they consider Sequence 1 to be the upper beds of the underlying Jilh Formation. They extended this depotectonic model for Minjur deposition into the subsurface as far as northeastern Saudi Arabia and published a log and lithofacies cross-section with biostratigraphic data. They recognized and correlated the Lower and Upper Minjur and correlate these units and the cycles recognized by Issautier et al. (2012a) from surface to subsurface. Their biostratigraphic data show the Upper Minjur to be the lateral equivalent of the Lower Marrat in Kuwait. Their isopach map of the Minjur clearly shows a northeastward-oriented sedimentary basin which likely continues into Kuwait (Issautier et al. 2019, Figure 11).

Sharland et al. (2001) originally placed their youngest Triassic MFS (Tr80) in the Upper Triassic and their oldest Jurassic MFS (J10) in the uppermost shales of the Lower Marrat, just below the base of the lithostratigraphically defined Middle Marrat.

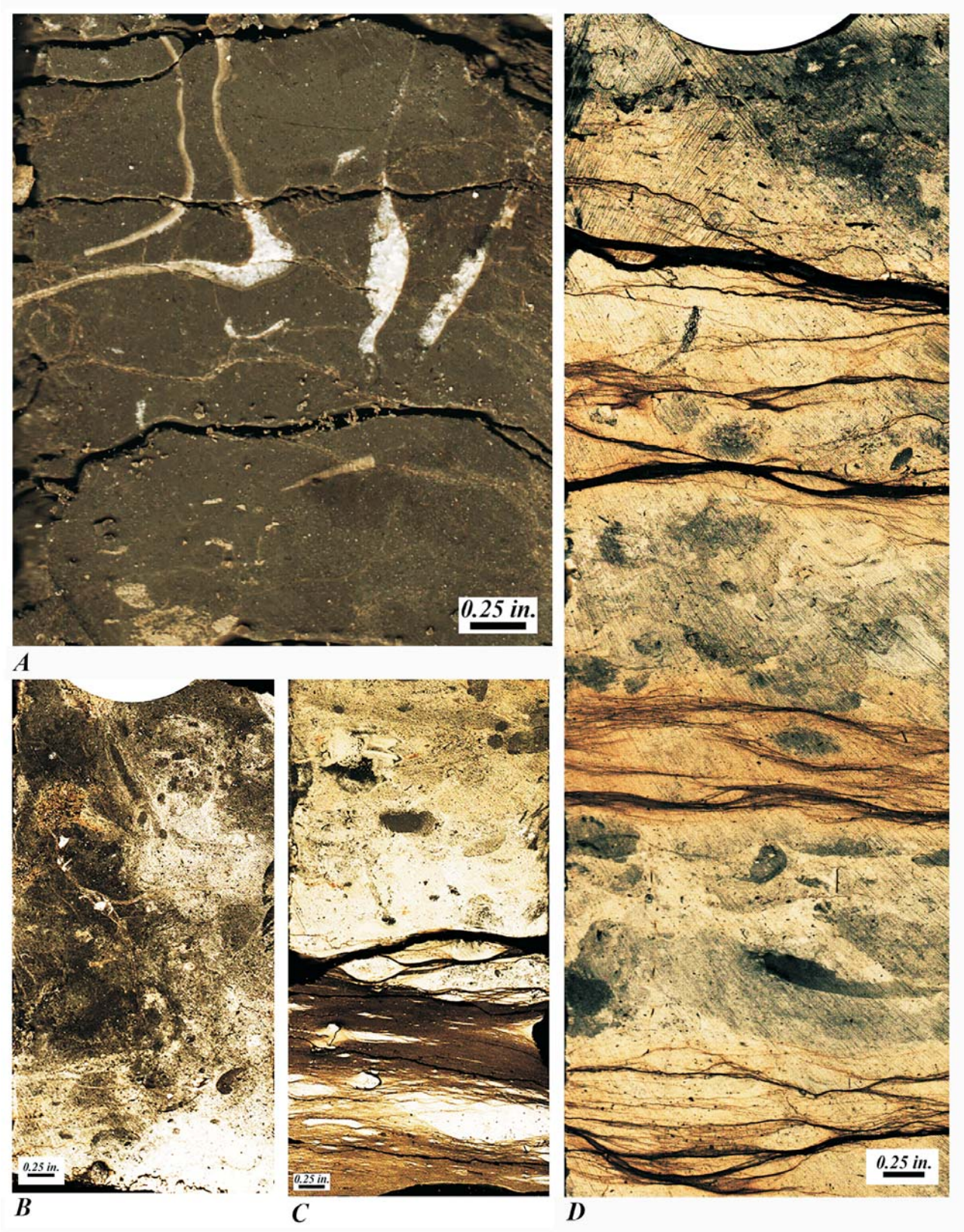

TEXT-FIGURE 26
Scanned images of core slabs from Well KK, showing lithofacies of the J06 TST and HST: (A) Skeletal wackestone to mud-dominated packstone with *Lithiotis* sp. shells (15710.3–15710.6 ft); (B) burrowed, peloidal skeletal wackestone deposited in shallow subtidal lagoonal environment (15709.2–15709.8 ft); (C) ripple-laminated, argillaceous peloidal mudstone of shallow subtidal environment, moderately bioturbated (15702.3–15703.0 ft); (D) alternately burrowed and ripple-laminated argillaceous mudstone to peloidal wackestone (15698.2–15699.0 ft).

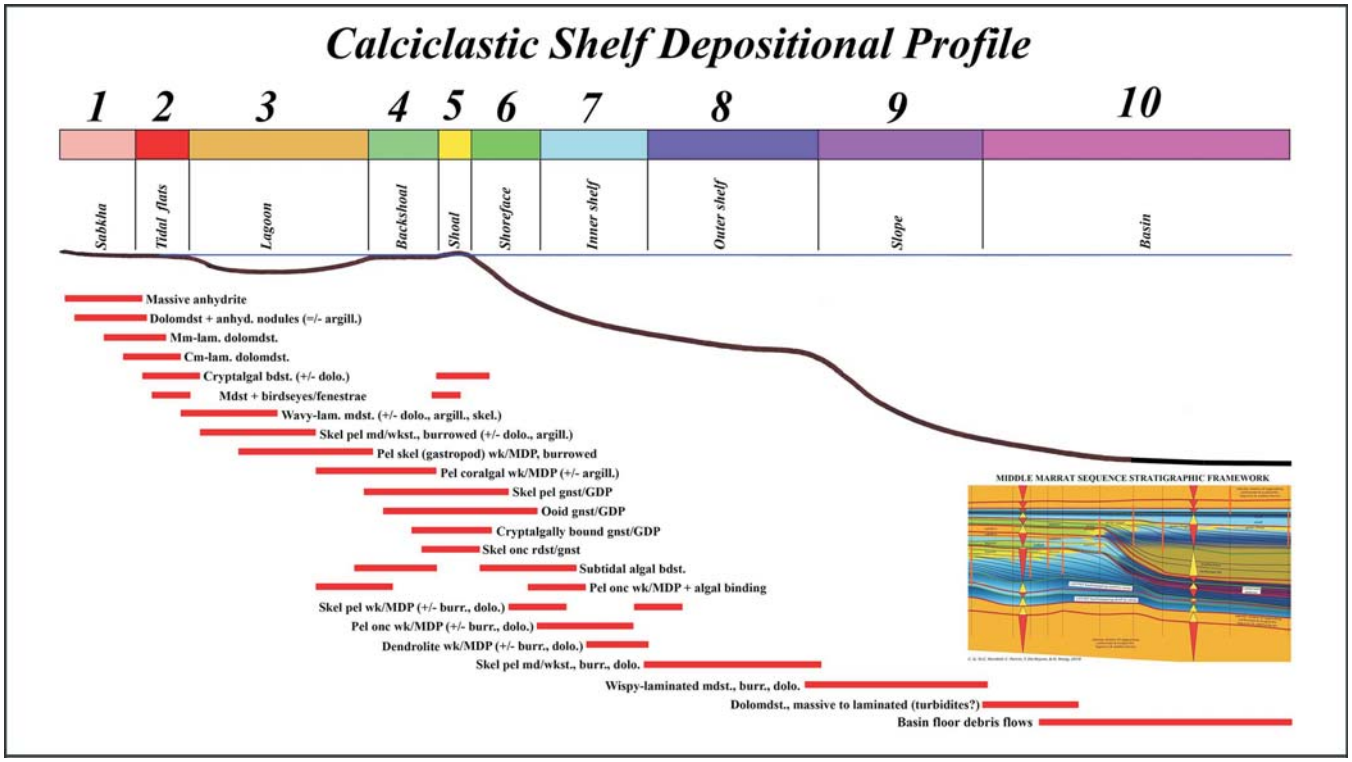

TEXT-FIGURE 27
The depositional profile of the calciclastic shelf depositional model is subdivided into 10 environments of deposition based on lithofacies (distribution shown), ichnofacies, and microbial growth forms. The depositional profile is divisible into platform (1–3), barrier (4–6), shelf (7, 8), and basinal (9, 10) settings (Modified after Neog et al. 2010).

MFS J10 was subsequently moved to a "drowning" unconformity (Kendall and Schlager 1981) in the Middle Marrat (Al-Eidan et al. 2009). At that time, much of the Middle Marrat below the proposed drowning unconformity had not been seen in core and was assumed to be a single sequence. It seems clear that placement of MFS J10 in a restricted platform carbonate-evaporite and nearshore siliciclastic succession just below the base of the open marine carbonates which form a regionally recognized marker horizon at the base of the Middle Marrat, Mus, Sekhaniyan and Surmeh formations was intentional (Sharland et al. 2001, p. 199). MFS J10 is herein placed in clean carbonates a short distance above the base of the Middle Marrat, as defined by core sedimentology. The remainder of the lower Middle Marrat, below the drowning unconformity, is herein assigned to S J11 and discussed further below.

Recently published Upper Triassic biostratigraphic data have changed the assumed ages of several formations and shown that Tr80 was originally assigned to three different stratigraphic events. Tr80 is now placed in the late Carnian-age "marker dolomite" of Lunn et al. (2019), equivalent to the Sefidar Dolomite of Iran (Szabo and Kheradpir 1978). New MFSs have been designated in the upper Jilh (S Tr90, lower Norian) and Lower Minjur (S Tr 100, upper Norian to early Rhaetian) (Lunn et al. 2019) (text-fig. 4). We propose two additional sequences, S Tr105 and S Tr110 (text-fig. 4). In revising the original Triassic sequence stratigraphy of Sharland et al. (2001), Davies and Simmons (2018) place the Tr60 MFS at the base of the Sefidar/Marker Dolomite. We illustrate the sequence enumeration of Lunn et al. (2019), with some minor differences.

Marrat Formation

Al-Eidan et al. (2009) discussed the lithofacies, depositional environments and reservoir geology of the Marrat Formation in Kuwait with emphasis on the Middle Marrat. Neog et al. (2010) discussed the sequence stratigraphy, evaporite lithofacies and depositional environments of the Marrat Formation. They also presented a model for deposition of the carbonate-evaporite cycles of the Gotnia Formation (Neog et al. 2010). The following discussion describes the lithofacies, systems tracts and sequence framework of the Marrat Formation based on all available core and integrates these data with the unpublished Fugro-Robertson (2009) study and the biostratigraphic data summarized in the previous section of this paper.

Lower Marrat Member

The Lower Marrat (middle or late Sinemurian to earliest Toarcian in age) is a southeastward-thickening wedge-shaped depositional unit consisting of thin-bedded carbonates and evaporites and minor calcareous shales. Lithofacies are nearly all representative of very shallow, low-relief, low-energy environments of deposition indicative of an extensive restricted platform. More than 1,000 ft (305 m) of core was described from the Lower Marrat. The lithofacies were assigned to precise depositional settings and their vertical succession and organization into cycles was used to define systems tracts and assign them to depositional sequences according to the model of Vail et al. (1977) (text-figs 5, 22).

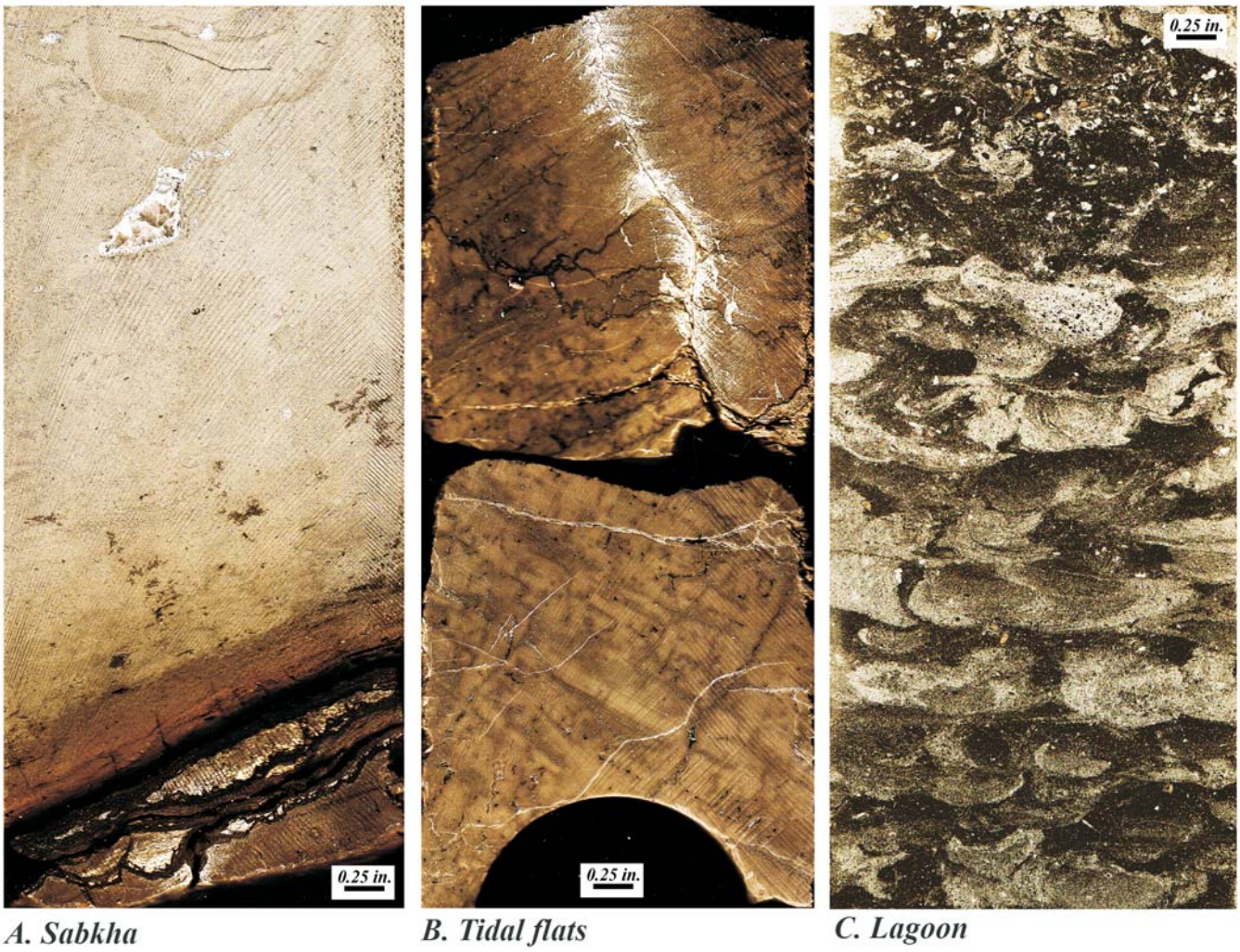

TEXT-FIGURE 28
Scanned images of core slabs, showing typical lithofacies of platform environments of deposition. A. Well AB, 15532.7–15533.2 ft. Microcrystalline dolomite overlies laminated mudstone and small anhydrite nodules with clay partings in this image of sabkha lithofacies. B. Well AB, 15533.3–1533.85 ft. This tidal flat image shows burrow-mottled lime mudstone with a desiccation crack bordered by a thin zone of dolomitization. C. Well UU, 15021.35–15021.9 ft. This lagoon image shows burrowing by *Asterosoma, Scolicia, Thalassinoides*, and *Chondrites*.

Lowstand Systems Tract

The best data for interpreting the lowstand systems tract (LST) depositional settings is from Sequence S J06. The interpreted LST of Sequence J06, when seen in slabbed core and on logs (low GR values, low neutron porosity and high density), appears to be a massive anhydrite. When slabbed and polished, delicate evaporative textures are clearly visible, indicating a predominantly sabkha depositional environment but with thin intervals of ponded or hypersaline intertidal lithofacies. There is typically a mix of nodular and palmate (subaqueous) crystal forms, interrupted by or intergrown with microbial layers (text-fig. 23). The microbial layers may be laminar or thrombolitic.

The base of the Sequence J06 LST is inferred to be an unconformity. Although this has not been confirmed by observation in core, the log character and succession bear a striking resemblance to the unconformity at the base of the J10 LST which was cored in four wells (JJ, MM, NN and II) (text-fig. 24). The top of the underlying J08 HST is a skeletal peloidal wackestone with common gastropod and bivalve fragments suggesting an open, normal marine platform depositional setting. These beds are overlain by a three-to-four ft zone of dolomitic shale of possible non-marine origin. The unconformity is picked at the base of this shale in core and at the point of highest GR and highest neutron porosity on logs (text-figs 5, 22). The same unconformable relationship is interpreted at the base of the J06 LST. The base of sequence J08 LST lacks such massive anhydrite beds as are seen in J06 and J10. Instead, there is an abrupt change from upward shoaling limestone and dolomite of the J06 HST platform to dolomite and anhydrite of sabkha, tidal flat and very shallow subtidal lagoon environments in the S J08 LST. The unconformable contact has been seen in three cored wells (text-fig. 24).

TEXT-FIGURE 29
Scanned images of typical lithofacies in barrier system environments of deposition. A. Well AB, 15609.6–15610.1 ft. Backshoal microbial boundstones. B. Well D, 15047.1–15047.7 ft Fenestral microbial laminites in shoal EOD. C. Well D, 15096.3–15096.85 ft Porous skeletal peloidal grainstone near top of shoreface.

The massive anhydrite of the J06 LST is abruptly overlain by intertidal, subtidal and shoal beds, indicating a flooding of the sabkha depositional surface at the base of the J06 TST (text-figs 23C, 25). The restricted circulation, hypersaline conditions and associated microbial growth forms of the LST were replaced by near normal marine lithofacies. In the calciclastic shelf model, these would normally be assigned to a lagoonal depositional setting but some of the lithofacies suggest a deeper setting that could also be described as open marine platform (text-fig. 26).

Above the microbial intertidal, shoal, and lagoon lithofacies, the J06 TST deepens rapidly upward to deep lagoon and marine platform depositional settings with clean limestones in which fragments of the aberrant pterioid bivalve *Lithiotis* sp. occur (text-fig. 26). These bivalves normally occur cemented together in dense accumulations, much like oysters, and would have been broken loose from these organic accumulations and transported into the adjacent lagoon. Similar buildups have been described in rocks of equivalent age in the central graben of the

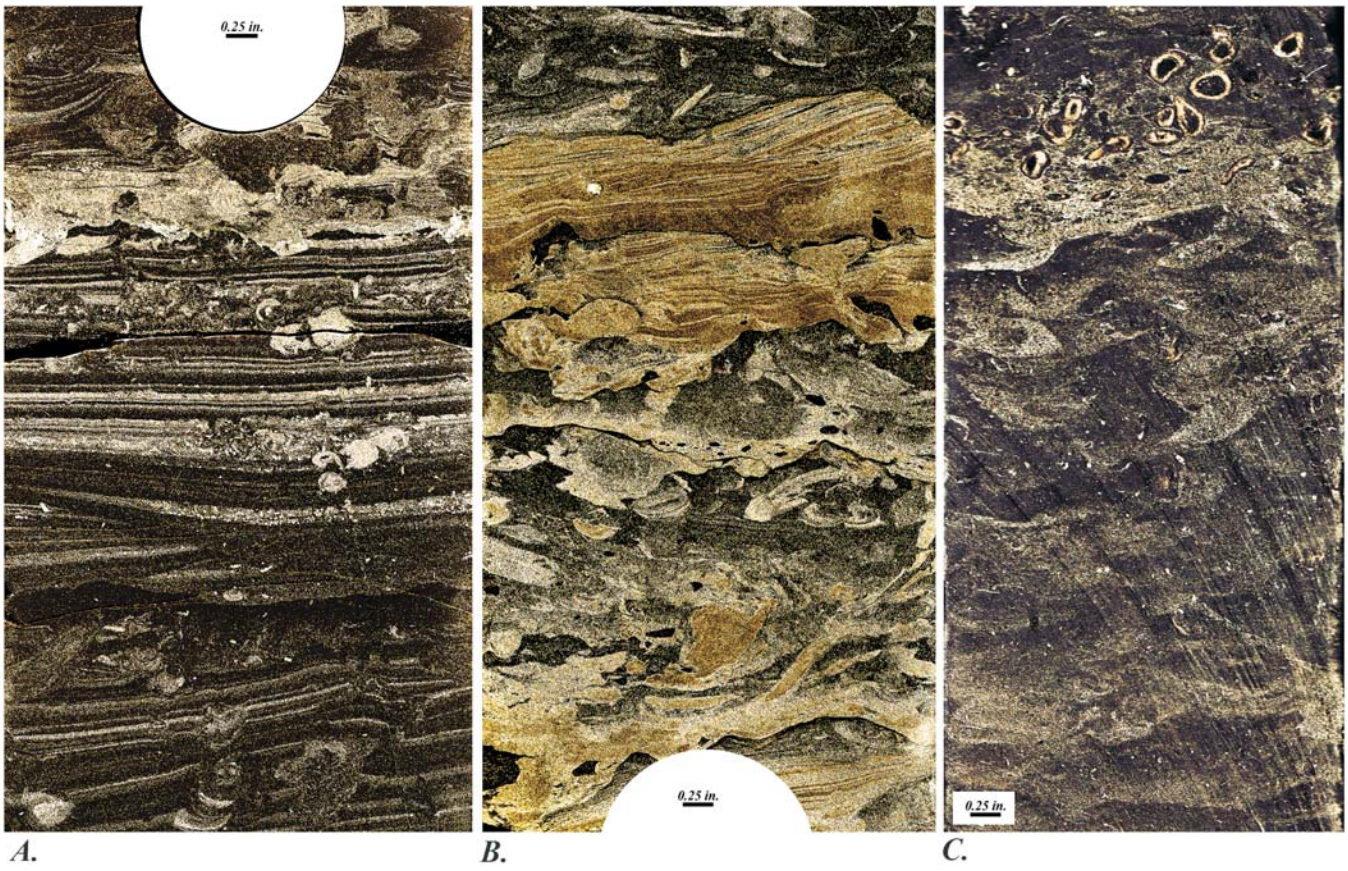

TEXT-FIGURE 30
Scanned images of core slabs, illustrating typical lithofacies of shelf depositional environments. A. Well B, 15157.0–15157.6 ft. Inner shelf, heavily burrowed. B. Well B, 15168.4–15168.9 ft. Shoreface transition with HCS. C. Well GG, 14978.4–14979.0 ft. Outer shelf mudstones with moderate to heavy bioturbation.

High Atlas in Morocco (Blomeier and Reijmer 1999; Scheibner and Reijmer 1999).

Highstand Systems Tract

Two complete HSTs (J06 and J08) were seen in core in the Lower Marrat and a third (J10) continues up into the Middle Marrat. These HSTs are most easily recognized on logs by the presence of limestone lithologies although in both J06 and J08, dolomite and anhydrite begin to dominate upward, toward the unconformable boundary with the LSTs of the overlying sequences. Although there is significant upward shoaling with the occurrence of common intertidal and sabkha lithofacies and exposure surfaces, the contacts with the overlying LSTs are sharply erosional and correlatable between wells in core and logs (text-figs 22, 26).

Middle Marrat Member

The depositional settings of the Middle Marrat have been described as a calciclastic shelf depositional model (Al-Eidan et al. 2009; Neog et al. 2010) (text-fig. 27). Before extensive coring revealed the existence of a drowning unconformity (MFS J10, herein redefined as MFS J11) and deeper water lithofacies representative of an intrashelf basin (ISB), the lithofacies of this member were described within a ramp depositional model, divided into inner, middle, and outer ramp depositional settings. The lithofacies beneath the drowning unconformity consist of a succession of open marine platform lithofacies with echinoderms, gastropods, bivalves and foraminifers that suggests shallowing downward toward the unconformity at the top of S J10.

The large, rapid sea level rise that marks the beginning of the Toarcian ISB, recognized worldwide as an oceanic anoxic event (T-OAE), caused the platform drowning and the regressive retreat of the platform margin. Depositional relief at that time would have been ramp-like, without a clearly defined barrier system separating platform from shelf and basin. Lowstands during subsequent high-frequency cycles shed packages of lime mudstone turbidites that downlapped onto the sediment-starved basin floor above the drowning unconformity. The ramp quickly steepened and differentiated into the rimmed platform geometry described in the calciclastic shelf depositional model (Al-Eidan 2009; Neog et al. 2010). Lowstands associated with the calciclastic shelf geometry were marked by an evaporitic lagoon which produced the dense, dolomitizing reflux brines which moved downward into the shelf mudstones and wackestones that became the prolific Middle Marrat dolomite reservoirs of north Kuwait (Neog et al. 2010).

Platform Lithofacies – Lithofacies of the platform include sabkha, tidal flat, and lagoon depositional settings. These environments and their representative lithofacies are all included in

the inner ramp classification when that model is applied but there is clearer differentiation and more variability in the platform geometry. Individual depositional cycles are typically very thin and occur in hierarchical sets attributable to 4th, 5th, and 6th-order Milankovitch cyclicity interpreted as orbital forcing. Cycle thickness ranges from a few cm to a few meters, with common discontinuities and minor unconformities.

The lagoon is the most extensive of these depositional settings and it is strongly affected by relative changes of sea level as well as being differentiated into proximal and distal settings, landward or seaward of the deepest midpoint, respectively (text-fig. 28). Late highstands, when the platform and barrier system are well developed, become evaporitic, with deposition of thick anhydrite layers that display both nodular/sabkha-like and palmate/subaqueous textures. The evaporitic lagoon also commonly contains stromatolitic microbial growth forms in which the cyanobacterial filaments trap gypsum crystals instead of micrite needles. The anhydrite layers are laterally extensive in the lagoons and provide an accurate means of mapping platform distribution within individual high-frequency sequences.

Barrier System Lithofacies **–** The barrier system consists of backshoal, shoal, and shoreface depositional settings and are referred to as middle ramp or platform rim in rimmed platform models (text-fig. 29). The best modern analog of the calciclastic barrier system is the study of Illing (1954) on the southeastern Bahamas Bank. The shoreface is the highest energy depositional setting, with the greatest rate of sediment production. This sediment is transported downslope onto the shelf by wave and tide action but is also carried landward across the shoal and pro-grades landward in the backshoal setting. Grain-supported lithofacies and microbial boundstones of several types are common in the shoal and backshoal. As in the platform, 4th, 5th, and 6th-order cyclicity is evident on the shoal but more typically forms meter-scale aggradational cycles in the backshoal (text-figs 29A, B).

The shoreface faces the open marine shelf and ISB, where waves and tides winnow the fine micrite mud, leaving porous ooid, skeletal, and microbial grainstones (text-fig. 29C). At their lower limit, these grainstones become finer-grained and storm beds interfinger with the mud-supported fabrics of the inner shelf in a zone called the shoreface transition or inner platform. Planar and trough crossbedding are common and *Diplocraterion* and *Ophiomorpha* burrows are fairly common, along with cryptic bioturbation that tends to obscure the lamination (*Skolithos* ichnofacies). The lower shoreface is also influenced by longshore currents which transport sediment into longer wavelength sedimentary structures, characterized by hummocky cross-stratification (HCS). In many areas of Kuwait, it is these grainstones of the shoreface clinoforms and tabular shoal and backshoal environments that form prolific reservoirs.

Inner and Outer Shelf Lithofacies **–** As defined in the calciclastic shelf depositional model, the inner shelf extends from the base of the shoreface, where grain-supported fabrics dominate, seaward with decreasing dip to the limit of storm wave-transported coarse-grained sediment (text-fig. 30). The inner shelf is dominated by mud-dominated packstones (MDP) and wackestones, commonly with large, complex oncoids, and is heavily bioturbated (*Cruziana* ichnofacies). Storm beds of grain-supported ooids and large skeletal fragments extend basinward from the base of the shoreface. The boundary with the outer shelf is typically marked as the transition to peloidal and skeletal lime wackestones and mudstones with small, simple oncoids, with moderate to heavy bioturbation by *Rhizocorallium* and *Zoophycos* (*Zoophycos* ichnofacies).

The presence of dense zones of *Chondrites* in some intervals suggests organic richness and is consistent with the interpreted depositional setting. The lower portions of the inner shelf and much of the outer shelf lithofacies are frequently partially or pervasively dolomitized, with occasional nodules of secondary anhydrite. Study of cores shows that the burrows act as conduits for the dolomitizing reflux brines, with the dolomite gradually extending from the burrows out into the matrix, creating excellent secondary porosity in these originally tight lithofacies. The dolomites are seemingly stratiform, extending downdip from the inner shelf to the outer shelf and not generally in contact with the dolomite bodies in successively younger clinoforms.

Intrashelf Basin Lithofacies – In the calciclastic shelf depositional model, the boundary between the shelf and the intrashelf basin, the shelf-slope break, is the limit of the deepest storm waves that are able to move and transport sediment. On the shelf, fine sediment is winnowed from the substrate during large storms, forming a dense hyperpycnal layer of suspended sediment that moves downslope under the influence of gravity, gradually settling out of the water column as wave action decreases. Beyond the shelf-slope break, gravity is the only effective mechanism of sediment transport and the accumulating sedimentary column on the slope is a mix of hemipelagic and subaqueous gravity flow beds. A number of cores in north Kuwait (text-fig. 31C) have lime mudstone turbidite lowstand intervals in which the beds have scoured bases, escape structures, and burrowed upper contacts, deposited along the base-of-slope and basin margin. Other cores, in wells farther from the platform margin, contain thin, dark, probably organic-rich intervals representative of the basin floor.

Sequence Framework of Middle Marrat **–** Neog et al. (2010) subdivided the uppermost Lower Marrat and the Middle Marrat into high-frequency sequences. Description of many additional cores and addition of numerous logged but uncored wells has not demonstrated the need for a change in this system of subdivision. The same high-frequency sequences identified by Neog et al. (2010) are still being identified and mapped. In this paper, we have used the same units but applied and extended the Sharland et al. (2001) nomenclature to these sequences, such that SB 3 to SB 7 of Neog et al. (2010) are here designated J12 to J16 (text-figs 5, 33).

The ten environments of depositional (EODs) of the calciclastic shelf model have also proved useful in integrating the sedimentology derived from core description into the sequence framework. This methodology is based on construction of a Waltherian aggradational profile, representing uninterrupted sedimentation at a point in the ISB from the basinal sediments through the entire aggradational and progradational cycle, culminating in sabkha lithofacies overlain by an unconformity (text-fig. 32). In describing cores, the interpreted EODs are plotted on a scale of 1-10, representing the onshore-offshore depositional profile. Increases in EOD represent transgressive events, while the dominant pattern is aggradational / progradational as shown by decreasing EODs. Breaks in the succession of EODs represent either unconformities with subaerial expo-

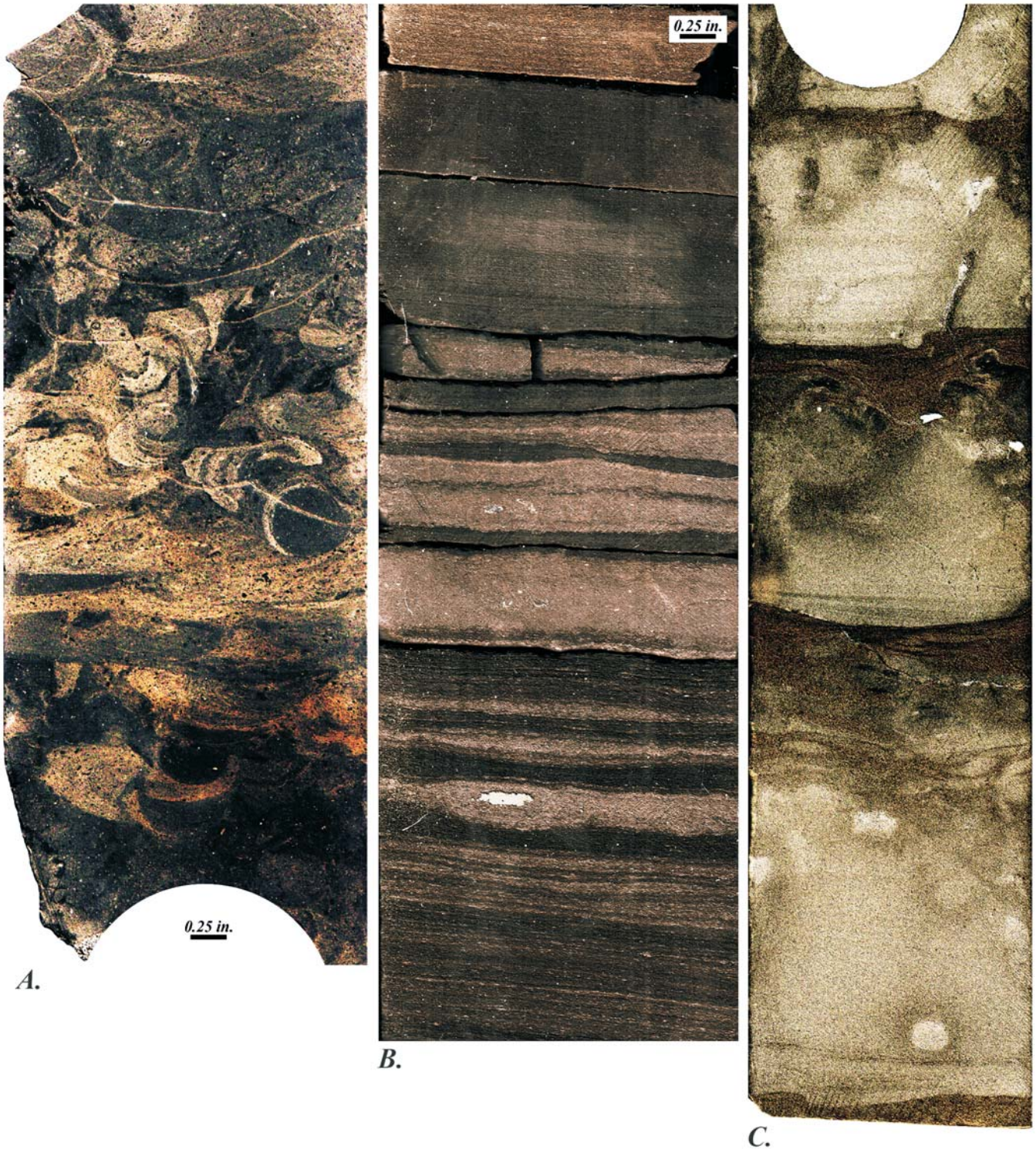

TEXT-FIGURE 31
Scanned images of core slabs, showing lithofacies of ISB depositional setting. A. Well AC, 14672.3–14,672.85 ft. Outer shelf or basin with prominent, large Zoophycos burrows. B. Well YY, 14994.9–14995.55 ft. Starved basin laminated mudstones with apparent high organic content. C. Well JJ, 15537.05–15538.0 ft. Lime mudstone turbidites with scoured bases and burrowed tops and interbedded laminated mudstones of basin floor.

sure or rapid lateral shifts of the depositional profile in response to relative changes of sea level and mark probable or potential sequence boundaries. The methodology is called a profile relay after the sedimentary relay concept of Lees and Miller (1985).

Upper Marrat Member

The Upper Marrat Member has been partially cored in 11 wells in north Kuwait, all of them in the lower or middle portions of the Member. No core data are available at this time for the upper portion of the Upper Marrat or the lowermost portion of the overlying Dhruma Formation. The member has been divided into three high-frequency sequences, designated J17, J18 and J19 (Crespo de Cabrera et al. 2019, 2020). The sequence boundary separating J17 and J18 was cored in three wells (EE, NN and QQ) and is recognizable as a disconformity on a thin dolostone unit, overlain by argillaceous limestones of deeper water appearance.

Sampled cuttings from the Upper Marrat Member (Unit A and upper Unit B of Yousif and Nouman 1997) did not yield useful palynological or micropaleontological information (Al-Moraikhi et al. 2014). Unpublished studies (Fugro-Robertson 2009) found J17 and J18 to be entirely Aalenian in age. Sequence J19 has not been seen in core but cuttings samples yielded data placing the Aalenian/Bajocian boundary within J19 (Fugro-Robertson 2009). The carbon isotope values from cuttings delineate a slight negative trend, starting at maximum values in the Middle Marrat Member (Unit C of Yousif and Nouman 1997). This trend is similar to the one recorded in the Late Aalenian to Early Bajocian globally stacked isotope data set (Al-Moraikhi et al. 2014).

SEQUENCE STRATIGRAPHY

Sequence Definition and Methodology

The modern concept of unconformity-bounded packages of strata began with Sloss (1963). At that time only six sequences could be identified on more than one continent. Studies designed to test and refine that model soon presented thick successions dated and correlated in basins on different continents. In the Gulf of Mexico, where shelf strata prograde out over thick slope and basin successions which are actively compacting and subsiding along growth faults, a method of correlation using facies successions led to the idea of maximum flooding surfaces (MFS) as a means of correlation (Frazier 1974). These became the basis for a methodology which identified genetic stratigraphic sequences (GSS) whose boundaries were these flooding surfaces (Galloway 1989a, 1989b).

Exxon Production Research developed the depositional sequence model into a full interpretation methodology based on reflection configuration and terminations on seismic profiles across plate margins (Vail et al. 1977). Their principal emphasis was on defining not only the MFS but the package of genetically related strata in which it occurred. The boundaries of this container were defined as the unconformities or correlative conformities separating it from adjacent sequences. The unifying concept responsible for these punctuations of the stratigraphic record was identified as eustasy. The Exxon methodology includes the construction of coastal onlap curves and chronostratigraphic cross-sections, scaled in time rather than depth. Within the sequences, sets of facies representative of distinct portions of the cycle of sea level change were identified, viz., lowstand, transgressive and highstand systems tracts. This is the depositional sequence model that has been followed in this study.

Sequence Changes in the Upper Triassic and Lower Jurassic of Kuwait

The Jurassic MFSs of Sharland et al. (2001) range from J10 to J110 and the youngest Triassic MFS was designated as Tr80. No MFS was designated between the Late Triassic Lower Minjur Formation and the revised position of J10 in the early Toarcian (Sharland et al. 2001; Al-Eidan 2009). Changed correlations in the Upper Triassic (Lunn et al. 2019), discussed in the following paragraphs, necessitated the addition of MFSs and are the basis for changed regional correlations proposed herein. Sedimentological data from detailed core descriptions and extrapolated to logs provide the context in which available micropaleontologic data have been evaluated to provide a new sequence framework for the Early and Middle Jurassic Marrat Formation.

Triassic chronostratigraphy has been significantly modified as the result of the recent paper by Lunn et al. (2019), which presents biostratigraphic data for the type outcrop exposures of the Baluti Shale and correlates them to a biostratigraphically dated subsurface section of the Baluti Shale and the overlying Sarki Formation. Their data show the Baluti to be late Carnian to earliest Norian in age. It had originally been tentatively assigned to the Rhaetian (van Belen 1959). More significantly, its subsurface position is above the Butmah Shale, which had been correlated to be above the Baluti and time-equivalent to the lower Sarki Formation (Lunn et al. 2019). According to Lunn (personal communication, 2021), the subsurface position of the Butmah shale "within the Lower Butmah Formation necessitated a reorganization of the subsurface stratigraphy. The Butmah was replaced by the Sarki, Baluti and the Kurra Chine A. The reorganization denies the previously accepted correlation of the basal Butmah dolomite (now the Kurra Chine A) of the subsurface to the basal Sarki dolomite at outcrop."

These new data also show the Baluti to overlie a regionally recognized dolomite marker unit in the A Member of the Kurra Chine Formation of Iraq, also called the Sefidar Dolomite in Iran (Szabo and Kheradpir 1978) and constrained the age of the regional dolomite marker to the late Carnian. Lunn et al. (2019) present several regional cross-sections based on these new and revised correlations, showing that the MFS at the base of this "marker dolomite" is actually MFS Tr80 rather than Tr60 as proposed by Davies and Simmons (2018). Two new Upper Jurassic MFSs were introduced by Lunn et al. (2019); Tr90 in the Jilh A of Kuwait (= lower Sarki) and Tr100 in the lower and middle members of the Minjur in Kuwait (= Lower Minjur in Saudi Arabia) (text-fig. 33). Tr100 is herein restricted to the Lower Member of the Minjur in Kuwait and a new sequence, S Tr105, is defined for the Middle Carbonate Member (text-fig. 33).

Lunn et al. (2019) correlated the Triassic/Jurassic boundary to the top of the middle member of the Minjur in Kuwait and designated that surface SB J01. Data presented in this paper, however, place the boundary at the base of the Lower Marrat Member in Kuwait, within a thin package of strata of indeterminate age, containing both Triassic and Jurassic palynomorphs (text-figs 4, 33). The strata in the upper member of the Minjur Formation which Lunn et al. (2019) designated Sequence J01 are, in this paper, shown to be Triassic in age and are herein renamed S Tr110. Lunn et al. (2019) also proposed SB J05 at the

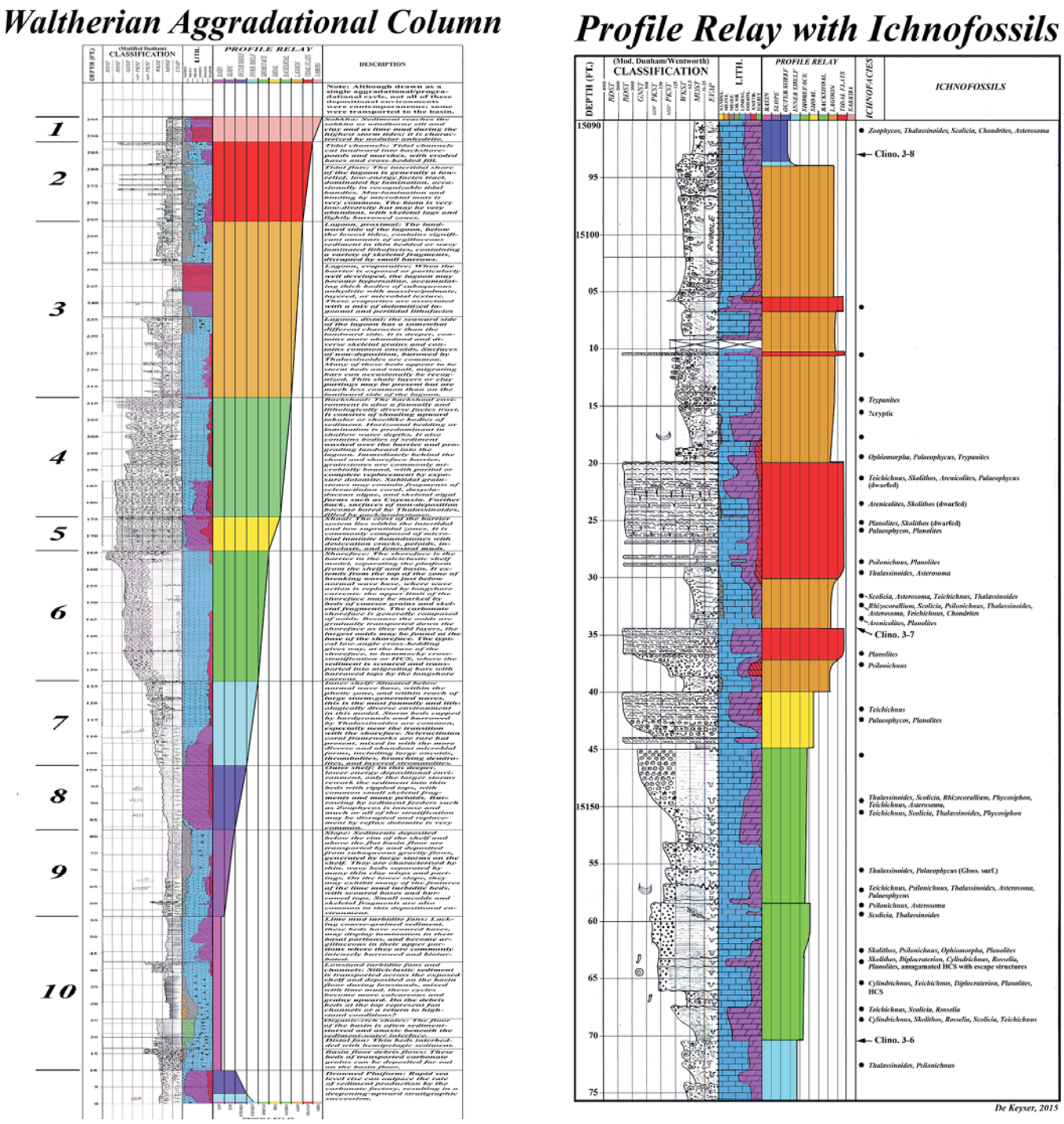

TEXT-FIGURE 32
Comparison of Waltherian aggradational column and profile relay plot for typical cored interval, showing ichnofossil distribution.

contact of the Minjur with the overlying Marrat. That suggestion has not been followed here because of the need to accommodate five sequences between J01 and J10 (text-figs 5, 33).

Little published biostratigraphic data was available to Sharland et al. (2001). Their chronostratigraphic sections for the Late Triassic and Early Jurassic lacked detail and left a gap from late Rhaetian to early Toarcian (2001, Encl. 2b; 2004, Encl. 1). In particular, there is considerable confusion about the age, stratigraphic position, and correlations of the Lower Marrat Member. The sedimentological and biostratigraphic data available to this study allow us to clarify some of those relationships and propose

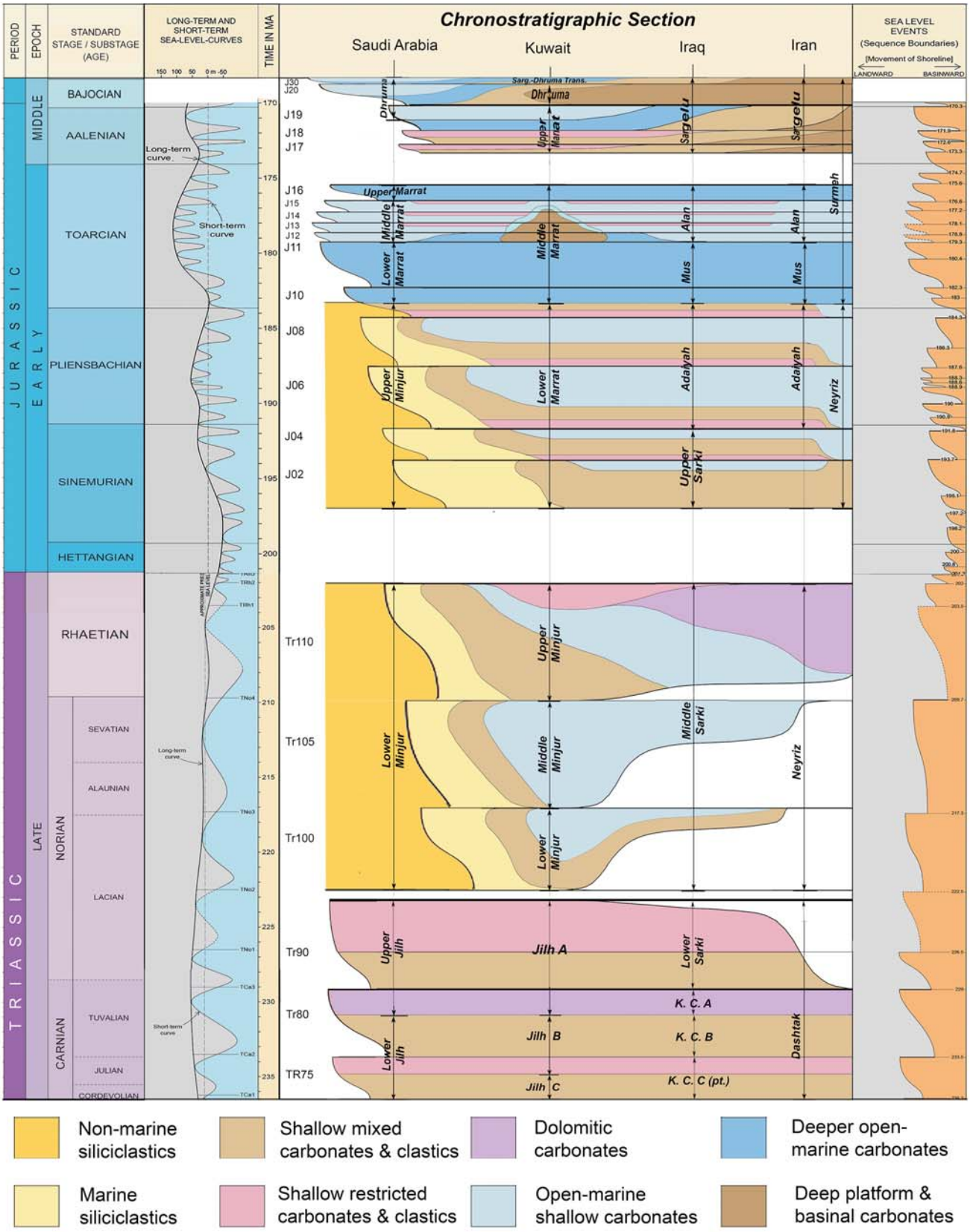

TEXT-FIGURE 33
Jurassic and Late Triassic chronostratigraphic chart of Kuwait and adjacent areas, incorporating proposed changes of Kadar et al. (2015), Crespo de Cabrera et al. (2019, 2020) and Lunn et al. (2019). The sea level curve and coastal onlap curve are from Haq (2017, 2018).

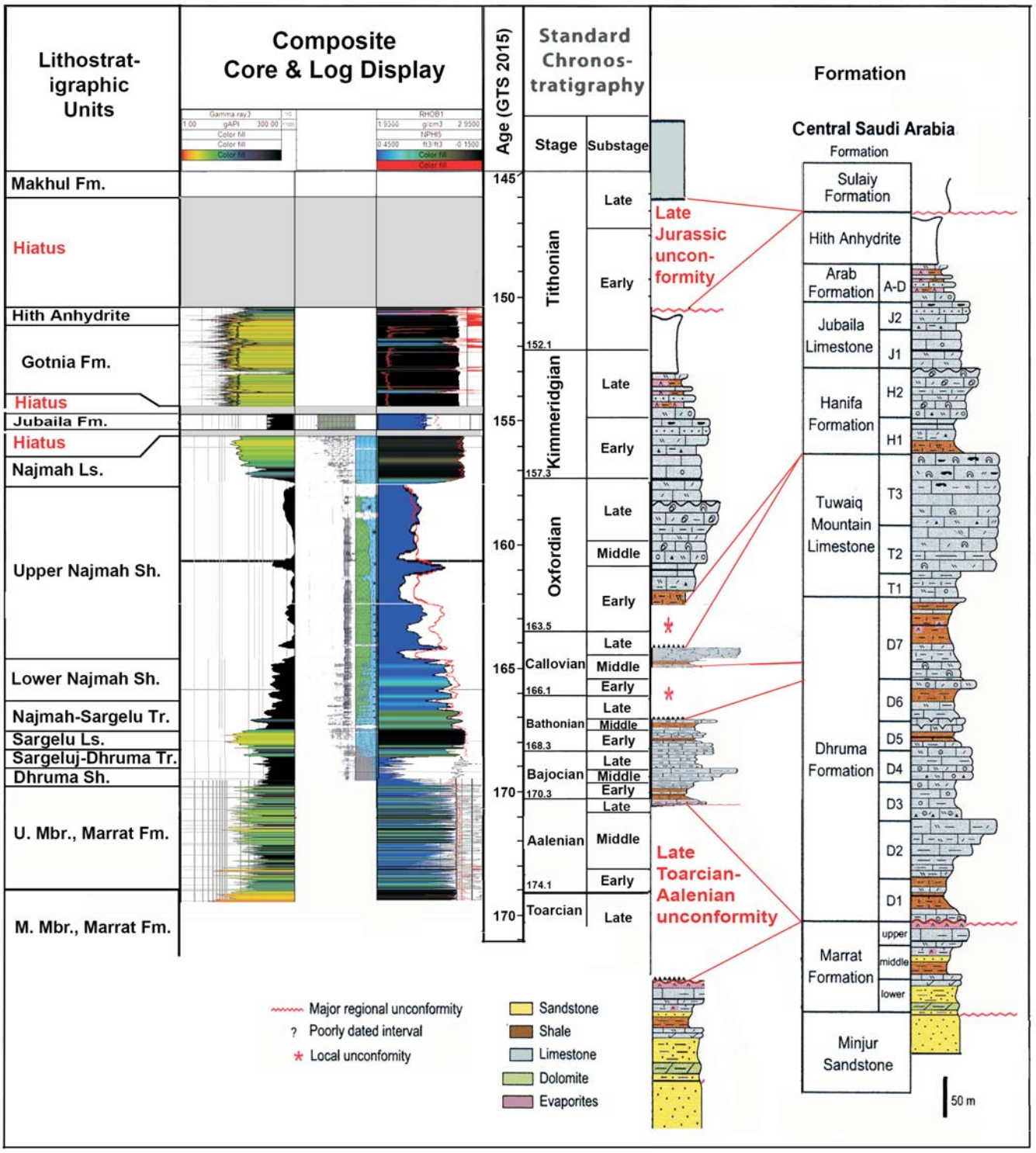

TEXT-FIGURE 34
Diagram comparing distribution of hiatuses in outcrop section in Saudia Arabia with a composite core and log from Kuwait plotted in time instead of depth. The hiatuses noted in Saudia Arabia (excluding the Tithonian) are represented by deposition of lowstand wedges (LSTs) in Kuwait. The two hiatuses identified in Kuwait are interpreted as tectonic and are not observed in Saudi Arabia. Modified after Al-Mojel et al. (2018).

a new, more detailed chronostratigraphic framework (text-figs 5, 30, 31, 33-36). Key features of this chronostratigraphy include:

• Placement of sequence boundaries at the base of the massive anhydrites in the Lower Marrat Member and recognizing them as LSTs;

• Recognition of the Sinemurian/Pliensbachian boundary at the base of the J06 TST;

• Recognition of the Pliensbachian/Toarcian boundary at the base of or within the J10 TST, just below the base of the Middle Marrat Member;

• Recognition of the Toarcian/Aalenian boundary coincident with the unconformable Middle-Upper Marrat contact; and

• Placement of the Aalenian/Bajocian boundary in the lower part of Sequence J19, in the Upper Marrat Member.

Other changes to the sequence framework will surely be proposed as more sedimentological and biostratigraphic data become available and differences of interpretation will occur. In their revision of the Triassic sequence stratigraphy, Davies and Simmons (2018) revised their assignment of the Sefidar Dolomite (Szabo and Kheradpir 1978) from Tr80 to Tr60, while Lunn et al. (2019) assigned it to Tr80. Other differences also exist in the Early Jurassic. Several principles have guided our proposals for new terminology.

• MFSs recognize distinct horizons in the stratigraphic succession of a given area and should be tied to that point as to a type section. The original definition of Tr80 by Sharland et al. (2001) was specifically tied to dolomites near the base of the Sarki Formation in outcrop in northern Iraq considered equivalent to the Sefidar Dolomite in Iran (van Bellen et al. 1959; Szabo and Kheradpir 1978; Sharland et al. 2001, p. 198). The Sefidar Dolomite was correlated to a marker dolomite at the base of the Jilh A in Kuwait by Khan (1989) and we follow Lunn et al. (2019) in maintaining that designation rather than the change to Tr60 (early Carnian) proposed by Davies and Simmons (2018).

• Recognition of sequence boundaries is critical to defining the size, shape, and extent of sequences. These can be Type 1 unconformities with physical evidence of erosion and at which a hiatus in deposition can be paleontologically demonstrated or Type 2, recognized by a major, abrupt shift in depositional profile and lithofacies but with no recognizable hiatus, e.g., the Middle/Upper Marrat boundary.

• Systems tracts determine the internal stratal configuration and lithofacies distribution and should be defined and sedimentologically described whenever possible.

• LSTs are often absent in platform settings where a sequence may have only a TST and an HST. In more basinal settings, such as Kuwait, however, the LST may form the bulk of a sequence, with the TST and HST represented by a thin, condensed section. LSTs are commonly time-equivalent to hiatuses in platform areas and their recognition is critical to construction of a complete stratigraphic and biostratigraphic succession.

• The goal of a comprehensive sequence stratigraphic framework should be a succession of 3rd-order sequences, approximately one to three MY in duration and within the capabilities of biostratigraphic zonation. This is the pattern that is emerging from study and dating of the Late Triassic to Early Jurassic succession in Kuwait. There will be controversies and conflicts in the nomenclature but the effort will be rewarded by improved success rates in exploration and development projects.

Systems tracts have been identified for most of the sequences defined or described in this paper. The lithofacies and depositional setting of these LSTs is different in the various portions of the Jurassic of Kuwait. The anhydrites described in the Lower Marrat provide a good example. In earlier studies, LSTs consisting of anhydrites have commonly been included in the HSTs of the underlying sequence and sequence boundaries placed at their upper surface (Al-Eidan et al. 2009; Neog et al. 2010; Fugro-Robertson 2009). Detailed sedimentological core description has identified unconformities at the base of these anhydrites. There is a shift in the depositional profile from open marine carbonates beneath the unconformity to predominantly tidal flat and sabkha lithofacies above. These anhydrites have been identified as LSTs in this study, e.g., J06 and J10. In Sequence J08, the anhydrite section has been subdivided into LST and TST and the upper, clean limestone portion of the sequence represents the HST.

In the Middle Marrat, the anhydrites occur in a platform setting, in the lagoon landward of the barrier system and are characterized by subaqueous textures (thin, cumulate beds, upright stromatolites composed of anhydrite (after gypsum), and upright palmate anhydrite pseudomorphs of original swallow-tail-twinned gypsum). These evaporitic units are overlain by unconformities and exhibit evidence of solution collapse and were placed in the underlying HSTs. The LSTs in the Middle Marrat are missing on the platform but occur instead at the base of clinoforms, in a toe-of-slope depositional setting (lime mud turbidites) or on the basin floor as distal debris flows during lowstand slope readjustment.

The anhydrites which occur in the Upper Marrat are predominantly sabkha lithofacies, deposited in a ramp-like setting (Neog et al. 2010). Two of the three sequences in the Upper Marrat have these sabkha anhydrites (J17 and J18). Sequence J19 appears to represent deeper lithofacies, from tidal flat and lagoon to open-marine platform. Most of this sequence has not been seen in core and many questions remain. It is clear, however, that the entire Upper Marrat lies seaward and down depositional dip from a late Toarcian to basal Bajocian hiatus in the outcrop belt and the entire Member is regarded here as a 2nd-order lowstand wedge.

Several of the stratigraphic units described by Kadar et al. (2015) and Crespo de Cabrera et al. (2019, 2020) also probably represent lowstands, including the Sargelu-Dhruma Transition, the Lower Wedge of the Lower Najmah Shale, and the Upper Wedge of the Upper Najmah Shale (Kadar et al. 2015; Crespo de Cabrera et al. 2019, 2020). A recent study by Al-Mojel et al. (2019) presented carbon and oxygen isotope data for the Jurassic outcrop section in Saudi Arabia. The authors identified four definite and one possible hiatus: at the Marrat/Dhruma boundary (late Toarcian-Aalenian), near the Dhruma D3-D4 boundary (Late Bajocian), in the Dhruma, from late D6 to early D7 (late Bathonian to mid-Callovian), between the Tuwaiq Mountain and the Hanifa formations (late Callovian to early Oxfordian), and between the Hith Anhydrite and Sulaiy Formation (Makhul

TEXT-FIGURE 35
Cross-section of Marrat Formation from Mutriba Field, across Northwest Raudhatain, Raudhatain and Sabriyah to Bahrah Field in north Kuwait. Depositional sequences proposed herein are compared with the biosequences proposed by Robertson Research (2009). Cored intervals are shown and referred to in text under discussion of Sequences J12 to J16. Note location of text-figure 34 in Well YY (red outline). Datum: top Middle Marrat.

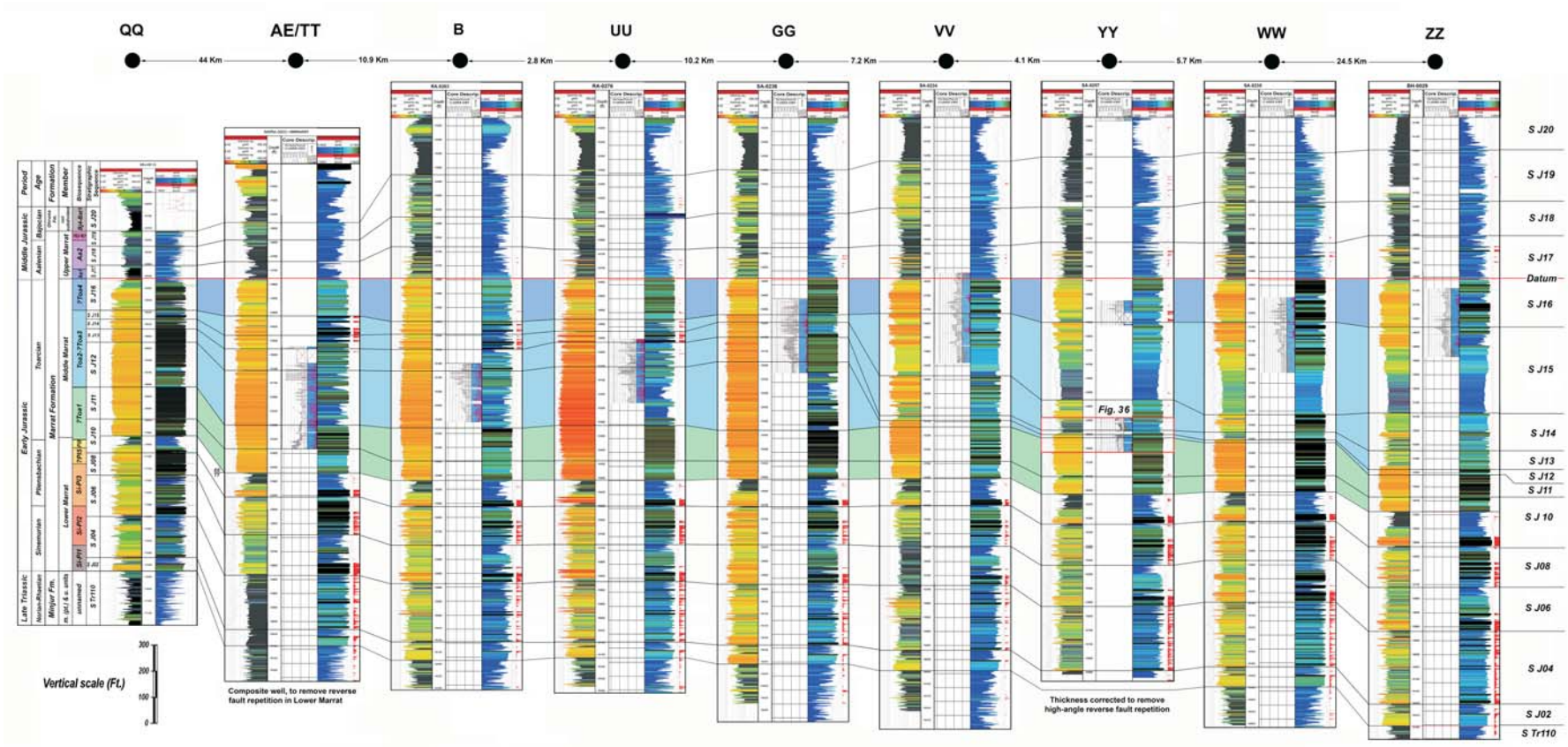

Formation in Kuwait) (middle to late Tithonian). The correspondence of these hiatuses to the LSTs proposed for the Jurassic is striking (text-fig. 34). The two hiatuses identified in the Jurassic section in Kuwait, i.e., below and above the Jubaila Formation, were interpreted to be tectonic in origin and are not evident in the outcrop section (Crespo de Cabrera et al. 2019, 2020).

Kuwait Sequence Terminology for Late Triassic and Early and Middle Jurassic

The chronostratigraphic section shown in text-figure 33 is extended nearly to the base of the Upper Triasssic to show the changes proposed by Lunn et al. (2019) and because some of the formations extend across the Triassic/Jurassic boundary and contain significant depositional/erosional hiatuses. This model of the chronostratigraphy fills some of the lengthy hiatuses and there is a pattern emerging of many more 3rd-order sequences of a few My duration. The few remaining sequences of longer duration, e.g. the Najmah Formation in the Upper Jurassic and the Lower Minjur have already been shown to contain several depositional cycles but these have yet to be subdivided. The revised framework of Upper Triassic and Lower Jurassic sequences in Kuwait is discussed in the following paragraphs.

Sequence Tr80 (Upper Triassic, late Carnian) (Lunn et al. 2019); formerly assigned to Tr70 by Sharland et al. (2001, 2004**)** and to Tr60 by Davies and Simmons (2018).

This 3rd-order depositional cycle was originally defined as having a sequence boundary at the base of the Jilh Salt in Kuwait (= Jilh B). The halite beds are overlain by a shaly interval and the Marker Dolomite (= Sefidar Dolomite) (Lunn et al. 2019). The basal evaporite / halite beds were interpreted as an early TST, the shale as the TST, and the Marker Dolomite with MFS Tr80 at its base, as the HST. Lunn (2020) redefined the sequence, placing the evaporite beds in S Tr75 as late HST deposits. Lithostratigraphically, the top of the Jilh B is placed at the top of the evaporite beds, such that S Tr80 includes portions of upper Jilh B and lower Jilh A.

Sequence Tr90 (Upper Triassic, late Carnian to early Norian) (Lunn et al. 2019, new)

The Marker Dolomite is locally overlain by an evaporitic interval (HST of S Tr80), followed by shaly, presumably more normal marine beds (TST), and by a shaly anhydritic interval (HST). Lunn et al. (2019) placed the MFS at the base of the HST (text-fig. 4). The top of the Jilh A unit is picked at the top of the HST and Sequence Tr90 encompasses the upper three-quarters of the Jilh A in Kuwait.

Sequence Tr100 (Upper Triassic, Norian to Rhaetian) (Lunn et al. 2019, revised, this paper)

The base of this sequence is the base of the Minjur Formation (= Lower Minjur in subsurface Saudi Arabia). The formation is divided into Lower, Middle, and Upper units in Kuwait (Khan 1989; Alsharhan et al. 2014). The succession begins with a shaly lower unit that becomes somewhat sandy and more calcareous upward. The middle unit becomes much more calcareous initially and overlies a significant unconformity (Khan 1989) (text-figs 33, 39). Lunn et al. (2019) place the top of S Tr100 at the top of the middle unit, where they also placed the Triassic/Jurassic boundary. Lunn et al. (2019) proposed a new sequence, S J01, for the upper unit of the Minjur Formation in Kuwait. This study places the Triassic/Jurassic boundary at or just below the contact between the Minjur and Marrat formations. Here, the top of S Tr100 is placed at the base of the middle carbonate unit and Sequence Tr105 is proposed for the middle member of the Minjur Formation. The proposed S J01 becomes S Tr110.

Sequence Tr105 (Upper Triassic, Late Norian to Rhaetian) (this paper, new)

The Middle Carbonate Member of the Minjur Formation unconformably overlies the Lower Member (Khan 1989) (text-figs 33, 39). It is easily recognizable and mappable throughout Kuwait and can be correlated to Iran and Iraq as the cleaner, more carbonate-rich upper portion of the Middle Sarki (Lunn 2020, Figure 6). It is overlain by the Upper Member of the Minjur, originally considered to be Jurassic and defined as S J01 by Lunn et al. (2019) and herein assigned to the Triassic and renamed S Tr110.

Sequence Tr110 (Upper Triassic, latest Norian to Rhaetian) (this paper, renamed, after Lunn et al. (2019) and Lunn (2020)

This sequence is comprised of all of the upper unit of the Minjur Formation in Kuwait. We have placed the base of the sequence at the base of the upper unit as was correlated by Lunn et al. (2019) who considered it to be Lower Jurassic and designated it S J01. The sequence is essentially equivalent to the upper portion of the siliciclastic Lower Minjur as recognized in the subsurface of Saudi Arabia. The upper surface, at the base of the Lower Marrat Formation is abrupt and appears conformable but has not been seen in core.

Sequence J02 (Lower Jurassic, middle (?) and late Sinemurian) (this paper, new)

The J02 sequence boundary is placed at the contact between the Minjur and the Lower Marrat. This surface was designated J05 by Lunn et al. (2019). They defined the J01 and J05 sequences in the upper member of the Sarki Formation, with J05 marking the boundary between the lower clastics and the upper carbonates and evaporites. Sequence J05, however, was defined to extend to the top of the Lower Marrat in the earliest Toarcian. That interval was subdivided into four sequences and a portion of a fifth in this study and J05 has not been used. The MFS of J02 is placed in the shaly beds above the first thick anhydrite beds and the top is placed at an assumed unconformity beneath the thick anhydrite beds that mark the LST of J04. S J02 has not been seen in core but appears to be a similarly interbedded unit of shale, limestone, dolomite, and anhydrite.

Sequence J04 (Lower Jurassic, late Sinemurian) (this paper, new)

The portion of the Lower Marrat below the massive anhydrites at the base of S J06 was originally assigned to a single sequence, J02, largely because of the lack of sedimentological data from cores. On logs, however, a persistent horizon beneath two thick anhydrite beds is recognized and correlated through all wells on logs. The Fugro-Robertson report (2009) recognized a second sequence in this interval, with a boundary just above these anhydrite beds. We assume the anhydrite beds represent the LST of that sequence and that the boundary for their biosequence was the base of the TST. We define J04 to include the interval from the base of the anhydrite beds to the unconformity beneath SJ06 (text-figs 5, 33 and 36).

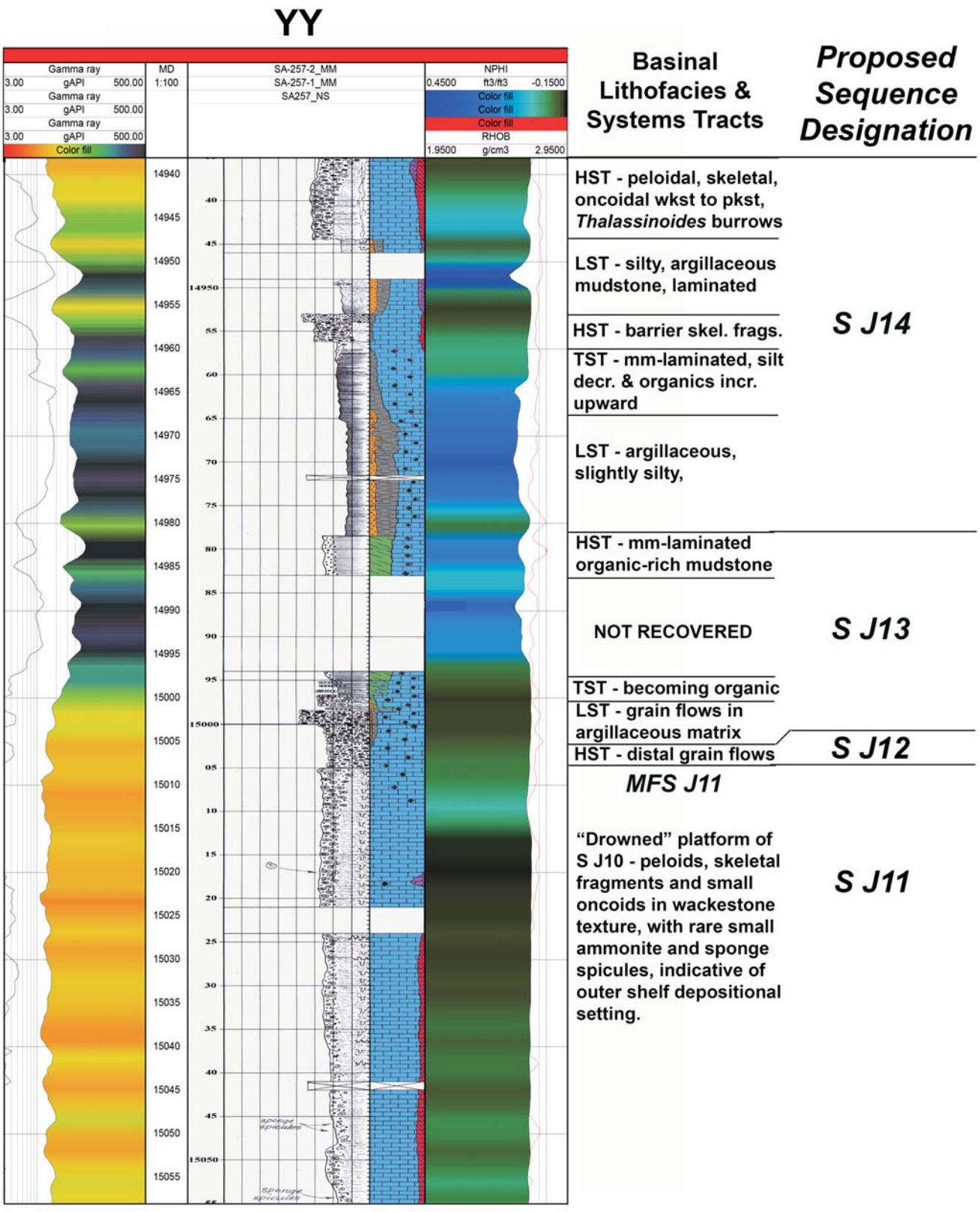

TEXT-FIGURE 36
Enlargement of a portion of the log and depth-shifted core description in Well YY (see text-fig. 33 for location in cross-section). The core reveals a succession of lithofacies which may be assigned to systems tracts based on their lithofacies and tentatively correlated to Sequences J12 to 15.

Sequence SJ06 (Lower Jurassic, late Sinemurian to Pliensbachian) (this paper, new)

The base of SJ06 is picked beneath a thick anhydrite interval where the HST of J04 is truncated by a presumed unconformity. The upper portion of the LST was cored in Well LL (text-fig. 10), where the anhydrites contain both nodular ("chickenwire") and palmate crystal fabrics, indicative of sabkha and ponded/salina depositional settings. The anhydrites are overlain by tidal flat settings rich in microbial fabrics (laminites and stromatolites) (Neog et al. 2018). The base of the TST is abrupt, with a change to shallow, normal marine mudstones and wackestones. A thin zone containing *Lithiotis* sp. shell fragments occurs a few feet above the base of the TST. Latest Sinemurian fossils were recovered from the top of the LST and early Pliensbachian fossils from the base of the TST (Fugro-Robertson 2009). The TST is mostly limestone with minor calcareous shale beds but quickly transitions to dolomites and anhydrites of the HST as accommodation space was filled. The HST is truncated at the base of S J08.

Sequence J08 (Lower Jurassic, Pliensbachian) (this paper, new)

S J08 contains four relatively thin shoaling upward cycles in the LST before abruptly deepening into a thin TST. The HST is a succession of skeletal peloidal mudstones and wackestones with occasional clotted peloidal microbial fabrics, shoaling abruptly at the top to microbial laminite boundstone and centimeter-laminated dolo-mudstone, overlain by millimeter-laminated argillaceous mudstone or dolo-mudstone with high GR values on logs. S J08 was completely cored in two wells (MM and II) and partially cored in three wells (JJ, LL, and KK).

Sequence J10 (Lower Jurassic, upper Pliensbachian to lower Toarcian) (this paper, new)

Sequence J10 comprises the upper portion of the Lower Marrat and the basal portion of the Middle Marrat. It was completely cored in one well (JJ) and partially in five additional wells (MM, NN, X, KK and II). The basal unconformity was cored in four wells (JJ, MM, NN and II), with complete recovery in three (JJ, MM and NN). On logs, the SB is picked in the high-GR zone beneath the thick evaporites of the LST. The evaporites contain abundant nodular ("chickenwire") and minor upright, tabular forms with occasional swallowtail twinning. The anhydrites are occasionally interbedded with dolomitized microbial laminate boundstones. The thick anhydrites are overlain by dolomitic and anhydritic mudstones with common intraclasts. The base of the TST is picked where dolomitic mudstones with intraclasts and nodular anhydrite are overlain by mm-laminated argillaceous mudstones with occasional skeletal fragments and minor bioturbation. The Pliensbachian-Toarcian boundary is placed at this contact in several wells (text-fig. 18) on the basis of the dinoflagellate *N. triceras* and the nannofossil *L. crucicentralis*. The TST is relatively thin, rapidly changing to clean, slightly dolomitic wackestones with bivalve, gastropod, and rare coral fragments at the base of the Middle Marrat. Sharland et al. (2001) originally placed MFS J10 in these shales. Al-Eidan et al. (2009) proposed moving J10 to the drowning unconformity higher in the Middle Marrat, described above. An additional sequence has since been identified at that horizon and the J10 MFS is herein located near the base of the Middle Marrat carbonates.

Sharland et al (2001, p. 204) placed MFS J10 in the lower beds of the middle member of the Sekhaniyan Formation, just below *Lithiotis*-bearing limestones, which were thought to be equivalent to the lower Mus Limestone. In Iran, they correlated it to the basal beds of the Surmeh Formation, again in proximity to the *Lithiotis* beds, dated only as Lower Jurassic by James and Wynd (1965). The placement of MFS J10 in Iraq and Iran correlates to its assigned position in this paper. In the Saudi Arabian outcrop belt, it is placed in shales near the base of the Upper Marrat, dated as the middle Toarcian *bifrons* Zone. Al-Mojel et al. (2018) and Le Nindre et al. (2022) also place J10 at that level. These authors place J10 of Al-Eidan et al. (2009), Kadar et al. (2015) and Simmons and Davies (2018) near the top of the Lower Marrat (early Toarcian, *serpentinum* Zone) and rename it J09.

Sequence J11 (Lower Jurassic, lower Toarcian) (this paper, new)

Sequence J11 comprises the portion of the basal platform carbonate section of the Middle Marrat that underlies and contains the drowning unconformity, proposed by Al-Eidan et al. (2009) as the redefined location of MFS J10. That horizon is herein renamed MFS J11 and considered to be the top of the TST with the HST condensed or absent above it. The SB was described in core in Well AR at 15,799.5 ft (MD, core) and corresponds to a thin interval of high GR values at 15,812 ft (MD, log) which can be traced throughout onshore Kuwait. The LST is approximately 25 ft thick and consists of mudstones to grain-dominated packstones and thin microbial boundstones with coated grains, microbially encrusted oncoids, echinoderm plates, molluscan fragments and *Cayeuxia* sp. The TST, is predominantly mudstones and wackestones with small oncoids, echinoderm plates, bivalve shell fragments and, near the drowning unconformity that forms the MFS, sponge spicules.

Sequences J12 to J16 (Lower Jurassic, Toarcian) (this paper, after Neog et al. 2010)

The rise in sea level for T-OAE and formation of the "drowning unconformity" at MFS J11 flooded the early Toarcian carbonate platform. The platform margin reestablished farther back from the plate margin, forming an intrashelf basin (ISB) (De Keyser and Kendall 2014). Five sequences, J12 to J16, record the development and infilling of the intrashelf basin. The first two, J12 and J13, record the evolution of the new platform margin from a low-relief, ramp-like setting to a steeper margin with a well-developed barrier system and lagoon in which thick anhydrite beds were precipitated. S J12 is comprised of several low-relief clinoforms which, during lowstands, shed packages of lime mudstone turbidites that downlap onto the "drowning unconformity" (text-fig. 30C). S J13 developed a mature depositional profile, with a high-energy barrier system, separating a broad lagoon from a graded shelf, slope and basin. As many as four or five clinoforms can be recognized in a single long cored interval but correlation of them is uncertain, biostratigraphy lacks sufficient resolution to distinguish them, and they are below the resolution of 3D seismic volumes.

S J14 and S J15 have thick lowstand wedges of argillaceous wackestones containing skeletal fragments derived from the barrier and lagoon, filling much of the relief in the intrashelf basin. The S J15 HST progrades rapidly across the infilled ISB and contains packages of grainstones with reservoir potential. Clinoforms deposited prior to these infilling lowstands are the steepest, have the greatest relief and contain coarse-grained, very porous and permeable shoreface grainstone lithofacies. The shoreface and shelf form a broad graded profile down to the

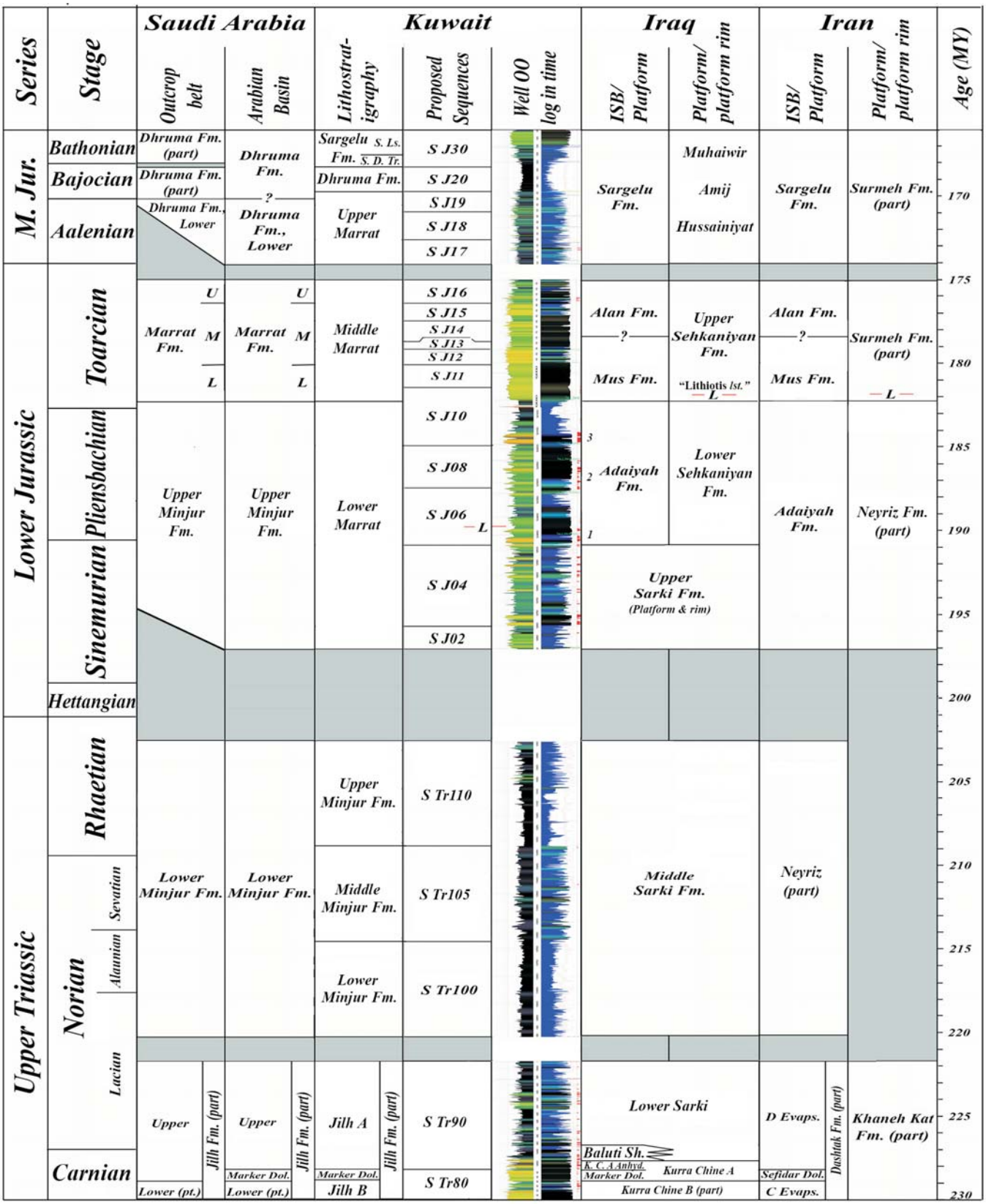

TEXT-FIGURE 37
Upper Triassic to Middle Jurassic correlation chart, showing the interpreted ages of the formations in the countries adjoining Kuwait, their relationship to the sequences discussed in this paper and the corresponding log character in Well OO, on the Burgan Arch. Age column on the right is scaled according to GTS 2015.

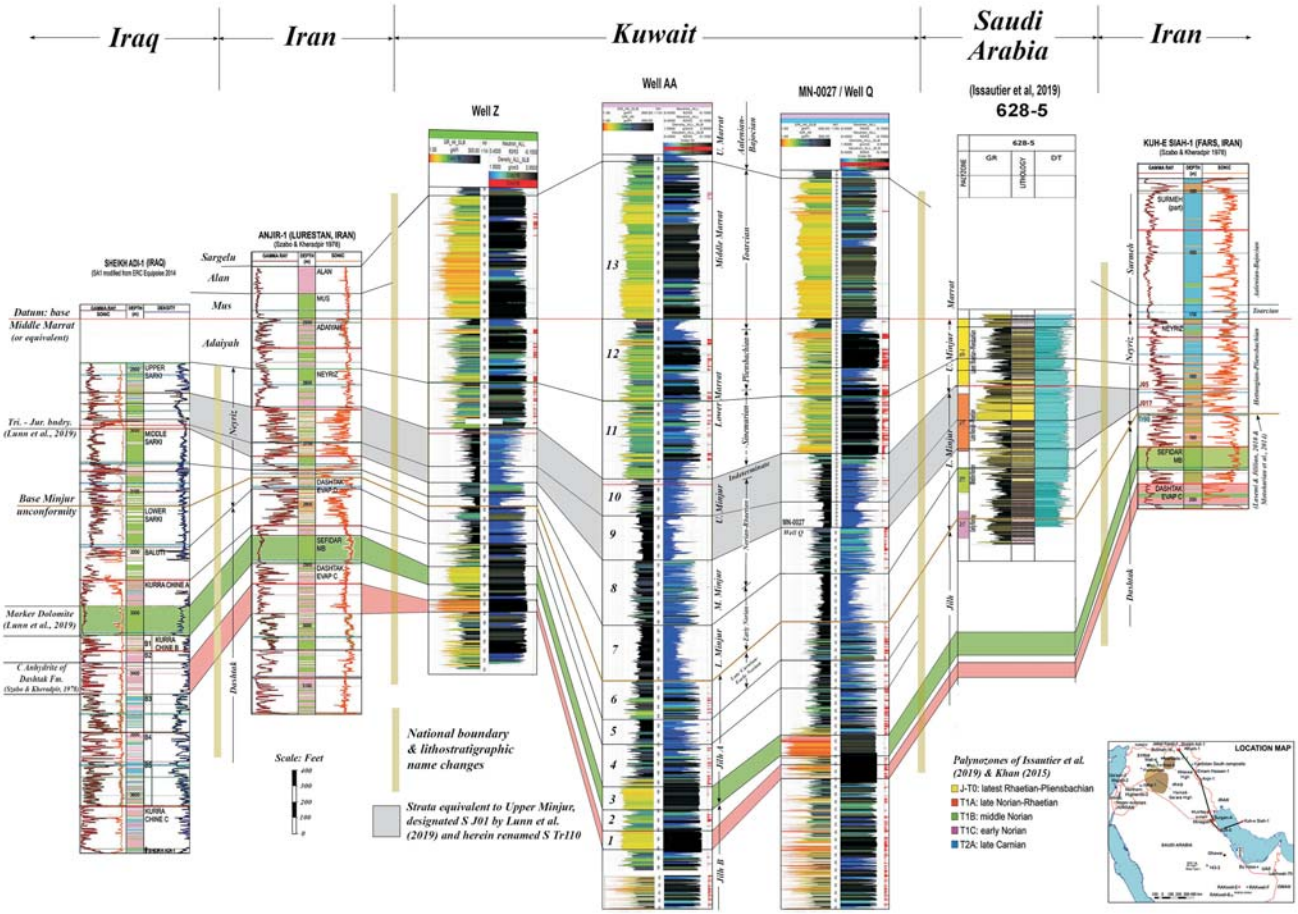

TEXT-FIGURE 38
Cross-section extending from northern Iraq to southwestern Iran, east of Kuwait with a datum at the base of the Middle Marrat. The cross-section incorporates lithostratigraphic terminology and biostratigraphic data from this study, Lunn et al. (2019), Lunn (2020), Szabo and Kheradpir (1978), Lasemi and Jillilian (2010), Motoharian et al. (2014) and Issautier et al. (2019). Yellow shaded bars mark locations of changes in lithostratigraphic nomenclature across national boundaries. The gray shaded area highlights strata assigned to Early Jurassic by Lunn et al. (2019) and Lunn (2020) and named S J01 but considered Late Triassic in this report and renamed S Tr110.

shelf margin at the limit of storm wave action and provide the conduit for hypersaline dolomitizing brines to flow down from the lagoons which prograde over them. The dolomitizing brines initially dolomitized the extensive burrow system before extending outward into the matrix of the shelf mudstones and wackestones, creating excellent reservoirs in the northern Kuwait fields.

S J16 was deposited during a larger relative rise of sea level and caused a larger shift of the depositional profile landward, resulting in an outer shelf *Zoophycos* ichnofacies to overlie *Cruziana* and *Skolithos* ichnofacies. The top of S J16 is the unconformable contact between the Middle and Upper Marrat and marks the Toarcian/Aalenian boundary. If S J16 can be proven to be middle Toarcian as suggested by the Fugro Robertson unpublished report (2009), it is likely to be equivalent to the Upper Marrat sequence where Al-Mojel et al. (2018) suggest placement of MFS J10. It is also possible that the Middle Marrat platform margin becomes younger in a basinal direction and that the top of S J16 is late Toarcian (see discussion above under biostratigraphy).

The cross-section shown in text-figure 35 combines the results of an unpublished 2009 study by Fugro-Robertson and the sequences recognized in this study. The sequences of the Lower Marrat have already been discussed above. The differences between the biostratigraphic and sedimentologic boundaries in the Lower Marrat sequences results from assignment of the thick anhydrites to LSTs rather than to the HSTs of the underlying sequences. As has already been discussed, these LSTs are underlain by unconformities and are transitional upward into the TSTs and HSTs. This differs from the anhydrites in the Middle Marrat, which are overlain by unconformities and show evidence of exposure and dissolution. The sequence boundaries in the Upper Marrat are unconformities and the thin sabkha anhydrites are not assigned to specific systems tracts.

The three biozones recognized in the Middle Marrat by Fugro-Robertson (2009) are color-filled between wells to show the correlation from the platform (wells QQ, TT/EE, B and UU, platform margin (Well GG) and ISB (wells VV, YY, WW and ZZ). Their oldest biozone (?Toa1) is equivalent to the upper TST and all of the HST of S J10 and all of S J11 and represents

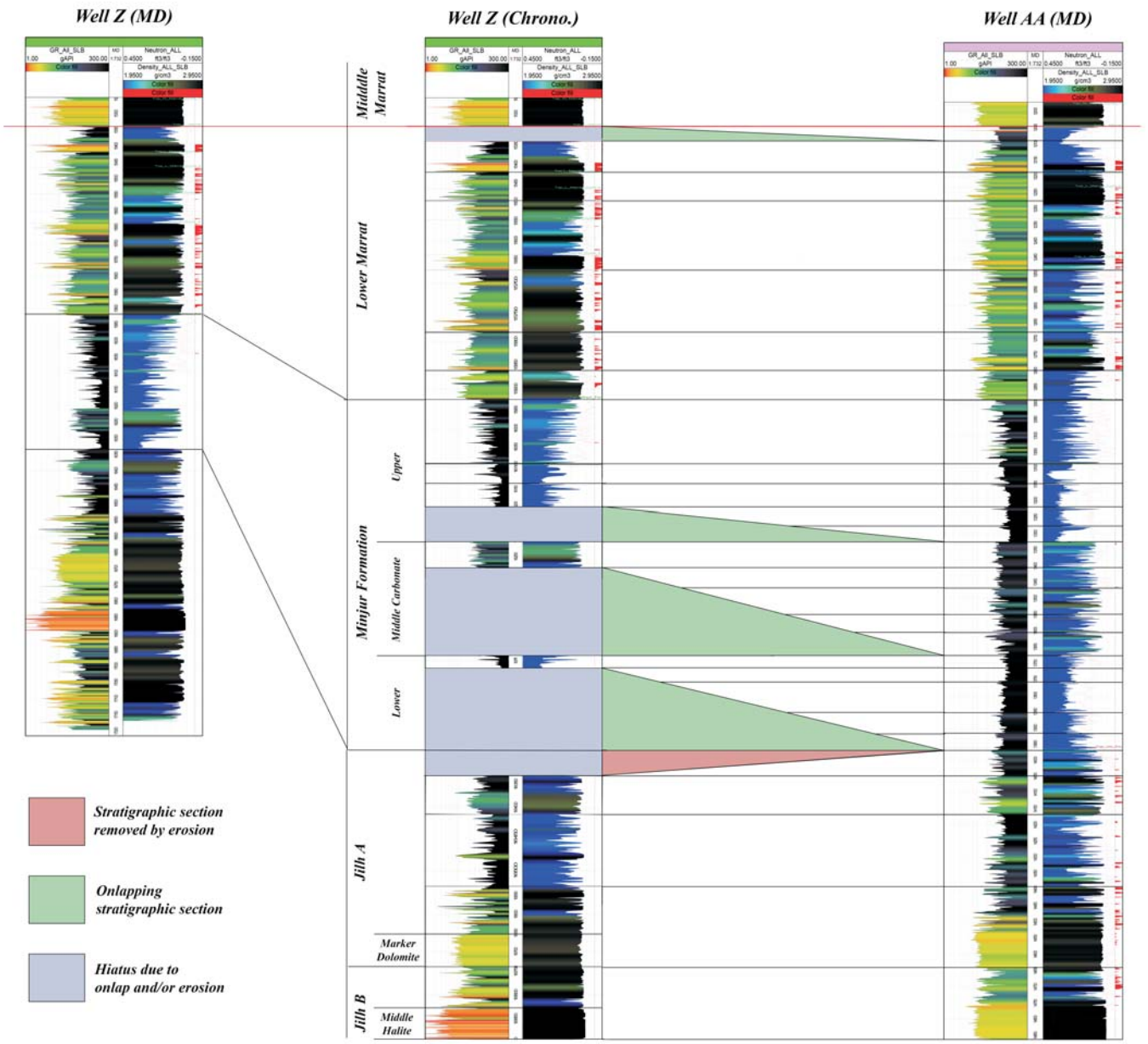

TEXT-FIGURE 39
Comparison of a basinal well (Well AA) in Burgan Field with a basin margin or platform well (Well Z) in NW Raudhatain Field. Depositional cycles have been identified in Well AA where the section is assumed to be nearly complete. Original log display for Well Z is in MD on the left and expanded in the center (Well Z, Chrono) by stretching (or shrinking) each cycle to match the thickness in Well AA. Cycles absent in Well Z are attributed either to erosion at the start of Qatar Arch uplift (top of Jilh Formation) or to onlap of the margins of the subsiding Arabian Basin. Hiatuses are present at the base of each member of the Minjur, decreasing upward as uplift ceased and basinal subsidence slowed. The change in sedimentation at the base of the Lower Marrat may represent onlap over the Qatar Arch. The minor onlap at the base of the Middle Marrat cannot be correlated, even locally, and is not considered significant.

the open marine platform succession that forms the lower portion of the Middle Member. Biozone Toa2-?Toa3 encompasses all of sequences S J13 to S J15 and represents the ISB and basin fill succession. Biozone ?Toa4 corresponds to the transgressive sequence that deposited outer shelf litho- and ichnofacies over platform lithofacies and forms the uppermost lithologic unit of the Middle Marrat.

The middle biosequence is of greatest interest because it corresponds to Sequences S J12–S J15 which represent the Middle Marrat ISB succession. At the west end of the cross-section (Well QQ), most of Toa2-?Toa3 is comprised of Sequences S J12 and S J13, up to the top of the band of anhydrite beds (density curve color-filled red above 2.8 gm/cm^3) visible in wells TT/EE, B and UU. The anhydrite beds represent late highstand lagoonal beds and are absent at and seaward of the barrier complex, visible at the same level in Well G. In the platform area, the overlying sequences (S J14 and S J15) consist predominantly of lagoonal, backshoal, shoal, and truncated shoreface lithofacies, reaching a thickness of 80–100 ft, up to the base of biosequence ?Toa4. Sea-

ward of the platform margin in Well GG, Sequences S J12 and S J13 thin rapidly into the basin and Sequences S J14 and S J15 thicken rapidly, largely because of thick argillaceous lime mudstone LSTs which are prominently visible on logs. This compensatory thickness relationship has been referred to as "wedge-on-wedge" and documented in western and central North America in sediments of Carboniferous (Tournaisian) age (Lane 1974; De Keyser 1979; Lane and De Keyser 1980). At the right end of the cross-section, Sequences S J12 and S J13 cannot be reliably identified and most of the thickness of biosequence Toa2-?Toa3 is represented by sequences S J14 and S J15 (text-fig. 36). Text-figure 36 is an enlargement of a core description and logs in the interval from the top of S J11 to the lower portion of SJ14, showing the thin basinal units overlying the drowned platform and the argillaceous mud/wackestone units that formed much of the basin fill.

Sequences J17 to J19 (Middle Jurassic, Aalenian to lower Bajocian) (Crespo de Cabrera et al. 2019)

The Upper Marrat has been regarded as having low hydrocarbon potential and therefore has been cored less than many other Jurassic units. Nevertheless, several long, continuous cores have provided excellent data for the lower approximately two-thirds of the Member and biostratigraphy has demonstrated the ages of the three sequences which have been described. S J17 and S J18 are both Aalenian in age and the Aalenian/Bajocian boundary is within S J19.

Sequence Correlation Across the Arabian Plate

Lunn et al. (2019) presented four cross-sections showing correlations of Triassic and Early Jurassic strata throughout the Arabian Plate and a sequence stratigraphic summary chart for the same interval. The revised correlations proposed in this paper are shown in text-figure 37.

Sequence Tr80, as revised by Lunn et al. (2019), is equivalent to the upper portion of Jilh B and the basal dolomitic unit of the Jilh A (= Marker Dolomite of Lunn et al. 2019) as recognized in Kuwait and is of late Carnian age. Lunn et al. (2019) considered the "middle halite" to be the early TST of the sequence, overlain by a thin, argillaceous TST in the upper part of the Jilh B. MFS Tr80 was placed at the base of the HST, their Marker Dolomite (text-figs 4, 35). They point out that the "middle halite" was interpreted as an argillaceous carbonate by Alsharhan et al. (2014). The very low GR value and low density (right track, red line) indicative of halite are clearly visible in the logs from Burgan Field (text-fig. 4). The Marker Dolomite is time-equivalent to the Sefidar Dolomite in Iran (Szabo and Kheradpir 1978). It was previously considered to be Norian in age and assigned to MFS Tr80. With the change in its age to late Carnian, the Marker Dolomite is now recognized as being older than most of the Jilh A and the lower unit of the Minjur and two new MFSs were recognized in the overlying Triassic section (Lunn et al. 2019).

Sequence Tr90, latest Carnian to early Norian in age, encompasses all of the Jilh A above the "marker dolomite" in Kuwait (text-fig. 4). The equivalent strata in Iraq include the anhydritic upper Kurra Chine A Member, the Baluti Shale and the Lower Member of the Sarki Formation of late Carnian and earliest Norian age. These units are equivalent to the "D" evaporites in Iran and to the upper Khaneh Kat Formation in the open marine platform margin region.

Sequence Tr100 is separated from Sequence Tr90 by a hiatus encompassing much of the early Norian, correlated to the unconformity at the base of the lower Neyriz Formation in Iran and the Minjur Formation in Kuwait (text-fig. 33). During this time, the Qatar Arch and the Ghawar structure were uplifted and eroded, accompanied by subsidence in the Arabian, Rub al Khali and Mesopotamian basins. The Dashtak is eroded down to the Sefidar Dolomite over the Qatar Arch uplift in the Fars area of onshore Iran and down as far as the B Evaporites of the Dashtak along its northeastward extension toward the Bandar Abbas area (Szabo and Kheradpir 1978). The Minjur Formation onlaps the Qatar Arch and the Marrat Formation thins over it as well. In Iraq, the Sarki Formation is divided into three units based on recognition of two prominent sequence boundaries and this hiatus separates the lower and middle units. The hiatus is dated in Iraq in Well Atrush-1, where the basal contact of S Tr100 with the underlying Lower Sarki is dated as latest Carnian or earliest Norian. The age of the top of the Lower Sarki is considered to be early Norian and the base of the Middle Sarki is definitively dated as late Norian (Lunn et al. 2019). The top of S Tr100 was dated as Norian to Rhaetian in age in Kuwait and Iraq (Lunn et al. 2019). In this paper, it is dated as late middle or early late Norian.

Sequence Tr105 is comprised of the Middle Carbonate Member of the Minjur Formation in Kuwait. Lunn et al. (2019, Figure 9) and Lunn (2020, Figure 6) correlate it to the upper, more carbonate portion of the Middle Sarki in Iraq and to the middle portion of the lower Neyriz in Iran.

Sequence Tr110 corresponds to the Upper member of the Minjur Formation in Kuwait and is dated as Norian to Rhaetian (text-fig. 35). This correlates to the shaly basal portion of the Upper Sarki in Iraq (well Sheikh Adi 1) and the lower, siliciclastic portion of the Neyriz in Iran (well Anjir 1) of Lunn et al. (2019, Figure 9). The top of the Middle Sarki has traditionally been equated with the Triassic/Jurassic boundary (Liu et al. 2017; Lunn, pers. comm., 2021) but data presented in this paper place it at the top of the lower, shaly portion of the Upper Sarki (Upper Jurassic).

Correlation to the outcrop belt of Saudi Arabia is problematic. Powers et al. (1966) considered the Minjur to be entirely Triassic in age and overlain unconformably by the Toarcian-age Marrat Formation. Issautier et al. (2012a) list the age of the Minjur Formation, divided into Upper and Lower Members, as Norian to Rhaetian, while Al-Mojel et al. (2018), in a study of the lower and middle Toarcian Marrat Formation, describe it as lying unconformably on the Triassic Minjur Formation. None of these outcrop studies except Powers (1968) recognized the possibility that some (or all) of the massive sandstones of the Upper Minjur could be Early Jurassic in age. Shallow core holes drilled on escarpments in the outcrop belt provided a complete section of the interval from the top of the Minjur Formation to the top of the Dhruma Formation. In that study the siliciclastics in the Minjur immediately below the Marrat Formation were dated as late Pliensbachian to earliest Toarcian, almost certainly correlative with the S J10 TST in Kuwait (Reid et al. 2016).

Stewart et al. (2016, Figure 6, Well A) employed data from that new reference section in a cross-section extending from southwest of Riyadh across the Qatar Arch into U. A. E. They correctly list the age of the Minjur Formation as Norian to Pliensbachian, equivalent to all of the Minjur and Lower Marrat

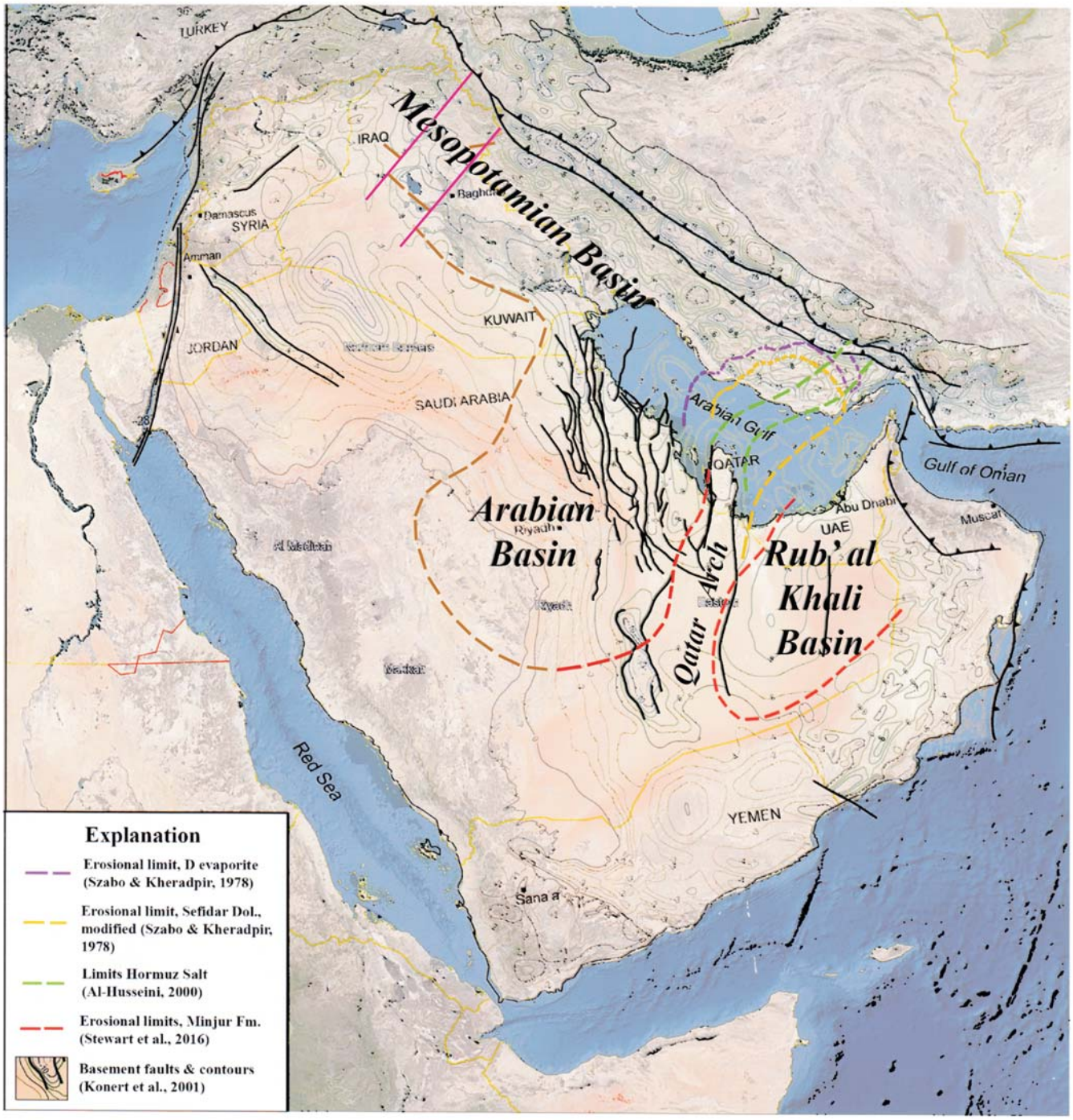

TEXT-FIGURE 40
Map of Arabian Plate, showing approximate boundaries of the Late Triassic to Early Jurassic Mesopotamian, Arabian and Rub' al Khali basins, separated by the Qatar Arch. Depth to basement (Km) and major faults are from Konert et al. (2001). Eroded edges of "D" evaporite and Sefidar Dolomite of the Dashtak Formation. and the boundary between Dashtak and Khaneh Kat formations modified from Szabo and Kheradpir (1978). Erosional limits of Minjur are modified from Stewart et al. (2016). Limits of the Hormuz Salt north and south of the Qatar Arch are from Al-Husseini (2000). Image is a screen capture from Google Earth.

in Kuwait. Their chronostratigraphic cross-section, extending from the Red Sea to the Rub' Al Khali Basin shows only siliciclastic sediments in the Minjur and a hiatus from late Rhaetian to mid-Sinemurian.

Issautier et al. (2019) reviewed and revised the earlier Minjur outcrop study of Issautier et al. (2012a, 2012b) and extended the study into the subsurface Arabian Basin. In reviewing the history of studies of the formation, they correctly note that while Powers

et al. (1966) assigned the Minjur to the Triassic, Powers (1968) recognized an Early Jurassic palynoflora in the upper portion of the formation. Palynological studies in the shallow subsurface allowed recognition of four palynozones ranging in age from latest Carnian or earliest Norian to Pliensbachian. They recognized four sequences in the Lower Minjur, the lowest assigned to the Jilh, and five in the Upper Minjur in outcrop and tentatively correlated them to the subsurface in a cross-section extending northeastward in the Arabian Basin (Issautier et al. 2019, Figure 12). It is interesting to note that this study also recognized three sequences in the Kuwait Minjur and five sequences in the Lower Marrat.

Lunn et al. (2019, Figure 11) present a cross-section extending southward from Kuwait, showing truncation beneath the Dhruma Formation, removing the Upper Minjur at Ghawar Field and truncation down to the Marker Dolomite (= Jilh B, S Tr80) over the Qatar Arch. In that cross-section and in Lunn (2020, Figure 6, Well 143-3) the Upper Minjur of Issautier et al. (2019) is correlated to the upper member of the Minjur in Burgan and Mutriba fields. We place the top of the Triassic at the base of the Lower Marrat and interpret these data to suggest that the Lower Marrat of Kuwait extends southward into northeastern Saudi Arabia and the Arabian Basin as an unnamed lithostratigraphic unit that is transitional westward and southward into the formally named Upper Minjur Formation. The five sequences of Issautier et al. (2019) may be correlative to the five sequences of the Lower Marrat recognized in this study. Sequence J01 of Lunn et al. (2019) is shown herein to be Late Triassic in Kuwait and renamed S Tr110.

Lunn et al. (2019) proposed Sequence J05 at the base of the Lower Marrat in Kuwait. As discussed above, we have not used that sequence designation because their S J05 extended upward to the base of the Middle Marrat and we needed to designate five sequences within that interval. However, they also show two MFSs and their corresponding sequence boundaries, labeled J01 (Hettangian) and J02 (Upper Sinemurian) (Kuwait) between wells Sheikh Adi-1/Jebel Kand-1 (Iraq) and Anjir-1 (Lurestan, Iran). The position of S J02 at the base of the Lower Marrat is consistent with this study but J02 was not discussed in their summary of the sequence stratigraphy. Their J02 is correlated to the upper unit of the Neyriz Formation and equivalent to the Adaiyah Formation.

We define Sequence J02 to extend from the base of the Lower Marrat to the thick anhydrite beds forming the LST of S J04. S J04 extends to the unconformity beneath the anhydritic LST of S J06. We correlate S J02 and S J04 to the Upper Sarki Formation in Iraq, to the lower portion of the Neyriz Formation where the Adaiyah Formation is recognized in Iran, and to the lower portion of the upper Neyriz Formation in Iran platform margin areas (text-fig. 37). These strata have not been seen in core in Kuwait but are shown in cross-sections by Szabo and Kheradpir (1978). They are unconformably overlain by the Surmeh Formation and the *Lithiotis* beds are just above the base of it, where they were dated only as Early Jurassic by James and Wynd (1965).

Sequences S J06, S J08 and S J10 below the base of the Middle Marrat are together correlated to the Adaiyah Formation in the platform interior in Iraq and to the Lower Sekhaniyan in the outer platform and rim in Iraq. Lunn (personal communication, 2021) notes that the three prominent anhydrite intervals in the Adaiyah in Iraq may be the equivalent of the anhydrites at the base of these three sequences.

Designation of Stratal Units

Integration of lithostratigraphic, sedimentologic and biostratigraphic data greatly facilitates construction of a sequence stratigraphic framework. Text-figure 38 summarizes these data in a long cross-section extending from northern Iraq to northwest Iran, Kuwait, Saudi Arabia and southwestern Iran. Lunn et al. (2019) and Lunn (2020) included the Iraq and Iran wells in several regional cross-sections and those data have proven very valuable to the present study. Issautier et al. (2019) summarized their data on the Minjur Formation in outcrop and extended that interpretation northeastward into the Arabian Basin with supporting biostratigraphic data.

The lines of correlation in text-figure 38 mark changes in lithostratigraphic nomenclature and sedimentary regime and are, for the most part, sequence boundaries. They enclose genetic increments of strata which can be correlated over much of the interior of the Arabian Plate. In text-figure 38, these stratal units (SU) have been numbered from 1 to 13 in the left track of Well AA (Burgan Field, Kuwait) and will be discussed in the following paragraphs.

Stratal Unit 1 (SU1) comprises the "middle halite" of the B Member of the Jilh Formation in Kuwait. It is the lateral equivalent of the C Anhydrite Member of the Dashtak Formation of Szabo and Kheradpir (1978). It is the uppermost unit of S Tr75 (Lunn et al., 2019). Pink color fill in text-figure 38 shows the correlation and lithostratigraphic equivalents of SU1.

SU2 and SU3 together represent S Tr80 of Sharland et al. (2001) as redefined by Lunn et al. (2019) and recognized herein. Lithostratigraphically, it consists of the upper unit of the Jilh B and the lowermost unit of Jilh A. SU3 is the lateral equivalent of the Sefidar Dolomite in Iran and recognized as the Marker Dolomite by Lunn et al. (2019). The pale green shading in text-figure 38 shows the correlations and lithostratigraphic equivalents of SU3.

SU4, SU5 and SU6 comprise S Tr90 of Lunn et al. (2019). Together with SU3, they comprise the Jilh A in Kuwait. The shaly middle unit (SU5) is laterally equivalent to the Baluti Formation in northern Iraq (Lunn et al. 2019) and is latest Carnian in age. The upper surface of SU6 is the unconformity of early Norian age separating it from the Minjur Formation (brown correlation line in text-figure 38).

SU7 is the Lower Member of the Minjur Formation in Kuwait. It is equivalent to the lower, more argillaceous portion of the Middle Sarki in northern Iraq. SU8 represents the Middle Carbonate Member of the Minjur. Lunn et al. (2019) combined SU7 and SU8 in defining S Tr100. Khan (1989) recognized a prominent unconformity at the base of SU8 and we have restricted S Tr100 to SU7 and defined SU8 as S Tr105. Both SU7 and SU8 exhibit onlap of multiple cycles from intrabasin to basin margin wells (text-figs 33, 39). Stewart et al. (2016) illustrated seismic images of equivalent onlap in the Rub al Khali Basin, south of the Qatar Arch.

SU9 and SU10 together comprise the Upper Member of the Minjur in Kuwait. Earlier studies have considered the Triassic/Jurassic boundary to be the top of the Middle Member of the Minjur, based on the distribution of the palynomorph *Vesica-*

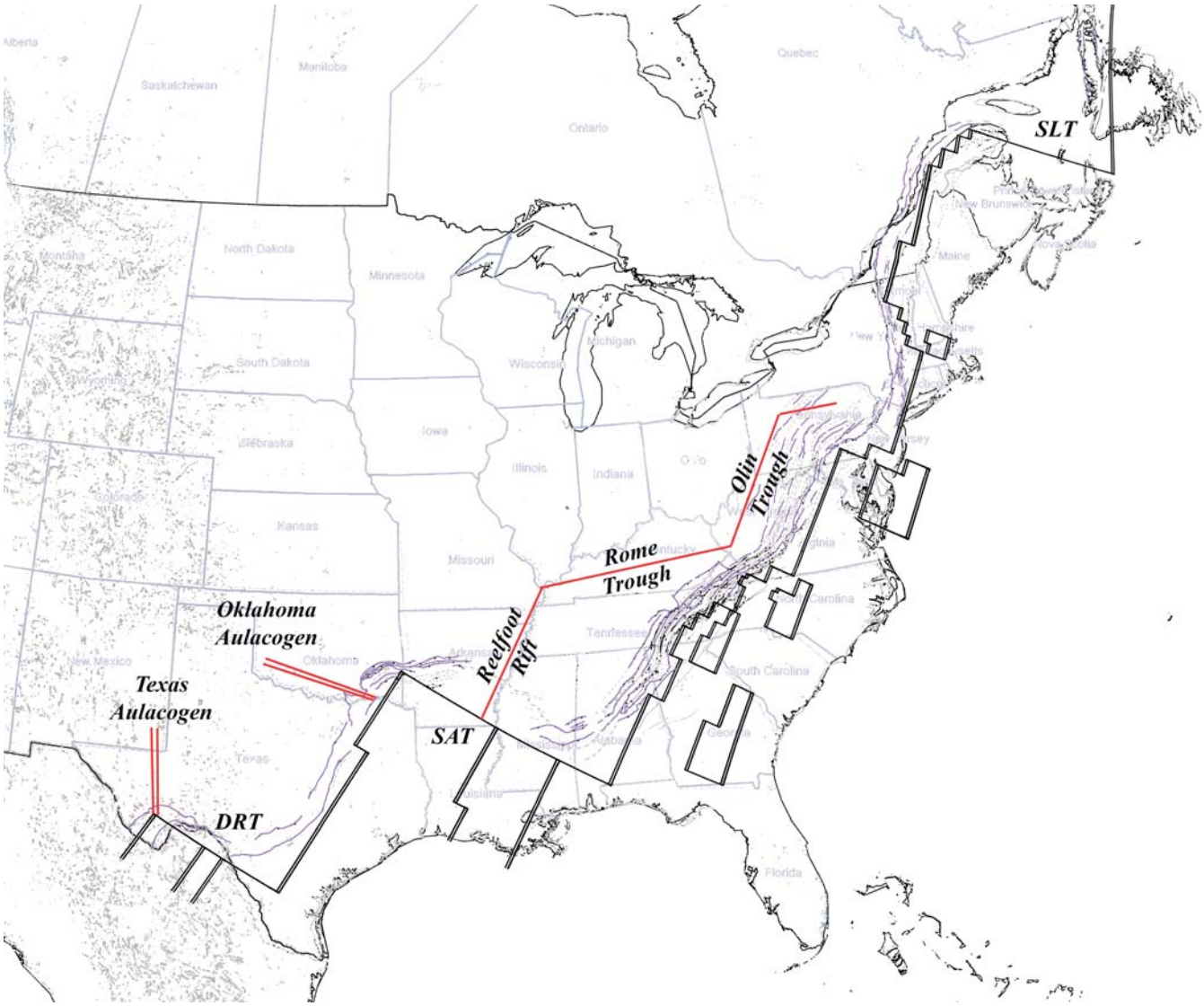

TEXT-FIGURE 41
Map of eastern North American Alleghenian orogenic system, showing the series of rifted margins and connecting transform faults (modified from Thomas et al. 1977) referred to as promontories and recesses. The Alleghenian system consists of the Marathon (southernmost), Ouachita, Appalachian and maritime Canadian thrust belts. The three long transform fault zones are the Devils River Transform (DRT) (southernmost), Southern Appalachian Transform (SAT) and St. Lawrence Transform (SLT). The Texas Aulacogen was inverted to form the Central Basin Platform and the Oklahoma Aulacogen was inverted to form the Arbuckle Mts. The Reelfoot Rift and Rome-Olin trough system are thought to be a failed Eocambrian rift system.

spora schemeli (Cameron 1974; Loutfi and Abdel-Satter 1987). The more detailed recent studies reported herein found *V. schemeli* near the top of SU10 in two wells. That and a thin interval of mixed Triassic and Jurassic species just below the base of the Lower Marrat have caused us to move the boundary to near the base of the Lower Marrat. We have correlated the top of SU10 to the boundary between the Lower and Upper Minjur as defined in Saudi Arabia (Issautier et al. 2019). Notably, in the cross-section of the Minjur published by Issautier et al. (2019, their Figure 12), the first downhole occurrence (FDO) of *V. schemeli* is at or just below that surface in all five wells. SU9 and SU10 together were named S J01 by Lunn et al. (2019), assuming them to be Early Jurassic in age. We have renamed this sequence S Tr110 and it is shaded light gray in text-figure 38.

SU11 is the lower portion of the Lower Member of the Marrat Formation, comprised of sequences S J02 and S J04 as defined herein, dated as early Norian to late Sinemurian in age. SU11 has been correlated to the upper, less argillaceous portion of the Upper Sarki Formation in Iraq and to the middle portion of the Neyriz Formation in northwestern Iran. In Saudi Arabia, they represent the lower, more siliciclastic portion of the Upper Minjur (Issautier et al. 2019).

SU12 extends from the base of S J06 to the base of the Middle Marrat in Kuwait and includes all of S J06 and S J08 and all of S J10 except the uppermost TST and all of the HST. It has been correlated to the Adaiyah Formation in Iraq and northwestern Iran. Where the Adaiyah is not recognized, it is correlated to the upper

portion of the Neyriz. In Saudi Arabia, it is equivalent to the upper, more carbonate portion of the Upper Minjur (Issautier et al. 2019). SU12 is dated as latest Sinemurian to earliest Toarcian.

SU13 comprises all of the Middle Marrat in Kuwait, including the upper portion of S J10 and all of sequences S J11 to S J16. It is correlated to the Mus and Alan formations in Iraq and northwestern Iran and to the lower, *Litthiotis*-bearing portion of the Surmeh Formation in southeastern Iran. SU13 is the equivalent of the entire Marrat Formation as defined in Saudi Arabia. Correlation of the Mus and Alan to the Middle Marrat is uncertain and has not been attempted in text-figure 38.

To summarize, the Upper Minjur of the outcrop belt is time-equivalent to the Lower Marrat (Sequences J 02, J 04, J 06, J08 and the LST and early TST of J10). The Marrat in the Saudi Arabian outcrop belt represents most or all of the Middle Marrat sequences J10 to J16. The upper Toarcian appears to be missing in outcrop due to non-deposition or erosion beneath the Aalenian unconformity. Most of the time represented by the Aalenian hiatus is preserved in the Upper Marrat of Kuwait (Sequences S J17 to S J19).

In Iran, the *Lithiotis* beds occur near the base of the Surmeh Formation (James and Wynd 1965; Setudehnia 1972; Szabo and Kheradpir 1978; Motaharian et al. 2014) and are equivalent to the S J10 HST. The Surmeh encompasses the entire Jurassic section above the Neyriz Formation in the Lurestan-Kuzestan area of Iran, northeast of Kuwait but to the northwest (Iraq) in the Lurestan Basin it is subdivided into the Mus, Alan, Sargelu and Najmah (=Naokelekan)-formations. In Fars, the Hith is also recognized at the top of the Surmeh. The areas of Surmeh deposition more closely resemble platform margins while the areas of subdivision should be thought of as platform interior or intrashelf basin depositional settings.

The Surmeh has been subdivided into five lithostratigraphic units: lower carbonate, lower shaly, middle carbonate, upper shaly and upper carbonate (Lasemi and Jililian 2010). The lower carbonate unit can be further subdivided into two subunits, a lower, *Lithiotis*-bearing dolomitic limestone of Toarcian age, separated from brown dolomites and interbedded gray limestones of Bajocian age by an unconformity (Motoharian et al. 2014). The Toarcian subunit is approximately correlative to the Middle Marrat in Kuwait. If Aalenian strata are in fact absent as reported by Motoharian et al. (2014), then no more than the upper portion of the Upper Marrat of Kuwait can be correlated to the lower portion of the upper subunit and the remainder is correlative to the Dhruma of Kuwait.

The Upper Marrat of Kuwait has never been recognized in the outcrop belt of Saudi Arabia, being replaced by a hiatus from middle Toarcian to early Bajocian (Powers et al. 1966; Powers 1968; Sharland et al. 2001; Al-Mojel 2018). More recently, Reid et al. (2015) report a condensed Aalenian (Lower D1 of Dhruma Formation) in the new composite reference section, just below an influx of *Callialasporites turbatus* interpreted to mark the base of the Bajocian (Reid et al. 2015; Stewart et al. 2016). Reid et al. (2015) interpret the Aalenian as a time of highstand progradation present in the subsurface of eastern Saudi Arabia based on the occurrence of thin anhydrite beds. The anhydrite beds in S J17 and S J18 in Kuwait are interpreted as sabkha deposits and of peritidal origin. We would interpret these sequences and much of S J19 as part of a lowstand wedge.

Chronostratigraphy and Hiatuses in the Minjur Formation

The lack of biostratigraphic data, combined with the depo-tectonic effects of uplift of the Qatar Arch and accompanying subsidence of the Arabian and Rub al Khali basins, have complicated efforts to describe the lithostratigraphy, correlate formations across national boundaries and construct a sequence stratigraphic framework for the Triassic of the Arabian Plate. The recent publications by Issautier et al. (2012a, 2012b), Reid et al. (2015), Stewart et al. (2016), Issautier et al. (2019), Lunn et al. (2019) and Lunn (2020) have provided the data and interpretation on which this paper has attempted to build an expanded sequence stratigraphic framework that includes the Lower and Middle Jurassic Marrat Formation and clarifies its relationship to the Minjur Formation of Saudi Arabia. The Minjur Formation as recognized in Saudi Arabia spans approximately 38–40 Ma, from early Norian to earliest Toarcian time.

Uplift of the Qatar Arch and formation of the Arabian Basin, however, was confined to the time span of the Minjur Formation as recognized in Kuwait, where it is divided into lower, middle and upper members, from early Norian to Rhaetian according to the biostratigraphic data presented herein. The thickness of the Minjur Formation varies greatly in Kuwait, from approximately 390 ft in the northwest to 1,060 ft in the southeast. The subjacent Jilh Formation and the superjacent Lower Member of the Marrat Formation display a platform morphology and lithofacies, bracketing the Minjur Formation with its rapid thickening southeastwards into a predominantly siliciclastic depocenter. The unconformity at its base is taken to represent the onset of uplift of the Qatar Arch.

Comparison of a well thought to represent the basin margin (Well Z) with a well near the axis of the basin (Well AA) shows that higher-order cycles recognizable on logs within the members of the Jilh, Minjur and Lower Marrat can be identified in both wells. Correlation lines were drawn to connect the cycles and it was found that many Minjur cycles evident in the basinal well (AA) were absent in the basin margin well (Z), while cycles in the Jilh and Lower Marrat were present in both wells with only slight thickness differences. To test this observation, a log display was built in which the basin margin well was stretched (or shrunk) to make all the cycles in both wells the same thickness (text-fig. 39). The missing cycles were represented by gaps in the log display and were assumed to equal the time during which the basinal cycles were deposited. The basinal cycles gradually onlapped the basin margin and deposition resumed in the upper cycles of each member. The missing cycle at the top of the subjacent Jilh Formation was assumed to represent erosion (compare this with text-figure 33).

Most of the missing stratigraphic interval is at the base of the Lower and Middle Carbonate Members, with only a couple cycles missing at the base of the Upper Member. Fourteen Minjur cycles were recognized in Well AA and only five in Well Z. The estimated duration of Minjur deposition is approximately 20 Ma and assuming these cycles averaged at least 1 my, the total amount of time represented by these hiatuses could easily be 8–10 My. Presently, the biostratigraphy can only identify a few subdivisions in the Late Triassic and Early Jurassic, such that each "zone" might contain four or five of these probable 4th-order cycles. Until such time as these Triassic and Early Jurassic formations are studied in greater detail and a more precise formal zonation can be constructed, sedimentology, physical stra-

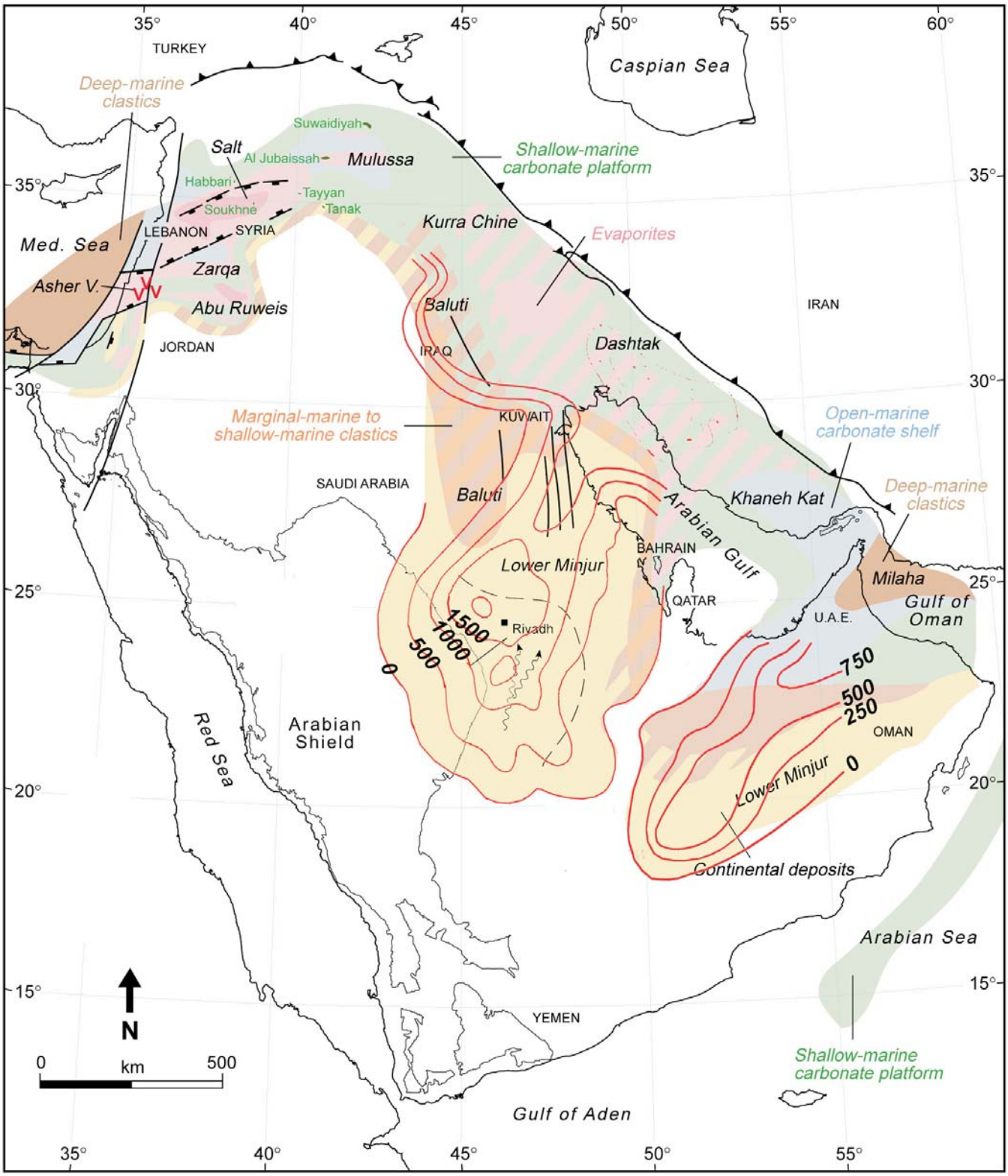

TEXT-FIGURE 42
Outline map of Arabian Plate with approximate size and position of the Arabian and Rub' al Khali basins and southwestern margin of the Mesopotamian Basin. Hypothetical restored Minjur isopachs (feet, red) are modified after Alsharhan (1993), Jassim and Goff (2006), Stewart et al. (2016) and Issautier et al. (2019).

tigraphy and well log correlations will be critical components of any sequence stratigraphic analysis.

PALEOGEOGRAPHY AND DEPOTECTONIC HISTORY

The Early, Middle and most of the Upper Triassic sediments of the Arabian Plate consist of a series of carbonate-evaporite cycles which can be correlated throughout the plate interior. The succession begins with the Aghar/Beduh Shale at the base of the Sudair Formation and continues upward to the top of the Jilh Formation in early Norian time. In Iran, these cycles were assigned to the Dashtak Formation based on the presence of four evaporite intervals, designated A through D (oldest to youngest) (Szabo and Kheradpir 1978). A dolomite unit in the "C" cycle was found to be regionally mappable and was named the Sefidar Dolomite (= Marker Dolomite of Lunn et al. 2019). The evaporites thin and terminate toward the plate margin where the time-equivalent massive carbonate is named the Khaneh Kat Formation (Szabo and Kheradpir 1978).

The long period of passive margin cooling and subsidence that began in the Permian ended when uplift occurred along the roughly north-south oriented Qatar Arch. The upper cycles of the Dashtak and Jilh were removed by erosion across the crest of the Arch to below the Sefidar Dolomite. Szabo and Kheradpir (1978) were able to map the erosional limit of the Sefidar Dolomite and the overlying "D" evaporites along the margin of the uplifted Arch (text-figure 40). Those limits can also be mapped along the south side of the uplift and together they define the shape of its northeastward extension out to the plate margin. Mapping also shows that the Hormuz Salt is absent beneath the northeastward extension of the Qatar Arch, serving to separate the northern and southern Gulf salt basins (Al-Husseini 2000). The depocenter of the Dashtak basin extends to the northwest as the Mesopotamian Basin and its extension beneath the northwestern Gulf. Szabo and Kheradpir (1978, Figure 15) (text-figure 40) mapped a linear depocenter up to 1130 m thick, extending northwestward past Kuwait before stepping southwestward in southern Iraq.

Thick wedges of Minjur Formation siliciclastic sediment were deposited both west and east of the Qatar Arch in the Arabian and Rub' al Khali basins (text-figure 42). The Minjur Formation, divided into Lower and Upper units, onlaps the Arch but is absent over the crest and the overlying Marrat Formation thins over it. In the Arabian Basin, the siliciclastics dominated sedimentation until the end of the Triassic. A combination of reduced sediment supply and relative rise of sea level began in the Early Jurassic (Sinemurian). In the northern Arabian Basin (Kuwait and northeastern Saudi Arabia), the siliciclastics of the Upper Minjur Formation were transitional to the carbonate-evaporite cycles of the Lower Marrat Formation discussed in this paper. The Qatar Arch continued to shed some siliciclastics until it was covered by the onlapping Marrat Formation in the Early Jurassic.

Further rise of sea level in earliest Toarcian time flooded the basin, forming a broad carbonate platform that extended southwestward to the outcrop belt in Saudi Arabia. A second large rise of sea level caused platform drowning and formation of an intrashelf basin on the platform, correlated to an early Toarcian oceanic anoxic event (T-OAE). Sedimentation infilled the ISB during the remainder of Toarcian time.

A new depocenter formed in the northern portion of the Arabian Basin during the Middle Jurassic Dhruma time (Bajocian) (Kadar et al. 2015; Stewart et al. 2016; Crespo de Cabrera et al. 2019, 2020). The Arabian Basin was separated from the Gotnia Basin by formation of the Rimthan Arch during the Callovian (Crespo de Cabrera et al. 2019, 2020). It is likely that the Rimthan Arch formed by reactivation of an older structure, based on the absence of the Silurian Qusaiba Shale in that location on the post-Hercynian subcrop map (Konert et al. 2001).

The four paleotectonic and lithofacies maps in text-figure 2 give a snapshot overview of the depo-tectonic history of the Arabian Plate during deposition of the Late Triassic and Early Jurassic. During Carnian and early Norian time, the northeast Arabian Plate margin was the passive margin of the paleo-ocean Neotethys. The interior of the plate was the site of deposition of a thick succession of carbonate-evaporite sequences which, together, comprise the Carnian saltern supersequence of Lunn et al. (2019). The second map (text-fig. 2b) shows the late Norian paleotectonics (Barrier et al. 2018) overlain with the paleofacies for Carrnian-Norian time. The late Norian plate reconstruction shows that a spreading center had formed along the northeast plate margin, forming the Southern Neotethys. Uplift and erosion along the Qatar Arch began at least by early Norian, accompanied by deposition of Minjur siliciclastics in the subsiding Arabian, Rub al Khali and Mesopotamian basins. The final two maps of text-figure 2 (2C and 2D) display the Toarcian paleotectonics (Barrier et al. 2018) overlain by the paleofacies for Rhaetian-Hettangian time, near the inception of Lower Marrat deposition and for the Sinemurian-Aalenian (Ziegler 2001). Uplift of the Qatar Arch ceased by the end of the Triassic and siliciclastic sediment input to the Arabian and Rub al Khali basins gradually diminished during deposition of the Upper Minjur/Lowerr Marrat as the Arch was onlapped and eventually covered.

Cessation of uplift of the Qatar Arch, therefore, closely preceded the inception of spreading and formation of the Southern Neotethys. Text-figure 40 shows the position of the Qatar Arch but also the limits of eroded Carnian saltern cycles (D evaporate and Sefidarr Dolomite) mapped by Szabo and Kheradpir (1978); the area extending northeastward to the plate margin in which the Hormuz salt is absent (Al-Husseini 2000); and the position and orientation of the Triassic depocenter beneath the Mesopotamian Basin.

One possible explanation for the uplift of the Qatar Arch and its northeastern extension to the plate margin is suggested by its shape: two linear uplifts and a subsiding basin extending out from a larger, central uplift at approximately 120-degree angles. Such features, with their series of promontories and reentrants are reminiscent of the rifted margins of plates. Such an origin has been suggested for the Appalachian-Ouachita orogenic system in North America (Thomas et al. 1977) (see text-fig. 41). The linear features connect upwelling hot spots located at the promontories and reentrants, called triple junctions (McKenzie and Morgan 1969). They undergo thermal uplift and erosion and, if extension continues long enough, will become either a new passive margin or an aborted rift zone or aulacogen. Two of the three arms undergo extension and the third arm of the triple junction becomes a failed rift zone or aulacogen (Burke and Dewey 1973). In the case of the Qatar Arch, the third arm of the Qatar triple junction is the Triassic depocenter which is aligned with the NW-SE-oriented Mesopotamian Basin and was later

overridden by the Zagros Deformation Front (text-fig. 41). It is hypothesized here that uplift and incipient rifting occurred at a Qatar hot spot during latest Carnian to early Norian time, then jumped to a location along the northeast Arabian Plate margin.

A modern, active analog is the Afar Triple Junction (Koptev et al. 2018), a mantle plume at which the East African Rift Zone, Red Sea and Gulf of Aden meet. Spreading is occurring along the Red Sea and Gulf of Aden branches while uplift, rifting and high heat flow characterize the East African Rift Zone. Hot spots, the surface expression of mantle plumes, are relatively stationary over long periods of geologic time and record the motions of plates over them (Wilson 1965; Morgan, 1971). The history of motion of the Arabian Plate relative to a reference point in Kuwait was illustrated by Sharland et al. (2001, Figure 3.3). The Afar hot spot is presently located at about 10N, 40E, in the Afar depression. During early Norian time, Kuwait was moving northwestward toward the present east African coast south of Somalia and may have crossed over the mantle plume, thereby causing the uplift and incipient rifting. Such interactions between plate boundaries and continental masses are well documented in the literature, one of the best-known examples being that of consumption of the Farallon Plate beneath western North America (Atwater 1970). The aborted rift represented by the Reelfoot Rift-Rome Trough-Olin Trough in eastern North America (Thomas et al. 1977) is directly analogous. It seems likely that other intra-plate tectonism, for example, the incipient rifting represented by the Palmyride depression in northern Syria, will be integrated into a comprehensive plate tectonic history of this region.

CONCLUSIONS

Incorporation of unpublished biostratigraphic data into an integrated sedimentological and sequence stratigraphic model for the Upper Triassic to lower Middle Jurassic strata of Kuwait provides a more detailed understanding of the depo-tectonic history and paleogeography of this region. More accurate dating of the included formations clarifies and, in some cases, alters the correlations with adjacent regions. The Lower and Middle Members of the Minjur Formation in Kuwait are assigned an early Norian age. The Upper Minjur Member is dated as late Norian-Rhaetian based on *Lunatisporites* spp. and *Vesicaspora schemeli,* together with *Rhaetogonyaulax* sp. and *Kyrtomisporis corrugatus.* The uppermost part of this member is assigned an undifferentiated Early Jurassic-Late Triassic age range, since Triassic markers and long ranging palynomorphs occur. The underlying Middle Carbonate Member is dated as Norian based on the presence of *Rhaetogonyaulax* spp. and *Minutosaccus crenulatus,* whereas an age range of Carnian-Norian is assigned to the Lower Minjur Member based on the co-occurrence of *Samaropollenites speciosus, Patinasporites densus* and *Elongatosaccites triassicus.* The lower part of the Lower Marrat is devoid of biostratigraphic age-diagnostic markers but a Sinemurian age based on $^{87}Sr/^{86}Sr$ isotope data (194.42–193.91 Ma) is proposed. A Pliensbachian age is assigned to the upper part of Lower Marrat based on the presence of *O. primaeva,* the LO of *Cymbriaella*, the FO of *N. triceras*, and the FO of *P. liassica* as well as on Sr isotope ages which indicates deposition in the late Pliensbachian. The base of the Middle Marrat is dated as earliest Toarcian on the basis of *L. crucicentralis,* an age which is further corroborated by the appearance of *M. croatica, E. praevirguliana, S. gibraltarensis,* and *P. liassica*, which have their LOs during the late Toarcian. The occurrence of *Timidonella sarda* (latest Toarcian-Bajocian) in the upper part of Middle Marrat, together with *Batiacasphaera* spp. in the Upper Marrat unit suggests a more nearly continuous sedimentation in the Toarcian-Aalenian interval, and a shorter hiatus in sedimentation than previously observed.

Kuwait was located on the southwest margin of the Mesopotamian Basin and on the northwest corner of the Arabian Basin. During large, rapid rises of sea level and periods of tectonic subsidence it was the locus of intrashelf basins (Marrat, Gotnia and Arabian basins). The stratigraphic section during these periods of deep-water deposition shows this region was sediment-starved and condensed, with very low rates of sedimentation. During lowstands, deposition was continuous in these basins and can be correlated to hiatuses on the platform margins.

Isochore maps of the Marrat Formation and its members demonstrate the geometry of the margins of the Mesopotamian and Arabian basins and their depositional and tectonic evolution. The isochore map for the total Marrat Formation reveals a uniformly eastward thickening wedge of sediments with no indication of a platform margin. This pattern is also shown by the Lower Marrat isochore map, with evenly spaced contours oriented north-south and apparently continuing into northeastern Saudi Arabia. The Middle Marrat shows a somewhat different pattern, with evidence of thickening into an intrashelf basin. By the time the Upper Marrat was being deposited, the basin had been infilled and the contour pattern shows an eastward thickening of a wedge of sediments that appears to continue southward into Saudi Arabia. The Dhruma is the first unit to show indications of a disruption of that pattern. Isochore maps of Crespo de Cabrera et al. (2019, 2020) suggest that formation of the Rimthan Arch occurred during late Middle and Late Jurassic time, segmenting the Mesopotamian Basin into Arabian and Gotnia basins. Patterns of sedimentation and paleobathymetry based on foraminifers support this interpretation.

Plots of biostratigraphy against an integrated display of core sedimentology and geophysical logs reveals a strong correlation between substage boundaries and the base of transgressive systems tracts. This is observable for the Sinemurian-Pliensbachian and Pliensbachian-Toarcian boundaries but is somewhat obscured by the presence of a karsted unconformity at the boundary between the Middle and Upper Marrat (Toarcian-Aalenian). The data for the Aalenian/Bajocian boundary are based on cuttings samples and can only place it within an indefinite stratigraphic interval in Sequence J19 of the Upper Marrat. The Bajocian/Bathonian boundary is associated with the MFS J30 TST, at the boundary between the Sargelu-Dhruma Transition and the Sargelu Limestone in Kuwait (Kadar et al. 2015; Crespo de Cabrera et al. 2019, 2020).

Plots of well logs versus time instead of depth provide a necessary and useful means of visualizing sequence stratigraphy. Whether displayed for single wells or as chronostratigraphic sections, such plots highlight varying rates of deposition, related to depositional setting. Sampling for biostratigraphy in thin basinal units with very low rates of deposition requires much closer spacing than in platform margin geometries, for example, and may reduce the duration of depositional hiatuses. Deposition does not cease during these hiatuses and the unconformity surfaces should be thought of as bypass surfaces, such that the missing sedimentary section should be looked for down-dip in the basins. Ultimately, many of these hiatuses will be narrowed or closed entirely.

ACKNOWLEDGMENTS

The authors wish to express their thanks to the Ministry of Oil, the State of Kuwait and the management of the Kuwait Oil Company for permission to publish this paper. The authors also acknowledge the support and encouragement from Mr. Mohammed Dawwas Al-Ajmi, Manager-Exploration, Kuwait Oil Company, Mr. Meshal Al-Wadi, KOC Exploration Studies Team Leader and Mr. Jarrah AI-Jenaie, KOC Geological and Geophysical Solutions Team Leader. We also express our gratitude to Dr. Darwin Kadar for reviewing the earlier version of the manuscript and to Millennia S.C. for providing supporting data. Grenville Lunn reviewed and edited the paper and provided valuable insights to the geology of Iraq and Iran. The authors wish to express our gratitude to the Editor-in-Chief of Stratigraphy, Dr. Jean Self-Trail for her critical review, constructive comments and editing of the manuscript.

REFERENCES

AL-EIDAN, A. J., NEOG, N., NARHARI, S. R., AL-DARMI, A., AL-MAYYAS, R. H., DE KEYSER, T. L. and PERRIN, C., 2009. Carbonate facies and depositional environments of the Marrat Formation (Lower Jurassic), North Kuwait. *Search and Discovery Article* 50223.

AL-MOJEL A., DERA, G., RAZIN, P. and LE NINDRE, Y. M., 2018. Carbon and oxygen isotope stratigraphy of Jurassic platform carbonates from Saudi Arabia: Implications for diagenesis, correlations and global paleoenvironmental changes. *Palaeogeography, Palaeoclimatology, Palaeoecology*, 511: 388-402.

AL-MORAIKHI, R., VERMA, N., MISHRA, P., HOUBEN, A. J. P., VAN HOOF, T. and VERREUSSEL, R., 2014. An updated chronostratigraphic framework for the Jurassic of the Arabian Platform: Towards a regional stratigraphic standard. *Search and Discovery Article*: 30333.

AL-SAHLAN, G., 2005. Letter to the Editor, *GeoArabia*, 10-3: 193–194.

ALSHARHAN, A. S., STROHMENGER, C. J., ABDULLAH, F. F. and AL SAHLAN, G., 2014. Mesozoic stratigraphic evolution and hydrocarbon habitats of Kuwait. In: Marlow, L. et al., Eds., *Petroleum Systems of the Tethyan Region.* American Association of Petroleum Geologists Memoir 106: 541–611.

AL-WAZZAN, H., HAWIE, N., AL-HAGGAN, H., AL-MERSHED, M.K., AL-SAHLAN, G. and AL-WADI, M., 2021. 3D forward stratigraphic modelling of the Lower Jurassic carbonate systems of Kuwait. *Marine and Petroleum Geology,* 123: 104699.

ARKELL, W. J., 1952. Jurassic ammonites from Jebel Tuwaiq, central Arabia. *Philosophical Transactions of the Royal Society of London B*, 236: 241–313.

ATWATER, TANYA, 1970. Implications of plate tectonics for the Cenozoic tectonic evolution of western North America. *Bulletin of the Geological Society of America,* 81: 3513–3536.

BARRIER, E. and VRIELYNK, B., 2008. Palaeotectonic maps of the Middle East. Tectono-sedimentary palinspastic maps from Late Norian to Pliocene. CCGM/CGMW, Paris, 14 maps.

BARRIER, E., VRIELYNCK, B., BROUILLET, J-F. and BRUNET, M-F., 2018. Paleotectonic reconsruction of the central Tethyan realm: Tectono-sedimentary-palinspastic maps from Late Permian to Pliocene. CCGM/CGMW, Darius Programme, Paris, 20 maps.

BARSS, M. S., BUJAK., J. P. and WILLIAMS, G. L., 1979. Palynological zonation and correlation of sixty-seven wells, eastern Canada. *Geological Survey of Canada,* 78-24: 1–117.

BAUDELOT, S. and TAUGOURDEAU-LANTI, J., 1986. Découverte d'une microflore dans les Pyrénées Catalanes attribuable au Norien–Rhétien. *Revue de Paléobiologie,* 5: 5–9.

BOUDAGHER-FADEL, M. B. K. and BOSENCE, D. W. J., 2007. Early Jurassic benthic foraminiferal diversification and biozones in shallow-marine carbonates of western Tethys. *Senckenbergiana Lethaea,* 87 (1): 1–39.

BOUDAGHER-FADEL, M. B. K., 2008. Evolution and Geological significance of larger benthic foraminifera. *Developments in Palaeontology and Stratigraphy* 21. Amsterdam: Elsevier, 1–544.

BRENNER, W., 1986. Bemerkungen zur Palynostratigraphie der Rhaet-Lias Grenze in SW-Deutschland. *Neues Jahrbuch für Geologie und Paleontologie Abhandlungen,* 173: 131–166

BRUGMAN, W. A., 1983. Permian-Triassic Palynology. *Laboratory of Palaeobotany and Palynology.* Utrecht: State University Utrecht, 121pp.

BUJAK, J. P. and WILLIAMS, G. M., 1976. Jurassic Palynostratigraphy of Offshore Eastern Canada. In: F. M. Swain, Ed., Stratigraphic Micropaleontology of Atlantic Basin and Borderlands. *Developments in Palaeontology and Stratigraphy,* 6. Amsterdam: Elsevier, 321–319.

BURKE, K. and DEWEY, J. F., 1973. Plume-generated triple junctions: Indicators in applying plate tectonics to old rocks. *Journal of Geology*, 81: 406–433.

BURKHALTER, R. M., BLASI, H-R. and FEIST-BURKHARDT, S., 1997. Der "Dogger" (oberes Aalenian) in den Bohrungen Herdern-1, Berlingen-1 und Kreuzlingen-1 (Nordostschweiz) und seine Beziehung zu den gleichaltrigen Schichten in Nordjura. *Eclogae Geologicae Helvetiae,* 90: 269–291.

CAMERON, D. K. JR., 1974. New Triassic Palynomorphs from the Arabian Peninsula. *Grana*, 14: 4–10.

CIRILLI, S., 2010. Upper Triassic lowermost Jurassic palynology and palynostratigraphy: a review. *Geological Society London Special Publication,* 334: 285–314

CRESPO DE CABRERA, S., DE KEYSER, T., AL-SAHLAN, G., AL-WAZZAN, H., KADAR, A. P. and KARAM, K. A., 2019. Middle and Upper Jurassic Strata of the Gotnia Basin, Onshore Kuwait: Sedimentology, Sequence Stratigraphy, Integrated Biostratigraphy and Paleoenvironments, Part 1. *Stratigraphy*, 16 (3): 165–193.

CRESPO DE CABRERA, S., DE KEYSER, THOMAS, AL-WAZZAN, HAJAR, AL-SAHLAN, GHAIDA, KADAR, ADI P., KARAM, KHALAF A., PACKER, STEPHEN, STARKIE, STEPHEN and KEEGAN, JAMES, 2020. Middle and Upper Jurassic strata of the Gotnia Basin, onshore Kuwait: Sedimentology, sequence stratigraphy, integrated biostratigraphy and paleoenvironments, Part 2. *Stratigraphy,* 17 (1): 1–37.

DAVIES, R. B. and SIMMONS, M. D., 2018. Triassic sequence stratigraphy of the Arabian Plate. In: Poppelreiter, M. C., Ed., *Lower Triassic to Middle Jurassic sequence of the Arabian Plate,* 101–162. Houten, The Netherlands: EAGE.

———, 2020. Dating and correlation of the Baluti Formation, Kurdistan, Iraq: implications for the regional recognition of a Carnier "marker dolomite," and a review of the Triassic to Early Jurassic sequence stratigraphy of the Arabian Plate by G. A. Lunn, S. Milleer

and A. Samarral [discussion], *Journal of Petroleum Technology*, 43: 95–108.

DE KEYSER T. L., 1979. "The Early Misssissippian of the Sacramento Mountains, New Mexico – an ecofacies model." Unpublished Ph.D. thesis, Oregon State University, 304 pp.

DE KEYSER, T., SAEID, E., KENDALL, C. and KELLOGG, J., in press. Normalized and color-filled logarithmic GR logs to enhance subsurface stratigraphic interpretation of carbonates and siliciclastics, *Interpretation.*

DICKINSON, W. R. and VIGRASS, L. W., 1965. Geology of the Suplee-Izee area, Crook, Grant, and Harney counties, Oregon, *Oregon Department of Geology and Mineral Industries, Bulletin* 58: 109 pp.

DIGBEHI, Z. B., DOUKOURE, M., TEA-YASSI, J., YAO, R. K., YAO N'GORAN, P., KANGAH, K. D. and TAHI, I., 2012. Palynostratigraphy and palaeoenvironmental characterization and evidence of Oligocene in the terrestrial sedimentary basin, Bingerville area, southern Côte d'Ivoire, northern Gulf of Guinea. *African Journal of Environmental Science and Technology,* 6 (1): 28-42.

DOLBY, J. H. and BALME, B. E. 1976. Triassic palynology of the Carnarvon Basin, Western Australia. *Review of Palaeobotany and Palynology*, 22: 105–168.

DOUBAN, A. F., AL-SAHLAN, G. and FENTON, J. P. G., 2001. Sequence Stratigraphic Distribution and Biostratigraphic Zonation of the Permo-Triassic Section in Kuwait. Abstract. AAPG Annual Convention, Denver, Colorado, US.

ENAY, R., LE NINDRE, Y. M., MANGOLD, C., MANIVIT, J. and VASLET, D., 1987. Le Jurassique d'Arabie Saoudite centrale: nouvelle données sur la lithostratigraphie, les paléoenvironnements, les faunes d'ammonites, les ages et les correlations, 1987. *Geobios*, Lyon, Special Memoir, 9: 13–65.

EVITT, W. R., 1961. The dinoflagellate *Nannoceratopsis* Deflandre; morphology, affinities and infraspecific variability. *Micropaleontology*, 7: 305–316.

FAROUK, S., AL-KAHTANY, K., EL-SOROGY, A. and EL-MOTAAL, E. A., 2018. High-frequency cycles and sequence stratigraphy of the Lower Jurassic Marra Formation, central Saudi Arabia, *Marine and Petroleum Geology*, 98: 369–383.

FISHER, M. J., 1972**.** The Triassic palynofloral succession in England. *Geoscience and Man,* 4: 101–109.

FRASER, N. M., BOTTJER, D. J. and FISCHER, A. G., 2004. Dissecting "*Lithiotis*" bivalves: implications for the Early Jurassic reef eclipse. *Palaios*, 19: 51–67.

FRAZIER, D. E., 1974. Depositional episodes: their relationship to the Quaternary stratigraphic framework in the northwestern portion of the Gulf basin: University of Texas at Austin, *Bureau of Economic Geology Geological Circular* 74 (1): 28 p.

FUGAGNOLI, A., 1999. *Cymbriaella*, a new Foraminiferal genus (Textulariina) from the Early Jurassic of the Venetian Prealps (Northeastern Italy). *Revue de Micropaleontologie,* 42 (2): 99–110.

———, 2004. Trophic regimes of benthic foraminiferal assemblages in Lower Jurassic shallow water carbonates from Northeastern Italy (Calcari Grigi, Trento Platform, Venetian Prealps). *Palaeogeography Palaeoclimatology, Palaeoecology,* 205: 111–130.

FUGRO-ROBERTSON LIMITED, 2009. Marrat Formation Stratigraphic Study, Onshore Kuwait, Biostratigraphic, Sequence Stratigraphic and Sr Isotope Investigation of 19 Wells. Volume 1: Text. Unpublished Report No. 7020/1b.

GALLOWAY, W. E., 1989a. Genetic stratigraphic sequences in basin analysis I: architecture and genesis of flooding-surface bounded depositional units, *American Association of Petroleum Geologists Bulletin*, 73: 125–142.

———, 1989b. Genetic stratigraphic sequences in basin analysis II: application to northwest Gulf of Mexico Basin, *American Association of Petroleum Geologists Bulletin*, 73: 143–154.

GHASEMI-NEJAD, E., HEAD, M. J. and ZAMANI, M., 2008**.** Dinoflagellate cysts from the Upper Triassic (Norian) of northeastern Iran. *Journal of Micropalaeontology,* 27: 125–134.

GOLDSMITH, P. J., HUDSON, G. and VAN VEEN, P., 2003. Triassic. In: Evans, D., Graham, C., Armour, A. and Bathurst, P., Eds. and co-ordinators, *The Millennium Atlas: petroleum geology of the central and northern North Sea,* 105–127. The Geological Society of London.

GOUBIN, N., 1965. Description and distribution of principal Permian, Triassic, and Jurassic pollenites of the Bore-Holes of the Morodava Basin (Madagascar). *Revue de l'Institut Francais du Petrole et Annales des Combustibles Liquides,* 20 (10): 1415–1461.

GRADSTEIN, F. M., OGG, J. G. and OGG, G., 2012. *The Geologic Time Scale* 2012. Elsevier Science Ltd, pp. 1–1176.

HAWIE, N., AL-WAZZAN, H. A., AL-ALI, S. and AL-SAHLAN, G., 2020. De-risking hydrocarbon exploration in lower Jurassic carbonate systems of Kuwait through forward stratigraphic models. *Marine Petroleum Geology*, 123: 104700.

HELBY, R., MORGAN, R. and PARTRIDGE, A. D., 1987a. A palynological zonation of the Australian Mesozoic. *Memoir of the Association of Australasian Palaeontologists* 4: 1–94.

HERNGREEN, G. F. W. and DE BOER, K. F., 1974. Palynology of Rhaetian, Liassic and Dogger strata in the eastern Netherlands. *Geologie en Mijnbouw*, 53 (6): 343–368.

HENNEBERT, M. and LEES, A., 1991. Environmental gradients in carbonate sediments and rocks detected by correspondence analysis: examples from the Recent of Norway and the Dinantian of southwest England. *Sedimentology*, 38: 623–642.

HORBURY, A., 2018. Petroleum geology and its relation to stratigraphic architecture of the Triassic to Middle Jurassic (Induan to Aalenian) interval on the Arabian Plate, In: Poppelreiter, M. C., Ed., *Lower Triassic to Middle Jurassic sequence of the Arabian Plate,* 49–100. Houten, The Netherlands: EAGE.

IBRAHIM, M. I. M., ABOUL ELA, N. M. and KHOLEIF, S. E., 2002. Dinoflagellate cyst biostratigraphy of Jurassic - Lower Cretaceous formations of the North Eastern Desert, Egypt. *Neues Jahrbuch für Geologie und Paläontologie Abhandlungen*, 224 (2): 255–319.

IBRAHIM, M. I. A., KHOLEIF, S. E. and AL-SAAD, H., 2003. Dinoflagellate cyst biostratigraphy and palaeoenvironment of the Lower – Middle Jurassic succession of Qatar, Arabian Gulf. *Revista Española de Micropaleontologia,* 35 (2): 171–194.

ILLING, L. V., 1954. Bahamian calcareous sands. *American Association of Petroleum Geologists Bulletin,* 38: 1–95.

ILYINA, N. W. and EGOROV, A. Y., 2008. The Upper Triassic of northern Middle Siberia: stratigraphy and palynology. *Polar Research,* 27: 372–392.

ISSAUTIER, B., LE NINDRE, Y. M., MEMESH, A., DINI, S. and VISEUR, S., 2012a. Managing clastic reservoir heterogeneity I:

sedimentology and sequence stratigraphy of the Late Triassic Minjur Sandstone at the Khashm al Khalta type locality, central Saudi Arabia. *GeoArabia*, 17(2): 17–56.

ISSAUTIER, B., LE NINDRE, Y. M., VISEUR, S., MEMESH, A. and DINI, S., 2012b. Managing clastic reservoir heterogeneity II: geological modelling and reservoir characterisation of the Minjur Sandstone at the Khashm al Khalta type locality (central Saudi Arabia). *GeoArabia*, 17(3): 61–80.

ISSAUTIER, B., LE NINDRE, Y. M., REID, C., MEMESH, A. and DINI, S., 2019. Depositional environments, age, and sequence stratigraphy of the Minjur Formation in outcrop and near subsurface – central Saudi Arabia. *American Association of Petroleum Geologists, Memoir,* 116: 141–184.

JAMES, G. A. and WYND, J. G., 1965. Stratigraphic nomenclature of Iranian oil consortium agreement area, *American Association of Petroleum Geologists Bulletin*, 49: 2182–2245.

JASSIM S. Z. and GOFF J. C., 2006. *Geology of Iraq*. Dolin. Brno: Moravian Museum, Prague, 318p

KADAR, A. P., DE KEYSER, T., NEOG, N. and KARAM, K. (with contributions from Le Nindre, Y. M. and Davies, R. B.), 2015. Calcareous nannofossil zonation and sequence stratigraphy of the Jurassic System, onshore Kuwait. *GeoArabia*, 20 (4): 125–180.

KENDALL, C. G. ST. C. and SCHLAGER, W., 1981. Carbonates and relative changes of sea level. *Marine Geology*, 44: 181–212.

KHAN, AIJAZ, 1989. Stratigraphy and hydrocarbon potential of Permo-Triassic sequence of rocks in the State of Kuwait, Unpublished Report, Exploration Department, Kuwait Oil Company, Kuwait, 25 pp.

KLAUS, W., 1963. Spores from the Southern Alpine Permian. *Jahrbuch fur Geologie,* 106: 299–363

KONERT, G., AFIFI, A. M., AL-HAJIRI, S. A. and DROSTE, H. J., 2001. Paleozoic stratigraphy and hydrocarbon habitat of the Arabian Plate. *GeoArabia,* 6 (3): 407-442.

KOPTEV, A., GERYA T., CALAIS, E., LEROY, S. and BUROV, E., 2018. Afar triple junction triggered by plume-assisted bi-directional continental break-up. *Scientific Reports.* 8:14742. DOI:10.1038/s41598-018-33117-3.

KÜRSCHNER, W. and HERNGREEN, G. F. W., 2010. Triassic palynology of central and northwestern Europe: a review of palynofloral diversity patterns and biostratigraphic subdivisions. In Lucas, S. G., Ed., *The Triassic Timescale*, Geological Society of London Special Publication, 334: 263–283.

KUSTATSCHER, E., ASH, S., KARASEV, E., POTT, C., VAJDA, V., YU, J., and MCLOUGHLIN, S., 2018. Flora of the Late Triassic. In: Tanner, L. H., Ed., *The Late Triassic World*, 46: 545–622.

LANE, H. R., 1974. Mississippian of southeastern New Mexico and west Texas – a wedge-on-wedge relation. *American Association of Petroleum Geologists Bulletin*, 58: 269–282.

LANE, H. R. and DE KEYSER, T. L., 1980. Paleogeography of the late Early Mississippian (Tournaisian 3) in the central and southwestern United States, In: Fouch, T. D. and Magathan, E. R., Eds., *Paleozoic paleogeography of the west-central United States,* 149–166. Denver, CO, USA: Rocky Mountain Section, Society of Economic Paleontologists and Mineralogists.

LASEMI, Y. and JILILIAN, A. H., 2010. The Middle Jurassic basinal deposits of the Surmeh Formation in the central Zagros Mountains, southwest Iran: facies, sequence stratigraphy, and controls. *Evaporites,* 25: 283–295

LE NINDRE, Y. M., MANIVIT, J. and VASLET, D., 1990. Stratigraphie sequentielle du Jurassique et du Crétacé en Arabie Saoudite, *Societé géologique de France, Paris, ser. 8,* 6: 1025–1034.

LEES, A. and MILLER, J., 1985. Facies variation in Waulsortian buildups. Part 2. Mid-Dinantian buildups from Europe and North America, *Geological Journal*, 20: 159–180.

LI, L. Q., WANG, Y. D., ZHOU, N., VAJDA, V. and LIU, Z. S., 2018. Late Triassic ecosystem variations inferred by palynological records from Hechuan, southern Sichuan Basin, China. *Geological Magazine* 155 (8): 1793–1810. Cambridge University Press.

LIU, C., ALWAYS, R., MORETON, D. J., SAMARRAI, A. and HMASALIH, F., 2017. Recommendations for a practical log-based stratigraphic framework for the Kurdistan region of Iraq. *AAPG Search and Discovery Article,* 30487.

LOUTFI, G., and ABDEL-SATTER, M. M., 1987. Geology and hydrocarbon potential of the Triassic succession in Abu Dhabi, U. A. E. *Society of Petroleum Engineers*, Paper no. 15698: 717–735.

LUNN, G., 2020. Dating and correlation of the Baluti Formation, Kurdistan, Iraq: implications for the regional recognition of a Carnier "marker dolomite", and a review of the Triassic to Early Jurassic sequence stratigraphy of the Arabian Plate [reply to discussion by R. B. Davies and M. D. Simmons. *Journal of Petroleum Technology*, 43: 109–126.

LUNN, G. A., MILLER, S. and SAMARRAL, A., 2019. Dating and correlation of the Baluti Formation, Kurdistan, Iraq: implications for the regional recognition of a Carnier "marker dolomite," and a review of the Triassic to Early Jurassic sequence stratigraphy of the Arabian Plate. *Journal of Petroleum Technology*, 42: 5–36.

MANGERUD G., PATERSON, N.W. and BUJAK, J., 2020. Triassic palynoevents in the circum-Arctic region. *Atlantic Geology* 57: 71–101.

MATTIOLI, E. and ERBA, E., 1999. Synthesis of calcareous nannofossil events in Tethyan Lower and Middle Jurassic successions. *Rivista italiana di Paleontologia e Stratigrafia*, 105 (3): 343–376.

MCKENZIE, D. P. and MORGAN, W. J., 1969. The evolution of triple junctions. *Nature*, 224: 125–133.

MORBEY, S. J., 1975. The palynostratigraphy of the Rhaetian stage, Upper Triassic in the Kendelbachgraben, Austria. *Palaeontographica Abteilung* B, 152: 1–75.

MORBEY, S. J., DUNAY, R. E., 1978. Early Jurassic to Late Triassic dinoflagellate cysts and miospores. In: Thusu, B., Ed., *Distribution of Biostratigraphically Diagnostic Dinoflagellate Cysts and Miospores from the Northwest European Continental Shelf and Adjacent Areas,* 100: 47-59. Continental Shelf Institute Publication.

MORGAN, W. J., 1971. Convection plumes in the lower mantle. *Nature*, 230: 42–43.

MOTAHARIAN, A., AGHANABATI, A., AHMADI, V. and MEISAMI, A., 2014. Biostratigraphy of Jurassic sediments in high Zagros belt (northeast of Shiraz-Iran), *MAGNT Research Report,* 2: 286–294.

NEOG, N., RAO, N. S.,AL-MAYYAS, R., DE KEYSER, T., PERRIN C. and KENDALL, C., 2010. Evaporite facies: A key to the mid Me-

sozoic sedimentary stratigraphy of North Kuwait. ICE Convention Abstract, Calgary, 2010.

ORBELL, G., 1973. Palynology of the British Rhaeto–Liassic. *Bulletin of the Geological Survey of Great Britain*, 44: 1–44.

PACKER, S. R. and KEEGAN, J. B., 2015."Biostratigraphic analysis of the Marrat Formation, onshore Kuwait." Unpublished report 782/14.

PACKER, S. R., KEEGAN, J. B. and STARKIE, S. P., 2018. "Biostratigraphic analysis of selected intervals from the Minjur, Jilh & Sudair Formations, onshore Kuwait." Unpublished report 855/18.

———, 2019. "Biostratigraphic analysis of selected intervals from the Minjur, Jilh & Sudair Formations, onshore Kuwait." Unpublished report 870/19.

PACYNA, C., 1914. Plant remains from the Polish Triassic. Present knowledge and future prospects. *Acta Palaeobotanica,* 54 (1): 3–33.

PATERSON, N. W. and MANGERUD G., 2015. Late Triassic (Carnian–Rhaetian) palynology of Hopen, Svalbard. *Review of Palaeobotany and Palynology*, 220: 98–119.

PFLÜG, H. D., 1953. Origin and development of the angiosperm pollen in earth history *Palaeontographica Abteilung* B, 95: 61–171

POWERS, R. W., 1968. Lexique stratigraphique international. Volume III, Asie, Fas. 10 b1, Arabia Saoudite. *Centre National de la Recherche Scientifique*, Paris, 177 pp.

POWERS, R. W., RAMIREZ, L. F., REDMOND, C. D. and ELBERG, E. L., Jr., 1966. Geology of the Arabian Peninsula: Sedimentary geology of Saudi Arabia. *United States Geological Survey Professional Paper* 560-D: 1–147 p.

REID, C., HOOKER, N., HUGHES, W., LINDSAY, R., DHUBEEB, A., MOJEL, A., BREUER, P., HENDERSON, A. and BAKHIET, A., 2015. A new reference section for the Lower to Middle Jurassic southwest of Riyadh: Detailed stratigraphic architecture and regional correlation with the subsurface of Saudi Arabia and Kuwait, *EAGE, 5th Arabian Plate Geology Workshop, Lower Triassic to Middle Jurassic evaporate-carbonate-siliciclastic systems of the Arabian Plate (Sudair to Dhruma and time-equivalent,* Kuwait: 8-11 February 2015.

REOLID, M., MATTIOLI, E., NIETO, L. M. and RODRIGUEZ-TOVAR, F., 2014. The early Toarcian oceanic anoxic event in the external Subbetic (Southiberian palaeomargin, westernmost Tethys): geochemistry, nannofossils and ichnology. *Palaeogeography, Palaeoclimatology, Palaeoecology*, 411: 79-94.

RIDING, J. B., D. J. MANTLE, and J. BACKHOUSE, 2010, A review of the chronostratigraphical ages of Middle Triassic to Late Jurassic dinoflagellate cyst biozones of the North West Shelf of Australia. *Review of Palaeobotany and Palynology*, 162: 543–575.

ROBERTSON RESEARCH INTERNATIONAL LIMITED, 1999. "Stratigraphic review of Permian-Triassic prospectivity in the State of Kuwait. Phase I: A Review of the Permo-Triassic Stratigraphy of Kuwait." Unpublished report No. 6049/Ib.

———, 2000. "Stratigraphic review of Permian-Triassic prospectivity in the State of Kuwait. Phases II and III: Biostratigraphic analyses and correlation of the Permian – Triassic stratigraphy of Kuwait." Unpublished report No. 6123/Ib.

———, 2004. "Biostratigraphic analysis of selected Jurassic core samples from the Marrat to Najmah Formations, Onshore Kuwait." Unpublished Report No. 6619/Ib.

SARTORIO, D. and VENTURINI, S., 1988. *Southern Tethys Biofacies.* Milan: Donato. Agip spa, 235 p.

SCHNEEBELI-HERMANN, E., HOCHULI, P.A., and BUCHER, H., 2017. Palynofloral associations before and after the Permian–Triassic mass extinction, Kap Stosch, East Greenland.*Global and Planetary Change,* 155: 178–195. https://doi.org/10.1016/j.gloplacha.2017.06.009

SENGOR, A. M. C. and NATAL'IN, B. A., 1996. Paleotectonics of Asia: fragments of a synthesis. In: Yin, A. and Harrison, T. M., Eds., *The tectonic evolution of Asia,* 486–640. Cambridge: Cambridge University Press.

SEPTFONTAINE, M., 1984. Biozonation (a` l'aide des foraminifères imperforé s) de la plate-forme interne carbonatée Liasique du Haut Atlas (Maroc). *Revue de Micropaléontologie,* 27: 209–229.

SETUDEHNIA, A., 1978. The Mesozoic sequence in southwest Iran and adjacent areas. *Journal of Petroleum Geology*, 1: 3–42.

SHA, J., VAJDA, V., PAN, Y., LARSSON, L., YAO, X., ZHANG, X., WANG, Y., CHENG, X. and JIANG, B., 2011: Stratigraphy of the Triassic–Jurassic boundary successions of the Southern Margin of the Junggar Basin, Northwestern China. *Acta Geologica Sinica,* 85: 801–840.

SHA, J., OLSEN P. E., PAN, Y., XU, D., WANG, Y., ZHANG, X. and VAJDA, V., 2015. Triassic–Jurassic climate in continental high-latitude Asia was dominated by obliquity-paced variations (Junggar Basin, ürümqi, China). *Proceedings of the National Academy of Sciences of the United States of America* 112: 3624–3629.

SHARLAND, P. R., ARCHER, R., CASEY, D. M., DAVIES, R. B. HALL, S. H., HEWARD, A. P., HORBURY A.D. and SIMMONS, M.D., 2001. Arabian Plate sequence stratigraphy. *GeoArabia* 2: 1–371.

SHARLAND, P. R., CASEY, D.M., DAVIES, R.B., SIMMONS, M. D. and SUTCLIFFE, O .E., 2004. Arabian Plate Sequence Stratigraphy – revisions to SP2. *GeoArabia*, 9 (1): 199–214.

SLOSS, L. L., 1963. Sequences in the Cratonic Interior of North America. *Geological Society of America Bulletin,* 74: 93–114.

STAMPFLI, G. M. and BOREL, G. D., 2002. A plate tectonic model for the Paleozoic and Mesozoic constrained by dynami plate boundaries and restored synthetic oceanic isochrons: *Earth and Planetary Science Letters*, 196: 17–33.

STANCLIFFE, R. P. W., 1996**.** Microforaminiferal linings. In: Jansonius J. and McGregor, D.C., Eds., *Palynology: Principles and Applications Vol 1*, 373-380. College Station, TX: AASP Foundation.

STEINEKE, M. and BRAMKAMP, R. A., 1952. Mesozoic rocks of Eastern Saudi Arabia (abstract). *American Association of Petroleum Geologists Bulletin*, 36: 909.

STEINEKE, M., BRAMKAMP, R. A. and SANDER, N. J., 1958. Stratigraphic relations of Arabian Jurassic oil. In: Weeks, L. G., Ed., *Habitat of Oil*, 1294–1329. American Association of Petroleum Geologists Symposium.

STEWART, S. A., REID, C. T., HOOKER, N. P. and KHAROUF, O. W., 2016. Mesozoic siliciclastic reservoirs and petroleum system in the Rub' Al-Khali basin, Saudi Arabia, *American Association of Petroleum Geologists Bulletin*, 100: 819–841.

SUNEBY L. B. and HILLS L. V. 1988. Palynological zonation of the Heiberg Formation (Triassic-Jurassic) eastern Sverdrup Basin, Arctic Canada. *Bulletin of Canadian Petroleum Geology*, 36 (4): 347–361.

SZABO, F. and KHERADPIR, A., 1978. Permian and Triassic stratigraphy, Zagros basin, southwest Iran. *Journal of Petroleum Geology*, 1-2: 57–82.

TAYLOR, D. G., 1982. Jurassic shallow marine invertebrate depth zones, with exemplification from the Snowshoe Formation, Oregon, *Oregon Geology*, 44: 51–56.

THOMAS, W. A., 1977. Evolution of Appalachian-Ouachita salients and recesses from reentrants and promontories in the continental margin. *American Journal of Science*, 277: 1233–1278.

TRAVERSE, A. 2004. Proposal to conserve the fossil pollen morphogeneric name *Classopollis* against *Corollina* and *Circulina*. *Taxon*, 53: 847–848.

———, 2008. Paleopalynology. *Topics in Geobiology,* 28: 813.

TRIPATHI, A. and RAM-AWATAR, 2006. *Atlas of Spores and Pollen from the Triassic Succession of India.* Uttar Pradesh: Birbal Sahni Institute of Palaeobotany Jubilee Special Publication, 128 pp.

TRUSKOWSKI, I., AL-SAHLAN, G. and YOUSSEF, A. , 2015. Lower to Middle Jurassic Marrat Formation in Kuwait: Biostratigraphy and paleoenvironments. Fifth Arabian Plate Geology Workshop. Lower Triassic to Middle Jurassic (Sudair to Dhruma and time equivalent) Evaporite-carbonate-siliciclastic system of the Arabian Plate. Abstract, 8-11 February, Kuwait City, Kuwait.

VAIL, P. R., MITCHUM, R. M., Jr., TODD, R. G., WIDMIER, J. M., THOMPSON, S., III, SANGREE, J. B., BUBB, J. N. and HATLELID, W. G., 1977. Seismic stratigraphy and global changes of sea level, In, Payton, C. E., Ed., *Seismic stratigraphy – applications to hydrocarbon exploration*. American Association of Petroleum Geologists Memoir 26, 49–212.

VAN BELLEN, R. C., H. V. DUNNINGTON, R. WETZEL and D. M. MORTON 1959-2005. Lexique Stratigraphique International. 03 10 Asie, (Iraq), 333 pages. Reprinted by permission of CNRS by Gulf PetroLink, Bahrain.

VAN BUCHEM, S. P., AL-HUSSEINI, M., MAURER, F. and DROSTE, H. F., 2010. *Barremian-Aptian stratigraphy and hydrocarbon habitat of the eastern Arabian Plate*. Bahrain: Manama, 614 pp.

VELIĆ, I., 2007. Stratigraphy and palaeobiogeography of Mesozoic benthic foraminifera of the Karst Dinarides (SE Europe). *Geologia Croatica*, 60 (1): 1–113.

VISSCHER, H. and BRUGMAN, W. A., 1981. Ranges of selected Palynomorphs in the Alpine Triassic of Europe. *Review of Palaeobotany and Palynology*, 34: 115–128.

WARRINGTON, G., 1978. Palynology of the Keuper, Westbury and Cotham Beds and the White Lias of the Withycombe Farm Borehole. *Bulletin of the Geological Survey of Great Britain*, 68: 22–28.

———, 1997. The Lyme Regis Borehole, Dorset - palynology of the Mercia Mudstone, Penarth and Lias groups (Upper Triassic - Lower Jurassic). *Proceedings of the Ussher Society,* 9: 153–157.

WARRINGTON, G. and WHITTAKER, A., 1984. The Blue Anchor Formation (late Triassic) in Somerset. *Proceedings of the Ussher Society,* 6: 100–107.

WHITTAKER, J. E., JONES, R. W. and BANNER, F. T., 1998. *Key Mesozoic benthic foraminifera of the Middle East.* London: Natural History Museum, 236 p.

WILLIAMS, G. L. and BUJAK, J. P., 1985. Mesozoic and Cenozoic dinoflagellates. In: Bolli, H. M., Saunders, J. B., Perch-Nielsen, K., Eds., *Plankton Stratigraphy,* 847–964. Cambridge: Cambridge University Press.

WILSON, J. T., 1965. Evidence from ocean islands suggesting movement in the earth. In: Blackett, P. M. S., Bullard, E. and Runcorn, A., Eds., A Symposium on Continental Drift. *Royal Society of London Philosophical Transactions*. Series A, 258: 145–167.

YAROSHENKO, O. P. and BASH IMAM, I. 1995. Age variability of palynomorph compositions of the Middle and Late Triassic of Syria and their relation to climate and facies–stratigraphy and geological correlation. *Stratigraphy and Geological Correlation*, 3-4: 375–392.

YOUSIF, S. and G. NOUMAN 1997. Jurassic geology of Kuwait. *GeoArabia,* 2 (1): 91–110.

ZIEGLER, M. A., 2001. Late Permian to Holocene paleofacies evolution of the Arabian Plate and its hydrocarbon occurrences. *GeoArabia*, 6 (3): 445–504.